University of Southampton Research Repository

Copyright © and Moral Rights for this thesis and, where applicable, any accompanying data are retained by the author and other copyright owners. A copy can be downloaded for personal non-commercial research or study, without prior permission or charge. This thesis and the accompanying data cannot be reproduced or quoted extensively from without first obtaining permission in writing from the copyright holder/s. The content of the thesis and accompanying research data (where applicable) must not be changed in any way or sold commercially in any format or medium without the formal permission of the copyright holder/s.

When referring to this thesis and any accompanying data, full bibliographic details must be given:

Thesis: Chloe L.C. Jones (2025) "*The (in)consistency of links across traits, species and communities in planktic foraminifera during Plio-Pleistocene climate change*", University of Southampton, School of Ocean and Earth Science, PhD Thesis, 155.

Data: Chloe L.C. Jones (2025) Traits, species and communities in planktic foraminifera during Plio-Pleistocene climate change. URI [https://doi.org/10.5258/SOTON/D3228]

University of Southampton

Faculty of Environmental and Life Sciences

Ocean and Earth Science

The (in)consistency of links across traits, species and communities in planktic foraminifera during Plio-Pleistocene climate change

by

Chloe Louise Cheryl Jones

ORCID ID: 0000-0003-0684-2404

Thesis for the degree of Doctor of Philosophy

May 2025

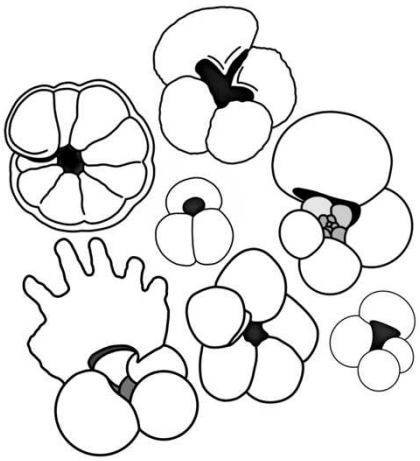

Supervisor

Thomas H.G. Ezard

Co-supervisor

Anieke Brombacher

The research presented in this thesis was carried out at the National Oceanography Centre in Southampton. This research was funded by the NERC grant NE/S007210/1 (3 years) and the Johanna M. Resig Foraminiferal Research Fellowship from the Cushman Foundation for Foraminiferal Research (1 year).

"*You are braver than you believe,*

stronger than you seem,

and smarter than you think."

- Winnie the Pooh

For Grandfather Jack Pile

University of Southampton

Abstract

Faculty of Environmental and Life Sciences

Ocean and Earth Science

Doctor of Philosophy

The (in)consistency of links across traits, species and communities in planktic foraminifera during Plio-Pleistocene climate change

by

Chloe Louise Cheryl Jones

This thesis aims to disentangle the roles of biotic and abiotic factors in driving extinction and shaping community dynamics in planktic foraminifera during the Plio-Pleistocene, a period characterised by a notable decline in species richness between 3.9 and 1.032 million years ago. Isolating biotic factors from environmental influences on planktic foraminiferal biodiversity remains challenging due to the complexity of environmental influence, difficulties in detecting biotic interactions from the fossil record, and the varying significance of measurements, even with large sample sizes. These factors, along with long-term evolutionary adaptations, make it difficult to clearly separate biotic influences from environmental pressures.

First, the thesis addresses the meaning of species and the challenges of their identification in deep time using *Menardella limbata* and *Menardella multicamerata* as exemplar case studies. Traditional methods, relying on qualitative traits, often lead to overlapping descriptions that complicate species differentiation rather than an evidence-based approach. Having defined what I mean by species in this chapter, this thesis further explores long-term ecological dynamics through extinction events.

Analysing 19 species extinctions of planktic foraminifera, the research uses Hill numbers to assess changes in community profiles across three extinction phases (pre-extinction, imminent-extinction, and post-extinction). Findings reveal how global temperature correlates with community structure differently in each phase, showing a loss of climate control closer to removing a constituent species. The final chapter extends this approach to examine the role of trait diversity in community dynamics during the same extinction events as the previous chapter. By integrating morphometric data from over 15,000 specimens, the research assesses how species size distributions impact key community metrics, offering insights into how trait diversity correlates with biodiversity dynamics and species identifications.

Overall, the thesis highlights the necessity of integrating trait, species, and community dynamics to comprehensively understand biodiversity changes. It provides valuable insights into the complex interactions driving ecological shifts and suggests directions for future research in understanding long-term biodiversity patterns.

Table of Contents

Abstract 7

Table of Contents 9

Table of Tables 12

Table of Figures 13

List of Accompanying Materials 20

Research Thesis: Declaration of Authorship 21

Acknowledgements 22

Chapter 1 Introduction 23

1.1 Biodiversity loss and accurate measures for prediction 23

1.1.1 Abiotic drivers of biodiversity loss 23

1.1.2 Biotic drivers of biodiversity loss 24

1.1.3 Biodiversity and ecosystem functioning 25

1.1.4 The importance of species in biodiversity measures 26

1.1.5 Accurate measures of biodiversity loss 26

1.2 Planktic foraminifera 28

1.2.1 Abundance and diversity in planktic foraminifera 29

1.2.2 Calcification and diversity in planktic foraminifera 30

1.2.3 Extinction in planktic foraminifera 32

1.2.4 Species identification in planktic foraminifera 32

1.3 Study period and location 33

1.3.1 The Plio-Pleistocene as a study period 33

1.3.2 ODP Site 925 as a study site 35

1.4 Thesis aims, outline and research questions 37

1.4.1 Thesis aims 37

1.4.2 Chapter outlines and research questions 37

Chapter 2 Updated species descriptions of the planktic foraminifera species *Menardella limbata* and *Menardella multicamerata* through quantitative analyses 40

2.1 Introduction 40

2.2 Materials & Methods 45

2.2.1 Materials 45

2.2.2 Methods 45

2.3 Results 49

2.4 Discussion 54

2.5 Species Descriptions 57

2.6 Conclusion 59

Chapter 3 Extinction unravels climate controls on community composition 61

3.1 Introduction 62

3.2 Materials and Methods 64

3.2.1 Materials 64

3.2.2 Methods 65

3.3 Results 69

3.4 Discussion 73

3.5 Conclusion 77

Chapter 4 Do size dynamics result from environmental changes or shifts in community composition? 78

4.1 Introduction 79

4.2 Materials & Methods 82

4.2.1 Materials 82

4.2.2 Methods 82

4.3 Results 85

4.4 Discussion 92

4.5 Conclusions 96

Chapter 5 Conclusion 99

5.1 Synthesis 99

5.2 Future work 101

5.3 Concluding remarks 102

Appendix A Supplementary Material for Chapter 2 104

A.1 Pilot study for Chapter 2 104

Appendix B Supplementary Material for Chapter 3 109

Appendix C Supplementary material for Chapter 4 121

Appendix D Neurodiversity: An Important Axis of Diversity in Ocean Sciences 125

References 130

Table of Tables

Table 2.1 Species characteristics of *Globorotalia Gr. (Menardella M.) limbata* (Fornasini, 1902) and *Globorotalia Gr. (Menardella M.) multicamerata* (Cushman and Jarvis, 1930) from Kennett and Srinivasan (1983). 43

Table A.1 The whole test area (√µm) range and mean of *Menardella limbata* and *Menardella multicamerata* for 3.101 and 3.402 Menardella and for 3.101 and 3.402 Ma combined (All), with standard deviation and 95 % confidence interval. 108

Table B.1 Last occurrence dates of individual species at Site 925, including ecogroups and morphogroups according to Aze *et al.* (2011). Global Age (Ma) is the last occurrence (LO) date from Aze *et al.* (2011) Shipboard Age (Ma) is the LO date from Chaisson & Pearson (1997), and LO (Ma) is the LO date from this study (see **3.2.2.1** for methodology). LO (Ma) age model is from Wilkens *et al.* (2017), and the oxygen isotope ($\delta^{18}O$ (‰)) is from Lisiecki and Raymo (2005). 115

Table B.2 Species count for assemblage counts conducted on sample 925D 8H2 140-142 cm, at 2.4285 Ma. 116

Table B.3 The last occurrence samples and the pre- (PR), imminent- (IM) and post-extinction (PO) samples for all 19 species extinction events, with the number of species observed in a 300-specimen assemblage count from the sample (Count), with the oxygen isotope ($\delta^{18}O$ (‰)) for each sample as a representative of the environment. The age model is from Wilkens *et al.* (2017), and the $\delta^{18}O$ (‰) data is from Lisiecki and Raymo (2005) 117

Table B.4 Observed and estimated *q* (0-2) values for pre- (PR), imminent- (IM) and post-extinction (PO) intervals for all 19 species extinction events, with the number of species observed in a 300-specimen assemblage count from the sample (Count). The age model is from Wilkens *et al.* (2017), and the oxygen isotope ($\delta^{18}O$ (‰)) is from Lisiecki and Raymo (2005)..... 119

Table C.1 The mean diameter (µm) per species in the pre- (PR) and imminent- (IM) samples for all 19 species extinction events, with the oxygen isotope ($\delta^{18}O$ (‰)) for each sample as a representative of the environment. The age model is from Wilkens *et al.* (2017), and the $\delta^{18}O$ (‰) data is from Lisiecki and Raymo (2005) 121

Table of Figures

Figure 1.1 Projected **a)** global surface temperature change relative to 1850-1900, with the projections for each of the five Shared Socioeconomic Pathways (SSPs) shown in colour (shades represent uncertainty ranges) and the black curves represent the historical data, and **b)** risks of species losses in the next 30-80 years, indicated by the percentage of assessed species exposed to potentially dangerous temperature conditions, at global temperature change of 1.5 °C, 2 °C, 3 °C and 4°C above historical temperatures (1850-1900). Adapted from IPCC (2021, 2023). 24

Figure 1.2 The relative frequencies of depth habitats **a)** and depth habitats of macroperforate planktic foraminifer species across the Cenozoic and **b)** deep-sea benthic foraminiferal oxygen isotope record and temperature difference from the present (ºC). Time in millions of years ago (Ma). Adapted from Ezard et al. (2011) and Westerhold et al. (2020). 35

Figure 1.3 Location of ODP Site 925, Ceara Rise, Atlantic Ocean (Shipboard Scientific Party, 1995). 36

Figure 2.1 Type images of *Menardella* species **a)** *archeomenardii*, **b)** *praemenardii*, **c)** *menardii*, **d)** *limbate*, **e)** *pseudomiocenica*, **f)** *miocenica*, **g)** *multicamerata*, **h)** *exilis*, and **i)** *pertenuis*. **a-d** and **f-g** are from Kennett and Srinivasan (1983) and **f** is from Boli and Bermudez (1965). 42

Figure 2.2 Proposed type specimens from this study of *Menardella multicamerata* **(a, c, e, g, i-j)** and *Menardella limbata* **(b, d, f, h)**. **a)** *M. multicamerata* and **b)** *M. limbata* – 6 chambers in final whorl, **c)** *M. multicamerata* and **d)** *M. limbata* – 7 chambers in final whorl, **e)** *M. multicamerata* and **f)** *M. limbata* – 8 chambers in final whorl, **g)** *M. multicamerata* and **h)** *M. limbata* – 9 chambers in final whorl, **i)** *M. multicamerata*– 10 chambers in final whorl, **j)** *M. multicamerata* – 11 chambers in final whorl. The scale bars are 200 µm. 46

Figure 2.3 Analysed morphological traits on planktic foraminiferal whole tests **a-f)** and final chamber **g-h)**. Specimens were imaged umbilical side up. The final-whorl chamber number was counted manually **a)** and area **b)**, aspect ratio **c)**, circularity (determined by how close the shape is to a perfect circle, see **Equation 1**) **d)**, roundness (determined by how the test fits within an idealized circular shape, see **Equation 2**) **e)**, and lobulation (determined by the number

of measurable areas between the test outline and smoothed outline) **f)** for the whole test and area **g)** and aspect ratio **h)** for the manually segmented final chamber were measured. 48

Figure 2.4 Principal component analysis (PCA) of whole test morphological measurements in *Menardella* specimens. The first 3 PCAs explain 69.2% of the variance. **PC1** = area (size), number of final-whorl chambers, aspect ratio, and explains 30.2 % of the variance. **PC2** = circularity, roundness, aspect ratio, and explains 24.1 % of the variance. **PC3** = age and lobulation and explains 14.9 % of the variance. Closed blue circles = *Menardella limbata* representatives and open yellow squares = *Menardella multicamerata* representatives.....50

Figure 2.5 Whole test trait based species clusters at 3.101 and 3.402 Ma combined, distinguishing between *M. multicamerata* and *M. limbata* via **a)** Kennet and Srinivasan (1983) species descriptions, **b)** Gaussian Mixture Model analysis with non-priori clustering, and **c)** suggested updated descriptions from this study. Closed blue circles = *Menardella limbata* representatives and open yellow squares = *Menardella multicamerata* representatives. Solid blue circle with black outline = *Menardella multicamerata* holotypes, and solid yellow squares with black outline = *Menardella limbata* hypotypes.....51

Figure 2.6 Principal component analysis (PCA) of final chamber +morphological measurements in *Globorotalia (Menardella)* specimens. The first 3 PCAs explain 92.6% of the variance. **PC1** = circularity, aspect ratio and roundness, and explains 60.3 % of the variance. **PC2** = area and roundness and explains 19.4 % of the variance. **PC3** = percentage size and roundness and explains 7.9 % of the variance. Closed blue circles = *Menardella limbata* representatives and open yellow squares = *Menardella multicamerata* representatives. 52

Figure 2.7 Final chamber size in relation (%) to the whole test size in *Menardella limbata* (light to dark blue) and *Menardella multicamerata* (light to dark yellow) across all final-whorl chamber numbers. 52

Figure 2.8 Final chamber trait-based species clusters at 3.101 and 3.402 Ma combined, distinguishing between *M. multicamerata* and *M. limbata* via **a)** Gaussian Mixture Model analysis with non-priori clustering and **b)** suggested update description from this study. Closed blue circles = *Menardella limbata* representatives and open yellow squares = *Menardella multicamerata* representatives.....53

Table of Figures

Figure 3.1 **a)** Schematic explanation of Hill numbers, including equation (Chao *et al.*, 2014) **b)** sample-sized based diversity accumulation curves; **c)** example of an even assemblage diversity curve; **d)** example of an uneven assemblage diversity curve. 63

Figure 3.2 Extinction dates (Site 925 last occurrences for each species, dark numbered circles), LR04 benthic foraminifera oxygen isotope compilation $\delta^{18}O$ (‰) (Lisiecki and Raymo, 2005) (where higher values of $\delta^{18}O$ mean lower temperatures and more continental ice, and vice versa (blue line)), and the number of species (dark blue line) through time (millions of years ago (Ma)) according to the Wilkens et al. (2017) age model. Species: **1)** *Hirsutella margaritae*, **2)** *Sphaeroidinella kochi*, **3)** *Dentoglobigerina baroemoenensis*, **4)** *Dentoglobigerina venezuelana*, **5)** *Dentoglobigerina altispira*, **6)** *Sphaeroidinellopsis seminulina*, **7)** *Sphaeroidinellopsis paenedehiscens*, **8)** *Hirsutella cibaoensis*, **9)** *Menardella limbata*, **10)** *Menardella multicamerata*, **11)** *Globoconella puncticulata*, **12)** *Menardella miocenica*, **13)** *Menardella pertenuis*, **14)** *Menardella exilis*, **15)** *Globigerinoidesella fistulosa*, **16)** *Neogloboquadrina humerosa*, **17)** *Neogloboquadrina acostaensis*, **18)** *Globigerinoides extremus*, **19)** *Globigerinoides obliquus*.....66

Figure 3.3 Sample ages for the LO sample (black line), pre-extinction (green line), imminent-extinction (yellow line), and post-extinction (red line) See **Figure 3.2** for species 1-19. The Grey dashed line represents the Pliocene-Pleistocene boundary and the onset of the 41-kyr glacial-interglacial cycles. 67

Figure 3.4 The number of species per sample on a natural log (ln) scale; the fitted line is a non-linear semi-log line with a 95% confidence interval. 68

Figure 3.5 Change in regression slopes and strengths for observed diversity values (*q*0, *q*1, and *q2*) and oxygen isotopes ($\delta^{18}O$ (‰)) (Lisiecki and Raymo, 2005) for pre- (green), imminent- (yellow), and post-extinction (red) intervals, with 95% confidence interval bands from linear regressions. 71

Figure 3.6 Diversity profiles for **a)** *q*1, **b)** *q*2, **c)** *q*2, and differences between **e)** *q*0-*q*1), **f)** *q*0-*q*2, and **g)** *q*1-*q*2 with 95% confidence interval bands from generalised additive models. 73

Figure 4.1 **a)** LR04 high-resolution benthic oxygen isotope ($\delta^{18}O$ (‰)) compilation (Lisiecki and Raymo, 2005) as a representative of environmental change (light blue) with **b)** species richness of planktic foraminifera from **Chapter 3** (dark blue) and

Chaisson and Pearson (1997), **c)** extinction rate of planktic foraminiferal species as species per 0.5 million years (Rate (per .5Myr); black line with open circles, and **d)** mean diameter (μm) per assemblage from this study (black line with closed circles) from ODP site 925 between 4.5 and 0.5 Myr. The vertical grey dashed line represents the boundary between the Pliocene and the Pleistocene, at 2.58 Ma, and the onset of the 41 kyr glacial-interglacial cycles. 83

Figure 4.2 Analysed morphological traits on planktic foraminiferal tests: **a)** specimens were imaged in umbilical view, and **b)** maximum diameter was measured on the extracted two-dimensional representation. 84

Figure 4.3 Change in regression slopes and strengths for mean assemblage diameter (μm)and diversity profiles ($q0$, $q1$, and $q2$) for pre- (green), imminent- (yellow), and post-extinction (red) intervals, with 95% confidence interval band from linear regressions. 88

Figure 4.4 Change in regression slopes and strengths for community assemblage diameter (μm; top panel) and extinct-going species diameter (μm; bottom panel) with diversity oxygen isotopes ($\delta^{18}O$ (‰); Lisiecki and Raymo, 2005) for pre- (green), imminent- (yellow), and post-extinction (red) intervals, with 95% confidence interval bands from linear regressions. Each colour (see key) represents each of the 19 species extinction events, with each point in the community assemblage representing a different species and each colour in the species diameters representing the extinct-going species. 89

Figure 4.5 Comparison of the difference in Akaike Information Criterion (AIC) values between the full model and the model with the named term removed; the height of the bar is the difference in AIC scores and thus the change in model likelihood and associated penalty for model complexity due to the named term (a bigger difference implies the term is more influential, and vice versa). Species identification (ID) is the random effect and is measured by comparing a generalised least square (GLS) without random effect to the full model, with Climate (represented by $\delta^{18}O$), extinction intervals (Intervals), each of the Hill numbers ($q0$, $q1$, $q2$) and the Climate: Interval interaction as fixed effects compared within linear mixed effect (LME) models. Both GLS and LME comparisons were made in the nlme package (Pinheiro et al., 2024). 91

Figure 4.6 Scaled regression coefficients of each fixed effect in the final linear mixed model. Coefficients were scaled to facilitate comparison, given the different measurement scales. Arrows denote the term associated with a shift from imminent- to pre-extinction phase (Imm -> Pre) and imminent- and post-extinction phase (Imm -> Post). The interactions, indicated using colons, show the difference between the slope/gradient of the climate relationship from the imminent- to pre-extinction phase (Climate:Imm -> Pre) and from imminent- to post-extinction phase (Climate:Imm -> Post). Error bars show 95% confidence intervals and highlight that while climate has the strongest influence on model fit (**Figure 4.6**), a proportional change in *q*1 or *q*2 can have a proportionally larger effect size on mean size. 91

Figure A1.1 Whole test trait based species clusters at 2.950, 3.101, 3.251 and 3.402 Ma combined, distinguishing between *M. multicamerata* and *M. limbata* via **a)** Kennet and Srinivasan (1983) species descriptions, **b)** Gaussian Mixture Model analysis with non-priori clustering, and **c)** hypothesised morphological differences from this study. Closed blue circles = *Menardella limbata* representatives and open yellow squares = *Menardella multicamerata* representatives. 105

Figure A.1 Type specimens of Miocene *Menardella* species: **a-b)** hypotype specimens of *Menardella limbata* and **c-d)** holotype specimens of *Menardella multicamerata*. The scale bar is 500 µm. 106

Figure A.2 Square root of the whole test area (√µm) of *Menardella limbata* (light to dark blue) and *Menardella multicamerata* (light to dark yellow) across 3.101 and 3.402 Ma. 107

Figure A.3 Number of specimens of *Menardella limbata* (light to dark blue) and *Menardella multicamerata* (light to dark yellow) across 3.101 and 3.402 Ma for each group of final whorl chamber number. 107

Figure B.1 Regression for observed diversity values (*q*0) and oxygen isotopes ($\delta^{18}O$ (‰) (Lisiecki and Raymo, 2005)) using a linear mixed model (t = -5.639), with a 95% confidence interval band. 109

Figure B.2 Extinction percentage heatmap by combined ecogroup and morphogroup for the 19 species extinctions at ODP Site 925 in the Plio-Pleistocene. The darker shades represent higher extinction rates. **Ecogroup:** 1 = Open ocean mixed layer tropical/subtropical, with symbionts, 2 = Open ocean thermocline, 4 =

Open ocean sub-thermocline. **Morphogroup:** 3 = Spinose, globular with supplementary apertures, 7 = Non-spinose, globular, 14 = Non-spinose, globorotaliform, keeled, 16 = Non-spinose, globorotaliform, non-keeled. Ecogroup and Morphogroup definitions are from Aze *et al.* (2011). 110

Figure B.3 Observed (solid line) and estimated (grey dashed line) diversity profiles for 1-5 of the individual species extinctions. *q* = 0 to 3, plotted with 95% confidence intervals (corresponding shading) across the three extinction intervals: pre-extinction (green), imminent-extinction (yellow), and post-extinction (red). **a-c)** *Hirsutella margaritae*, **d-f)** *Sphaeroidinella kochi*, **g-i)** *Dentoglobigerina baroemoenensis* and *Dentoglobigerina venezuelana*, **j-l)** *Dentoglobigerina altispira,* **m-o)** *Sphaeroidinellopsis seminulina*, and **p-r)** *Sphaeroidinellopsis paenedehiscens*. 111

Figure B.4 Observed (solid line) and estimated (grey dashed line) diversity profiles for 6-10 of the individual species extinctions. q = 0 *to* 3, plotted with 95% confidence intervals (corresponding shading) across the three extinction intervals: pre-extinction (green), imminent-extinction (yellow), and post-extinction (red). **a-c)** *Hirsutella cibaoensis*, **d-f)** *Menardella limbata* and *Menardella multicamerata***,** **g-i)** *Globoconella puncticulata*, **j-l)** *Menardella miocenica*, **m-o)** *Menardella pertenuis,* and **p-r)** *Menardella exilis*. 112

Figure B.5 Observed (solid line) and estimated (grey dashed line) diversity profiles for 11-15 of the individual species extinctions. *q* = 0 to 3, plotted with 95% confidence intervals (corresponding shading) across the three extinction intervals: pre-extinction (green), imminent-extinction (yellow), and post-extinction (red). **a-c)** *Globigerinoidesella fistulosa*, **d-f)** *Neogloboquadrina humerosa*, **g-i)** *Neogloboquadrina acostaensis*, **j-l)** *Globigerinoides extremus*, and **m-o)** *Globigerinoides obliquus*. 113

Figure B.6 Change in regression slopes and strengths for estimated values (*q*0, *q*1, and *q*2) and oxygen isotopes ($\delta^{18}O$ (‰) (Lisiecki and Raymo, 2005)) for pre- (green), imminent- (yellow), and post-extinction (red) intervals, with 95% confidence interval band from linear regressions 114

Figure C.1 Regression for the mean assemblage diameter (μm) and oxygen isotopes ($\delta^{18}O$ (‰) (Lisiecki and Raymo, 2005)) using a linear mixed model ($r = -0.279$, $p < 0.05$), with a 95% confidence interval band 123

Figure C.2 Change in regression slopes and strengths for assemblage diameter and species richness (*q*0; dark blue), evenness (*q*1; orange), and dominance (*q*2; purple), with a 95% confidence interval band from linear regressions. 123

Figure C.3 Change in regression slopes and strengths for the assemblage size (μm) and oxygen isotopes ($\delta^{18}O$ (‰); Lisiecki and Raymo, 2005) for pre- (green), imminent- (yellow), and post-extinction (red) intervals, with 95% confidence interval bands from linear regressions. 124

List of Accompanying Materials

Data for this thesis is available at: https://doi.org/10.5258/SOTON/D3228

Research Thesis: Declaration of Authorship

Print name: Chloe Jones

Title of thesis: The (in)consistency of links across traits, species and communities in planktic foraminifera during Plio-Pleistocene climate change

I declare that this thesis and the work presented in it are my own and has been generated by me as the result of my own original research.

I confirm that:

1. This work was done wholly or mainly while in candidature for a research degree at this University;
2. Where any part of this thesis has previously been submitted for a degree or any other qualification at this University or any other institution, this has been clearly stated;
3. Where I have consulted the published work of others, this is always clearly attributed;
4. Where I have quoted from the work of others, the source is always given. With the exception of such quotations, this thesis is entirely my own work;
5. I have acknowledged all main sources of help;
6. Where the thesis is based on work done by myself jointly with others, I have made clear exactly what was done by others and what I have contributed myself;
7. Parts of this work have been published as:
   Wilson, J.D., E. Sibert, M. Grigoratou, C.L.C. Jones, L. Rubin, and Z. Smilli. 2023. Neurodiversity: An important axis of diversity in ocean sciences. *Oceanography* 36(4):60–61, https://doi.org/10.5670/oceanog.2024.103.

Signature:

Date: 16/05/2025

Acknowledgements

First, I would like to express my deepest gratitude to my supervisors. Tom, I mostly want to thank you for your patience while guiding me through R and stats, those hours have been (brain-achingly) invaluable to my research results. I also want to thank you for your unwavering support, guidance, and encouragement throughout this (seemingly) long journey. Anieke, you set me on the path to foram taxonomy, which I'm still not sure whether to thank you for! Both of your expertise, insightful feedback, and patience have been vital to my development as a researcher, and I could not have asked for better mentors.

To my colleagues and friends that I have made throughout my academic journey, thank you for creating such a welcoming and inspiring environment. A special thank you to Jamie (for all the cinema trips) and Alex (for all the wine), who have been there for me from the start, even through the tough times. You are now stuck with me forever. To Rehemat, you created a safe space for me to vent, rant and ponder about both life and science, which is so greatly appreciated!

To the Bratton Lot, I'm not sure any of you truly understand what it is I do, but you have, and always will be, my best friends. Time with you brings me so much joy, and knowing you are always there for me has helped me get through this journey.

A special thanks to my family, especially my Mum and Dad, whose constant support and belief in me provided the strength I needed to persevere through this journey. Your encouragement has meant the world to me, and this achievement would not have been possible without you. And to my Grandfather Jack, you inspired me to study geology and set me on the path to becoming a scientist. Your influence and guidance have shaped my journey, and I will forever be grateful for having you in my life.

To my absolute favourite person, Dan. You joined me late in my PhD journey, but your support has undoubtedly meant the most – you dove in at the deep end with your endless support and belief in me in the final months of this 5-year project. You provided me with a shoulder to cry on and a place to call home for this last hurdle. I would not have made it without you, your love and your undying optimism.

To myself, for not giving up. This PhD has taught me as much about research as it has about myself. It is a testament to the idea that growth comes not just from what we achieve, but from the persistence and courage to continue, even when the path is uncertain.

To everyone who contributed in some way to this thesis, thank you from the bottom of my heart. This accomplishment is as much yours as it is mi

Chapter 1 Introduction

1.1 Biodiversity loss and accurate measures for prediction

There is an ongoing decline in biodiversity (Díaz *et al.*, 2006; Cardinale *et al.*, 2012). Large research collaborations suggest we have entered a sixth mass extinction (Barnosky *et al.*, 2011; Ceballos *et al.*, 2015) and their predictions indicate that future extinction rates may surpass the Big Five mass extinctions (Ceballos *et al.*, 2015). Biodiversity is crucial for regulating many ecosystem processes and provides essential goods and services for humanity, including food, materials, and medicines (Díaz *et al.*, 2006; Worm *et al.*, 2006). Additionally, it offers indirect services such as maintaining climatic conditions suitable for human life (Díaz *et al.*, 2006; Cardinale *et al.*, 2012). Consequently, continued significant declines in biodiversity levels will result in the loss of these beneficial systems over time. Environmental changes, including shifts in temperature, atmospheric carbon dioxide (pCO_2) levels, salinity, and ocean circulation, are known to impact global biodiversity (Condamine, Rolland and Morlon, 2013). Rapid environmental changes, predicted by the Intergovernmental Panel on Climate Change (IPCC) for the next 30-80 years (IPCC, 2021; **Figure 1.1a**), are expected to exacerbate current biodiversity loss. For example, a global temperature rise exceeding 2^{o}C could result in a 100% species loss, particularly in tropical regions (IPCC, 2023; **Figure 1.1b**).

1.1.1 Abiotic drivers of biodiversity loss

These predictions for biodiversity loss are based on the diversity of life on Earth having long been linked to abiotic factors, such as climatic and tectonic changes, with temperature rise, ocean acidification, anoxic events and habitat loss all driving extinction (Cifelli, 1969; Lipps, 1970; Hallock, Premoli Silva and Boersma, 1991; Peters, Kelly and Fraass, 2013). The Big Five mass extinctions are key examples of abiotic-driven biodiversity loss. The Permian-Triassic Extinction, approximately 252 million years ago (Ma), is proposed to be driven by a combination of increased temperatures, ocean acidification and anoxic events linked to large-scale volcanic eruptions (e.g., Dal Corso *et al.*, 2022) with a loss of up to 94 % of marine life and 70% of terrestrial vertebrates. The Cretaceous-Paleogene Extinction (~ 65 Ma) saw a loss of 75% of all species from a combination of climatic changes from volcanic activity and a meteor impact (Schulte *et al.*, 2010). More recently, during the Last Glacial Maximum in the Pleistocene (~10,000 years ago), rapid climatic changes, including temperature rise and altered precipitation patterns, contributed to the extinction of many large-bodied mammals (Koch and Barnosky, 2006).

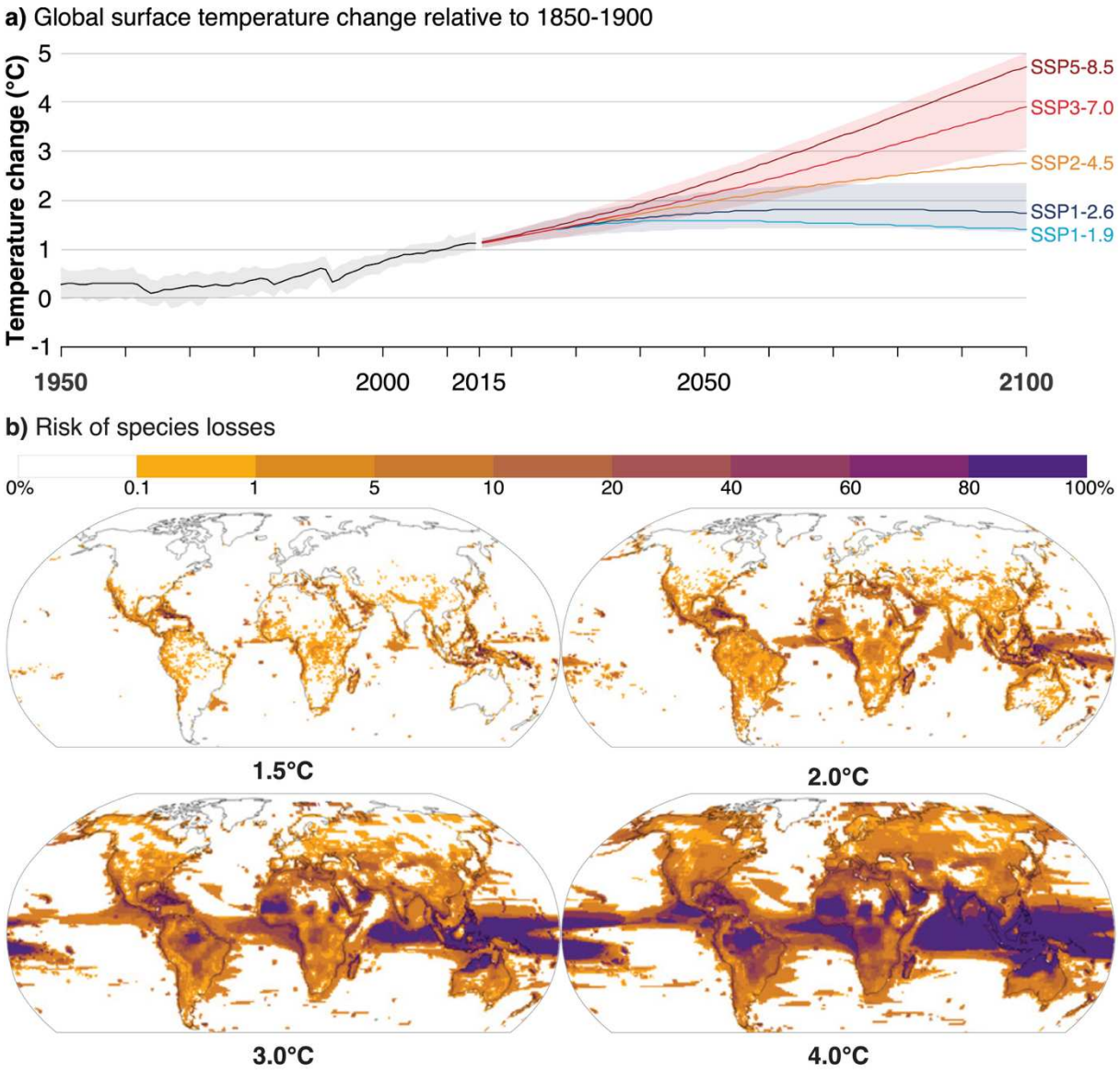

Figure 1.1 Projected **a)** global surface temperature change relative to 1850-1900, with the projections for each of the five Shared Socioeconomic Pathways (SSPs) shown in colour (shades represent uncertainty ranges) and the black curves represent the historical data, and **b)** risks of species losses in the next 30-80 years, indicated by the percentage of assessed species exposed to potentially dangerous temperature conditions, at global temperature change of 1.5 °C, 2 °C, 3 °C and 4°C above historical temperatures (1850-1900). Adapted from IPCC (2021, 2023).

1.1.2 Biotic drivers of biodiversity loss

Biotic factors, such as predation and competition, also impact biodiversity (Ives, Cardinale and Snyder, 2005; Cardinale *et al.*, 2012; Isbell *et al.*, 2015). Biodiversity itself has the potential to buffer against abiotic impacts (Cardinale *et al.*, 2012; Pires, Srivastava and Farjalla, 2018; Lucini *et al.*, 2020). For example, high species richness, one of the most basic indicators of biodiversity, enhances ecosystem stability, resilience, and adaptability (Ives, Klug and Gross, 2000; Loreau *et al.*, 2001). Species within an ecosystem often have differing ecological optima and fill unique ecological niches, meaning they respond differently and are potentially more

tolerant to environmental change (Ives, Klug and Gross, 2000; Loreau *et al.*, 2001). However, diverse ecosystems often exhibit greater functional redundancy, where multiple species perform similar ecological roles, ensuring that the loss of any single species will not necessarily disrupt key ecosystem processes (Loreau, 2004; Fetzer *et al.*, 2015). Ecosystems with higher biodiversity can, therefore, better absorb disturbances and better adapt to environmental changes, reducing the likelihood of cascading extinctions, where the loss of one species triggers a domino effect leading to the decline of additional species (McCann, 2000; Hooper *et al.*, 2005). While species richness and associated functional redundancy within an ecosystem undoubtedly help prevent cascading extinctions and maintain overall ecological health, the biodiversity impact of the loss of a species cannot be simply extrapolated from taxonomic counts.

1.1.3 Biodiversity and ecosystem functioning

Species richness alone does not capture ecosystem functioning (Hooper *et al.*, 2005). Communities are composed of individual organisms and species, each characterised by a unique set of traits contributing to their ecological roles within their respective habitats (Petchey and Gaston, 2006). This concept, known as functional diversity, emphasises the importance of the different functions and roles that species play in their ecosystems (Tilman, Isbell and Cowles, 2014). Unlike species richness, which simply counts the number of species, functional diversity assesses how the variety of traits within a community influences ecosystem processes and responses to environmental changes.

Measuring functional diversity provides crucial insights into how ecosystems adapt to long-term environmental changes and their overall ability to cope with shifting conditions. By linking species' traits directly to ecosystem processes, functional diversity enables researchers to predict how changes in species composition might occur in response to environmental pressures. Ecosystems with a broad range of functional traits are often more resilient to environmental changes. For example, diverse functional traits can offer different responses to stressors, which can help maintain ecosystem functions even under adverse conditions (Elmqvist et al., 2003; Mouillot et al., 2013). Therefore, ecosystems with high functional diversity tend to exhibit greater biological stability, meaning they can resist and recover from disturbances more effectively than ecosystems with lower functional diversity (Goswami et al., 2017). Thus, examining changes in morphological traits provides an alternative method for quantifying biodiversity and ecosystem stability. This approach goes beyond species richness to offer a more nuanced understanding of how trait variations within communities contribute to their resilience and stability (Loreau et al., 2001; Stachowicz, Bruno, and Duffy, 2007; Laureto, Cianciaruso, and Samia, 2015; Swain et al., 2024). By focusing on functional traits, we can

better understand how biodiversity influences ecosystem functioning and stability in the face of environmental change.

1.1.4 The importance of species in biodiversity measures

Accurate species definitions are crucial for measuring diversity changes because they ensure the reliability and validity of biodiversity assessments (Agapow *et al.*, 2004). Precise species definitions influence our understanding of species richness, distribution, and ecological roles, all of which are essential for assessing changes in biodiversity over time (Agapow *et al.*, 2004; see **1.1** and references within). Misidentification or incorrect classification can lead to inaccurate data on the number of species present, which can skew diversity metrics and impact our understanding of ecological changes (Dayrat, 2005; Kürzel *et al.*, 2022). Additionally, accurate species definitions help in understanding the ecological roles and functions of species within their communities (Petchey and Gaston, 2006). Different species may have distinct ecological functions, and misidentification can lead to incorrect assumptions about these roles and their contributions to ecosystem processes (Hooper *et al.*, 2005; Petchey and Gaston, 2006; Mouillot *et al.*, 2013). While trait-based and community-based approaches each provide valuable insights into biodiversity dynamics, integrating both approaches offers a complete understanding of how trait variations contribute to community resilience and stability (Elmqvist *et al.*, 2003; Hooper *et al.*, 2005; Petchey and Gaston, 2006). This integrative approach helps to identify communities that are not only diverse in terms of species but also resilient due to the distribution and overlap of functional traits.

1.1.5 Accurate measures of biodiversity loss

While species richness is a basic indicator of biodiversity change, it does not represent true species diversity and the ecological role within a niche alone (Akçakaya *et al.*, 2020); biodiversity is complex and cannot be represented by a singular number. For example, it does not capture the relative abundances of species within an ecosystem, giving the evenness and dominance. The evenness of an assemblage is indicative of community stability: high evenness is often associated with greater resilience to environmental changes because the ecosystem is not overly reliant on a particular species (Cusson *et al.*, 2015). Conversely, high dominance can reduce overall biodiversity, as other species may be suppressed or excluded (Cusson *et al.*, 2015). While common taxa are generally easily detectable and can be informative of diversity drivers as influential components of ecosystems (Lennon *et al.*, 2004; Gaston, 2008; Hannisdal *et al.*, 2017), less is known about the functional role of the rare species in ecosystems (Lyons *et al.*, 2005) that could act as “ecosystem canaries” in providing early warning signals of ecosystem collapse (Doncaster *et al.*, 2016).

Furthermore, what is absent from a sample ("dark diversity"; Pärtel, Szava-Kovats and Zobel, 2011), could be important for understanding the drivers of ecosystem changes, particularly when studying extinction events. This is because the absence of certain species may signal underlying environmental or ecological stressors that are not immediately apparent from the presence of species alone (Pärtel, Szava-Kovats and Zobel, 2011). Therefore, in the study of extinction events, knowing what species are missing from an ecosystem, when they are usually present, can provide insights into the conditions that may have led to their extinction. Since biodiversity is not univariate, broad representations of community composition are beneficial for predicting how assemblages will respond to environmental change. Biodiversity encompasses a range of factors, including genetic diversity, species interactions, ecosystem processes, and functional roles, which all contribute to the stability and resilience of ecosystems (Loreau *et al.*, 2001; Hooper *et al.*, 2005; Díaz *et al.*, 2006; Cardinale *et al.*, 2012). As such, a singular measure, such as species richness, cannot fully capture the complexity of biodiversity. Understanding the interactions and functional contributions of different species, both common and rare, allows for a more comprehensive view of ecosystem health and the potential impacts of environmental change.

Hill numbers (Hill, 1973), or "the effective number of species" (Chao *et al.*, 2014), are used to characterise the diversity of an assemblage (Chao *et al.*, 2014) by integrating richness, evenness and dominance of taxa (Hill, 1973). Hill numbers are ideal for extracting biologically meaningful signals, as they provide a nuanced approach to quantifying biodiversity that accounts for both species richness and the relative abundance of species in an integrated framework that yields insights into ecological diversity often missed by species richness alone (Hill, 1973; Chao and Jost, 2012). They also provide a standardised measure that accounts for the different diversity measures across different communities and, via bootstrapping, uncertainty bounds were a sampling exercise to be repeated (Chao *et al.*, 2014). Hill numbers have been applied in this study to track long-term biodiversity trends and compare ecosystems throughout climate-driven extinction events by identifying shifts in species composition and functional diversity, which allows for a deeper understanding of ecosystem stability and the impacts of environmental changes. Therefore, Hill numbers provide a robust framework for understanding biodiversity changes over time, enabling researchers to track long-term extinction dynamics and better predict the ecological consequences of environmental shifts. However, to be meaningful, Hill numbers require adequate sample sizes, which calls for extensive diversity records. Tracking extinction dynamics through the sorts of mass extinction events outlined previously necessitates that those extensive diversity records span the long-term.

Fossil records are invaluable for understanding long-term biodiversity trends, but they often lack comprehensive trait data. Functional diversity analysis requires a detailed understanding of how

traits are distributed and how they interact within communities (Bernard-Verdier *et al.*, 2012; Brown *et al.*, 2023). Many existing fossil databases focus primarily on taxonomic diversity, such as The Paleobiology Database (Uhen *et al.*, 2023), the Triton foraminifera database (Fenton *et al.*, 2021) and the New and Old Worlds Database of fossil mammals (NOW; The NOW Community, 2024), which give species richness without providing detailed information on their functional traits. This limitation hinders our ability to reconstruct functional diversity accurately over geological timescales. While databases like Phenomes10K (Goswami, 2015) have been developed to address the gap in functional trait data of vertebrates, by compiling trait information from fossils, they still face challenges in providing a comprehensive view of trait interconnectedness within communities. However, measuring very long-term functional diversity requires fossil record studies, and very few records allow for such reconstructions. Therefore, to accurately reconstruct long-term functional diversity, it is crucial to integrate comprehensive trait data from fossil records, enhance existing databases to include functional traits and analyse the interactions of these traits within communities.

1.2 Planktic foraminifera

Planktic foraminifera are marine protists, roughly 100-1000 µm in size (Haynes, 1981; Armstrong and Brasier, 2004), with most species possessing a calcareous test of calcium carbonate (Haynes, 1981), that are preserved when they sink to the sea floor after death. Planktic foraminifera represent a useful model system for understanding biodiversity in deep time due to their extensive 200 million-year fossil record, coupled with their wide geographic distribution and high taxonomic resolution (Kennett and Srinivasan, 1983; Kucera, 2007; Aze *et al.*, 2011; Fraass, Kelly and Peters, 2015; Yasuhara *et al.*, 2017). This excellent fossil record can be used to understand biodiversity changes through the abrupt climatic upheavals that lead to both mass extinctions and species loss following background climate changes (Fraass, Kelly and Peters, 2015).

Despite the extensive planktic foraminiferal record, significant gaps remain in our understanding of their functional traits (e.g., Rutherford, D'Hondt and Prell, 1999; Schmidt, Thierstein and Bollmann, 2004; Lombard *et al.*, 2009; Hönisch *et al.*, 2012). However, their morphological traits - such as test size, shape and calcification - have been well documented and studied (e.g., Barker and Elderfield, 2002; Schmidt, Thierstein, *et al.*, 2004; Kucera, 2007) and provide some insight into their functionality within a community. Planktic foraminiferal morphological traits help define their ecological roles, adaptation to environmental changes, and evolutionary success (Rutherford, D'Hondt and Prell, 1999; Schiebel and Hemleben, 2005; Kucera, 2007). With planktic foraminifera living in a range of depths in the ocean, identifiable geochemically, the significant information available on their niche habitats and morphologies

(Kennett and Srinivasan, 1983; Aze *et al.*, 2011; Antell *et al.*, 2021; Boscolo-Galazzo *et al.*, 2022) provides a better signature than genetic information on how species live, making fossils better suited for biodiversity studies.hill

1.2.1 Abundance and diversity in planktic foraminifera

The abundance and diversity of planktic foraminifera species are useful indicators of how planktic foraminiferal assemblages react to changing environments. Planktic foraminiferal assemblages have five major faunal provinces: tropical, subtropical, temperate, subpolar and polar (Bé, 1977), roughly following global temperature and salinity patterns (Schiebel and Hemleben, 2005). Contemporary planktic foraminifera species richness generally decreases from the tropics to the poles, peaking at the mid-latitudes (Rutherford, D'Hondt and Prell, 1999; Kucera, 2007). This global trend of increased species richness towards the tropics is largely controlled by increased stratification and, therefore, larger vertical temperature gradients and greater niche availability (Schmidt, Renaud, *et al.*, 2004).

Most planktic foraminifera live in the uppermost 50 m of the water column, in the mixed layer. Yet, many species can live much deeper than this, up to 2000 m along the thermocline (Schiebel and Hemleben, 2005). The higher temperature variability in the water column in the tropics means that the vertical separation of species is more obvious than in the poles (Schiebel and Hemleben, 2005), with greater niche stability at the poles than in the tropics (Waterson *et al.*, 2017). It is less clear how species' optimum niche changes through time, although Antell *et al*. (2020) have found that abiotic niches are stable across glacial-interglacial changes in the last 700,000 years.

However, species richness responds to multiple abiotic drivers other than temperature, such as ocean circulation (Ottens and Nederbragt, 1992) and productivity (Fenton *et al.*, 2016). Brombacher *et al.* (2018) questioned whether spatial abiotic drivers of morphological change within a species translate to temporal changes, advocating a more complex role for climate than temperature alone. The complexity of the drivers of change in diversity calls for a deep-time study of eco-evolutionary dynamics that tests diversity responses to both biotic and abiotic variables.

Abundance counts of 300 specimens of planktic foraminifera within an assemblage are traditionally used to track diversity changes (Al-Sabouni *et al.*, 2018). However, as abundance counts are inadequate to represent true species diversity (Ezard and Purvis, 2016; Hannisdal *et al.*, 2017; Akçakaya *et al.*, 2020), using abundant foraminiferal fossil assemblages to plot Hill number profiles of assemblage counts across extinction events allows a more in-depth, comparative look at complex communities (Yasuhara *et al.*, 2020; Kearns *et al.*, 2021).

1.2.2 Calcification and diversity in planktic foraminifera

Planktic foraminiferal morphological traits can also be used to measure diversity changes in relation to environmental change. The growth of planktic foraminifera calcite tests is controlled by several environmental factors, including ocean acidification, temperature, salinity, light, oxygen levels, nutrients, and food availability (Kucera, 2007), and the size and shape of their tests indicate their success in a changing environment. The shape and size of planktic foraminiferal tests can determine the organism's ability to float at different depths in the water column, affecting its access to light and nutrients (Berger, 1969; Coxall *et al.*, 2007). Additionally, the complexity of the shell's surface can enhance feeding efficiency by increasing surface area for capturing food particles (Anderson *et al.*, 1979; Schiebel and Hemleben, 2017; Grigoratou *et al.*, 2019). For example, species with spines can capture zooplankton prey, often larger than themselves (Anderson *et al.*, 1979; Schiebel and Hemleben, 2017), whereas non-spinose species feed on smaller zooplankton and dead organic matter (Anderson *et al.*, 1979; Schiebel and Hemleben, 2017). The different morphologies of species tests also impact their susceptibility to dissolution, with most spinose species having a higher tolerance than non-spinose species (Lombard *et al.*, 2009; Fox *et al.*, 2020; Béjard *et al.*, 2023). These morphological traits, therefore, not only reflect the ecological niches occupied by different species but also provide insights into how these organisms have responded to past climatic events and how they might fare in future environmental changes.

Morphological changes in the test can also be an indicator of environmental stress (e.g., Brombacher *et al.*, 2017; Weinkauf *et al.*, 2019, 2019). Characteristics of growth in individual foraminifera are reflected in both the chambers of their tests (Weinkauf *et al.*, 2014) and overall morphology, which are known to change depending on environmental parameters such as temperature (Bijma, Faber and Hemleben, 1990; Schmidt, Renaud and Bollmann, 2003; Schmidt *et al.*, 2016; Todd *et al.*, 2020). Studies show that within species, shell shape is limited under extreme stress (Caron, Faber and Bé, 1987; Weinkauf *et al.*, 2014, 2019). Hence, more variability is seen under optimum growth conditions. A study on marine bivalves (Kolbe, Lockwood and Hunt, 2011) found that greater morphological variability buffered against extinction by “enhancing species adaptations to changing conditions” or by increasing their geographical range. Further studies are needed across a wider species range to see if this applies to planktic foraminifera. However, the theory is useful for assessing the implications of biotic controls as a buffering mechanism, as a community may exhibit greater morphological variability before an extinction event. Therefore, it is important to study the size of planktic foraminifera before, during, and after an extinction to test biotic factors as a buffer against extinction when it occurs at a global scale.

While other traits, such as test shape as discussed, are informative of trait changes, test size remains one of the most commonly measured traits due to the ease and accuracy of measurements (Barker and Elderfield, 2002; Schmidt, Renaud, *et al.*, 2004; Schmidt, Thierstein, *et al.*, 2004; Kucera, 2007; Todd *et al.*, 2020). Test size is a straightforward morphological trait that can be easily and precisely measured using microscopes and/or image analysis software (e.g., Todd *et al.*, 2020). It provides consistent, repeatable data, which makes it highly valuable for statistical analyses and large-scale studies (Kucera, 2007). Size in planktic foraminifera also has a well-understood relationship with environmental factors. The general trend in foraminiferal size is that they are larger in warm tropical/subtropical zones with a decrease towards the poles (Kucera, 2007) due to a combination of environmental parameters: carbonate ion saturation, faster metabolic rates, higher light intensity and greater niche diversity due to stronger stratification (Schmidt, Renaud, *et al.*, 2004; Lombard *et al.*, 2010). This trend is complicated by the close correlation with salinity (Bijma, Faber and Hemleben, 1990; Weinkauf *et al.*, 2014, 2019), where reduced salinity hinders calcification in some species. For example, the reduced surface salinity from ca 39 psu to 34 psu during the influx of freshwater into the Mediterranean 126.4 ka saw the reduction in shell calcification and increased trait asymmetry and variance of planktic foraminifera (Weinkauf *et al.*, 2014). Furthermore, there is an increase in size with more food and nutrient availability (Kucera, 2007; Aldridge, Beer and Purdie, 2012), as less energy is needed. Ultimately, each species has differing optimum growth conditions (Darling and Wade, 2008), outside of which growth decreases and reproduction ceases (Schmidt *et al.*, 2006), resulting in extinction.

The ”Lilliput Effect” refers to a phenomenon observed during periods of significant environmental stress or rapid environmental change, where the size of these organisms becomes smaller than usual (Urbanek, 1993), and is often observed following mass extinctions in planktic foraminifera (Keller, 1988; Keller and Abramovich, 2009). However, dwarfing in planktic foraminifera has been proposed as a common stress-induced reaction prior to extinction (Wade and Olsson, 2009). Yet, Abramovich *et al.* (2010) observed this effect as a possible result of increased reproduction during the late Maastrichtian warm event. Dwarfed species, that had very low abundance pre- and post-event, became more abundant during the warming, whereas those species that retained their ‘normal’ size saw a drop in abundance (Abramovich *et al.*, 2010). Dwarfing before extinction, therefore, implies an opportunistic approach to reproduction to niche takeover. It has also been found that the maximum test size of planktic foraminifera often coincides with the maximum abundance and occurs at specific optimum temperatures (“optimum-size hypothesis”; Schmidt *et al.*, 2004; Moller, Schulz and Kucera, 2013), that support enhanced metabolic processes, growth, and reproduction. Overall, size changes in organisms are important as they reflect adaptive responses to environmental

stress, influence reproductive strategies, and indicate shifts in ecological niches and species abundance during periods of change or extinction.

1.2.3 Extinction in planktic foraminifera

The links between environmental change and foraminiferal extinctions have been studied extensively. For example, Ezard *et al*. (2011) show that changes in oxygen isotope ($\delta^{18}O$) levels (indicative of temperature, salinity and continental ice levels (Shackleton, 1977; Shackleton and Vincent, 1978)) are an important predictor of extinction, with mass extinctions being more strongly linked to abiotic rather than biotic factors (Abramovich *et al.*, 2010; Aze, 2022). Many individual background extinctions have also been linked to temporal climate fluctuations (Banerjee and Boyajian, 1997; Abramovich *et al.*, 2010; Peters, Kelly and Fraass, 2013; Fraass, Kelly and Peters, 2015; Weinkauf *et al.*, 2019). For example, the extinction of the species *Gansserina gansseri* (~65.78 Ma) is linked to global warming in the Maastrichtian (Abramovich *et al.*, 2010). Contrastingly, there is a selective extinction of warm-water taxa during the Eocene-Oligocene climate transition (~34 Ma) directly related to the global cooling event (Peters, Kelly and Fraass, 2013). While climate change has been widely linked to extinction events, its impacts differ amongst distinct ecological groups (Ezard et al. 2011), and little is known about if and how species interactions influence them.

The planktic foraminiferal fossil record suggests that net diversification (speciation - extinction) is strongly controlled by competition among species (Ezard *et al.*, 2011): with limited resources, species with similar ecological preferences compete for resources, resulting in less abundant communities (Rillo *et al.*, 2019). However, there is no evidence of competition in extant species (Rillo *et al.*, 2019), as there are too few living individuals within an ecological space to feasibly limit resources (Rillo *et al.*, 2019). Yet, speciation has a stronger link to biotic factors than extinction, potentially due to niche availability (Ezard *et al.*, 2011) and the most common mode of reproduction where gametes are released into the water column and subsequently fuse (Hemleben, Spindler and Anderson, 1989; Meilland *et al.*, 2021; Weinkauf, Siccha and Weiner, 2022). This suggests that while species interactions shape diversification, abiotic factors such as climate change currently remain a predominant driver of extinction events in the foraminiferal record.

1.2.4 Species identification in planktic foraminifera

Identifying planktic foraminifera species relies on several key methodological approaches important for understanding their abundance, diversity, and ecological significance. Morphological identification remains the primary method for classifying foraminifera based on the distinct features of their calcareous shells (Wiens, 2004). However, this approach can be

limited by the presence of cryptic species that are morphologically similar but genetically distinct (Huber et al., 1997; De Vargas et al., 1999; Darling and Wade, 2008). To address this, molecular techniques like DNA barcoding and sequencing are increasingly used to complement morphological identification, providing more precise species identification and helping to uncover hidden diversity (Darling *et al.*, 1996; Morard *et al.*, 2024). While this method cannot be applied to extinct species (Darling and Wade, 2008) because the molecular techniques rely on DNA and/or other molecular markers which are no longer preserved in fossils, all genetic diversity reported to date (Morard *et al.*, 2024) is monophyletically distributed within morphologically identified clades. Thus, the delimitation of species is still reliant on morphological differences and that multiple lines of evidence support delimitation as some form of meaningful taxonomic boundary. Distinguishing species within a sample remains difficult due to the overlapping features of closely related species (e.g., Tabachnick and Bookstein, 1990; Knappertsbusch, 2007; Mary and Knappertsbusch, 2013). Furthermore, outdated taxonomical descriptions can result in misidentifications and inaccuracies in species delimitations (e.g., Fabbrini et al., 2021; Fayolle and Wade, 2021; Poole and Wade, 2019; Scott, 2011; Torres-Silva and Hohenegger, 2024). Ultimately, it is essential to have precise and updated species descriptions, and taxonomic revisions to accurately measure diversity changes in planktic foraminifera and meaningful insights can be drawn through the abundance of fossils available.

1.3 Study period and location

1.3.1 The Plio-Pleistocene as a study period

The Pliocene (5.3 to 2.6 Ma) is frequently used as an analogue for future climate scenarios. During the Pliocene, global temperatures were approximately 2-3°C warmer than pre-industrial levels (Dowsett and Caballero Gill, 2010), which aligns closely with the temperature increases projected for the next century under high emission scenarios (IPCC, 2021; **Figure 1.1**). This makes the Pliocene a valuable period for studying how ecosystems and climate systems might respond to similar levels of warming. On the other hand, while the Pleistocene (2.6 Ma to 11.7 ka) is cooler than the Pliocene (Martínez-Botí *et al.*, 2015), it is characterised by significant climate variability, with 41-kyr glacial and interglacial cycles (Lisiecki and Raymo, 2005, 2007). Therefore, this increased amplitude of climate change in the Pleistocene provides a historical analogue for understanding how ecosystems and species might respond to a combination of current and future climate fluctuations. The climatic shifts between glacial and interglacial periods offer insights into how rapid temperature and ice cover changes can impact global and regional ecosystems.

The Plio-Pleistocene has great age control due to the LR04 stack, a high-resolution benthic $\delta^{18}O$ compilation (Lisiecki and Raymo, 2005), which allows us to accurately pinpoint sample ages and thus species' extinctions. The Plio-Pleistocene is also well-documented with extensive environmental records (e.g., Lisiecki and Raymo, 2007; Bartoli, Hönisch and Zeebe, 2011; Hönisch *et al.*, 2012; Badger *et al.*, 2013; Martínez-Botí *et al.*, 2015; Da *et al.*, 2019). The LR04 stack also provides knowledge of the glacial-interglacial climate change throughout the Plio-Pleistocene, which will help study climatic effects on extinction (**Figure 1.2**).

There has been a steady decline in planktic foraminiferal diversity over the last 5 Myr (Aze *et al.*, 2011; Ezard *et al.*, 2011), during a time when we see a shift from the warm Pliocene climate to the cooler Pleistocene, where it was cold enough to support ice sheets at both poles (Westerhold *et al.*, 2020; **Figure 1.2**). It is, therefore, widely suggested that climate played an important role in this decline of planktic foraminifera (Lipps, 1970; Thunell, 1981; Wei and Kennett, 1986; Peters, Kelly and Fraass, 2013; Fraass, Kelly and Peters, 2015). Sea surface temperature is suggested as the strongest predictor of large-scale diversity changes through time and is linked to the strength of ocean stratification (Rutherford, D'Hondt and Prell, 1999; Fenton *et al.*, 2016). More specifically, the decline in planktic foraminiferal diversity observed during the Pliocene and Quaternary is likely a result of both large-scale palaeoceanographic fluctuations, beginning ~6 Ma, and high-frequency climate oscillations related to the glacial-interglacial cycles that began ~ 2.5 Ma (Wei and Kennett, 1986; Peters, Kelly and Fraass, 2013; Fraass, Kelly and Peters, 2015).

Planktic foraminiferal test size is smaller in the Pliocene than in the Pleistocene, with the Plio-Pleistocene planktic foraminiferal test size smaller than in the Modern (Schmidt, Renaud and Bollmann, 2003; Schmidt, Thierstein, *et al.*, 2004; Todd *et al.*, 2020). This trend in increasing size over time is suggested to be as a result of a combination of both an evolutionary increase in species size and an increase in the abundance of the largest species (Malmgren, Berggren and Lohmann, 1983; Schmidt *et al.*, 2016; Todd *et al.*, 2020). However, we still see the same trend in the Plio-Pleistocene of larger sizes in warmer temperatures as we do in the Modern (Schmidt, Thierstein, *et al.*, 2004; Kucera, 2007; Todd *et al.*, 2020). The fact that larger sizes are consistently associated with warmer temperatures from the Pliocene through the Pleistocene and into modern times indicates that this relationship is robust across different climate periods. Therefore, size change in foraminifera is not only a reliable trait to track through time but is also a reflection of changes in the composition of foraminiferal communities. Given the Plio-Pleistocene's potential for excellent age control, a series of species extinctions/decline in biodiversity in planktic foraminifera and contemporaneous environmental records, a study site in the tropics with high initial diversity and good age models would provide the ideal site to investigate how biodiversity changes at trait, species and community levels.

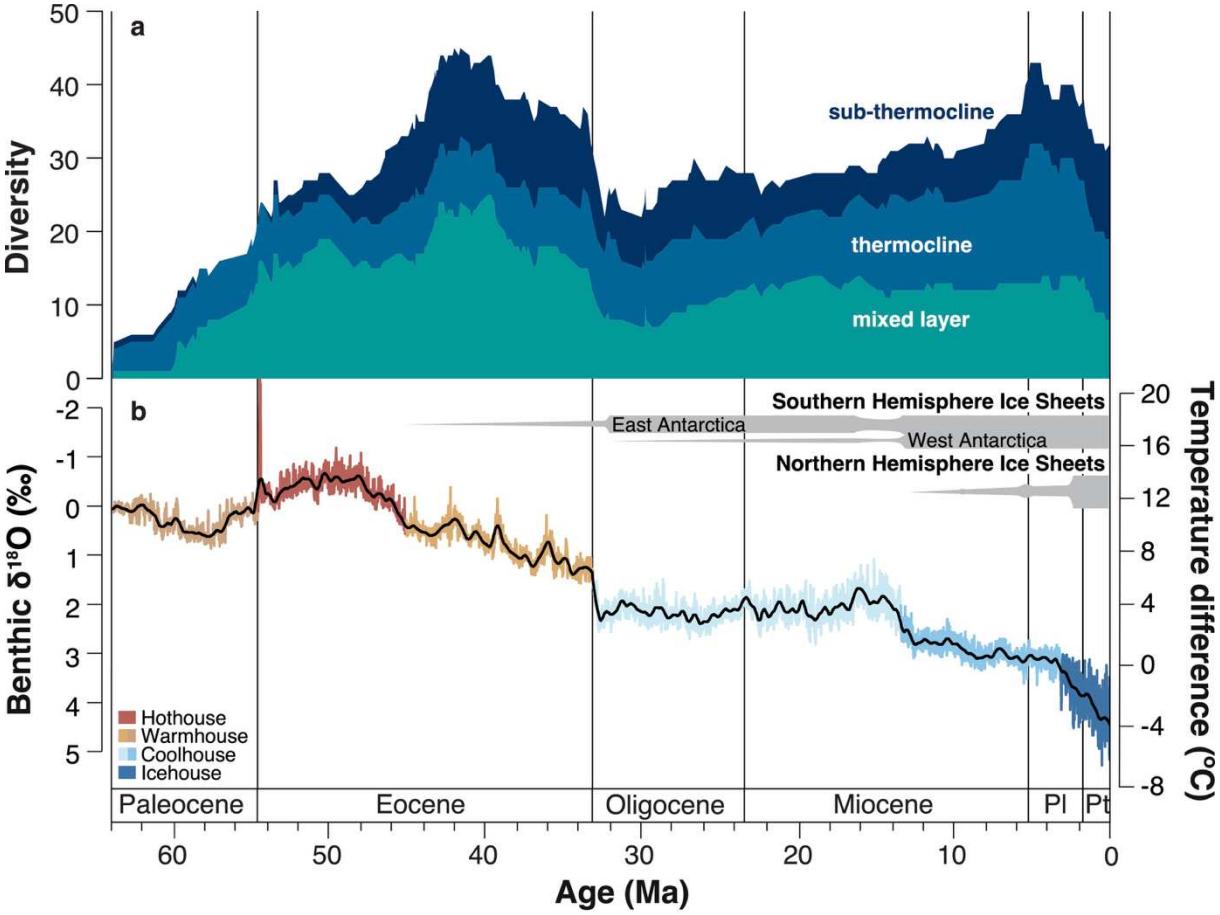

Figure 1.2 The relative frequencies of depth habitats **a)** and depth habitats of macroperforate planktic foraminifera species across the Cenozoic and **b)** deep-sea benthic foraminiferal oxygen isotope record and temperature difference from the present (ºC). Time in millions of years ago (Ma). Adapted from Ezard et al. (2011) and Westerhold et al. (2020).

1.3.2 ODP Site 925 as a study site

Ocean Drilling Program (ODP) Site 925, located on the Ceara Rise in the tropical equatorial Atlantic Ocean (4°12.256'N, 43°29.349'W) (Shipboard Scientific Party, 1995; **Figure 1.3**), makes for a good study site to investigate biodiversity changes. There is minimal change in palaeolatitude between 5 Ma (1.882°, 95% CI = 0.59583°, 3.17361°) and present day (Hinsbergen *et al.*, 2015; Vaes *et al.*, 2023). The seafloor at ODP Site 925 is 3040 meters below sea level (mbsl; Shipboard Scientific Party, 1995), which is above the current carbonate lysocline of 4-5 kilometres (km) in the Atlantic (Zeebe and Wolf-Gladrow, 2009); the depth in the ocean at which the rate of dissolution of calcium carbonate begins to increase significantly. The carbonate compensation depth (CCD; when the rate of dissolution is equal to the rate of supply) in the equatorial Atlantic was generally around 4.5 km in the Pliocene, deepening to around 5 km in the Pleistocene (Dutkiewicz and Müller, 2022). The lack of proximity to the lysocline and CCD makes ODP Site 925 a good site for preserving calcareous material, with well-preserved planktic foraminifera with no signs of severe dissolution (e.g. thinning of the test, changes in shape and size, and fragmentation; Chaisson and Pearson, 1997; Barker and Elderfield, 2002).

Test preservation is somewhat “frosty” but chambers are still well defined (Sexton, Wilson and Pearson, 2006).

The samples used in this thesis are from Holes 925B (4°12.248’N, 43°29.349’W, water depth: 3041.1 meters below sea level (mbsl)), 925C (4°12.256’N, 43°29.349’W, water depth: 3040.6 mbsl) and 925D (4°12.260’N, 43°29.363’W, water depth: 3040.5 mbsl) (Shipboard Scientific Party, 1995). All the Holes recover material down to the early Miocene (Shipboard Scientific Party, 1995), meaning we have a continuous record of the Plio-Pleistocene. Following the updated spliced age record (Wilkens *et al.*, 2017), multiple Holes are used for sampling in this thesis, also providing an accurate age model tuned to the LR04 stack (Lisiecki and Raymo, 2005; see Section **1.3.1**). The Shipboard planktic foraminifer biostratigraphy provides a record of species present and the last occurrence dates of 28 extinct-going species at ODP Site 925, at a sampling resolution of 333.3 kyr (Chaisson and Pearson, 1997).

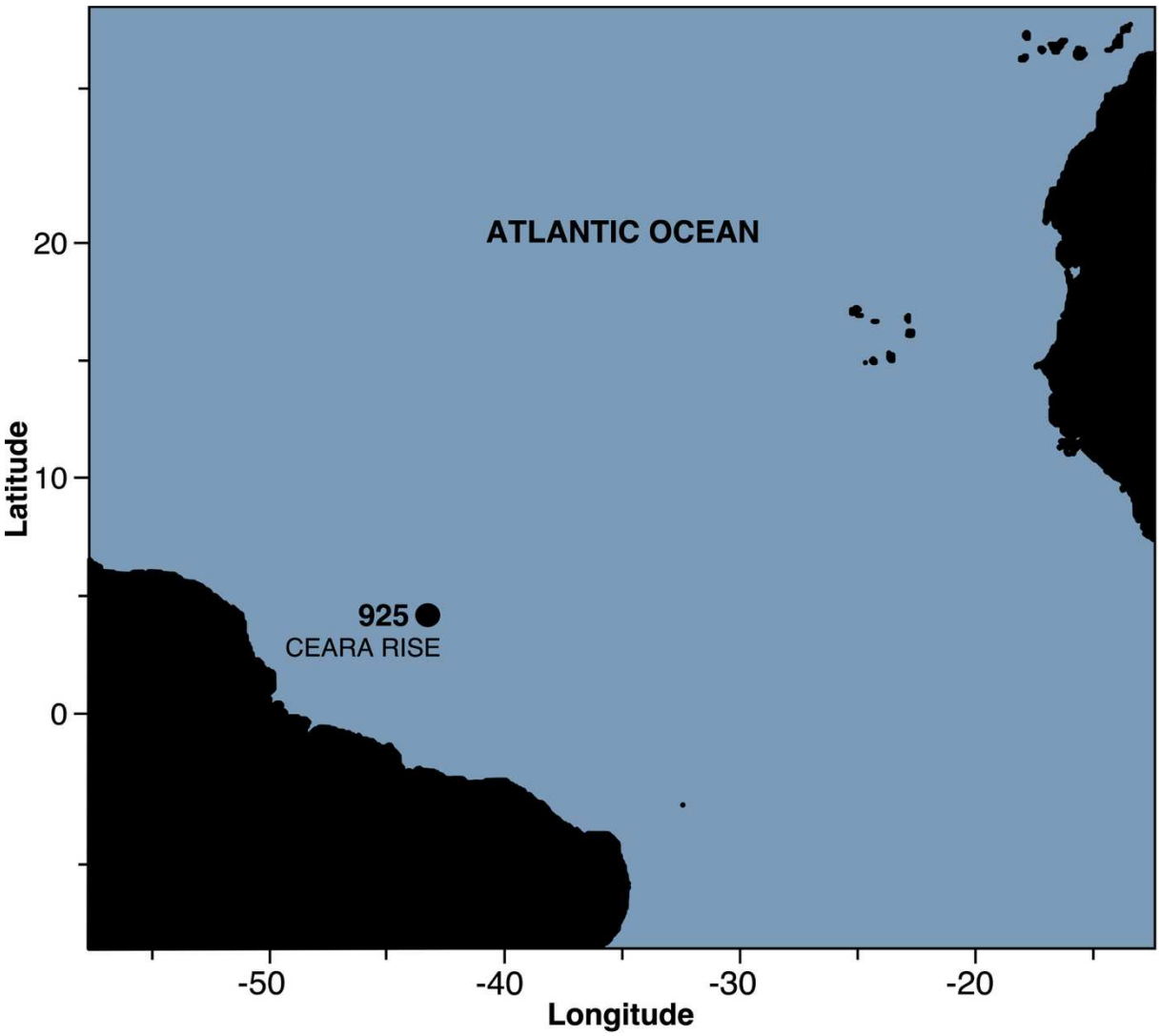

Figure 1.3 Location of ODP Site 925, Ceara Rise, Atlantic Ocean (Shipboard Scientific Party, 1995).

1.4 Thesis aims, outline and research questions

1.4.1 Thesis aims

The aim of this thesis is to use the exceptional fossil record of planktic foraminifera from the last 5 Myr to explore the potential effects of biotic controls on extinction and community dynamics during a time of environmental change. Central to my goals are to examine the interconnectedness of traits, species, and community dynamics across a period that would be caricatured as "simple" biodiversity loss due to the fall in species richness (39 to 25) from 3.900 to 1.032 Ma.

1.4.2 Chapter outlines and research questions

This thesis consists of 3 principal chapters, which aim to address a series of research questions in a coherent way.

Chapter 2 sets out what I mean by "species" using a case study on two putative *Menardella* species, *Menardella limbata* and *Menardella multicamerata*, and what this means for the broader fields of taxonomy, palaeoceanography and biostratigraphy. These species have traditionally been differentiated based on qualitative traits such as the circularity of the test and the number of chambers in the final whorl. However, these traits often overlap, making accurate species identification difficult. The data presented of 1,000 Menardella specimens uses quantitative morphometric analyses, including Gaussian additive mixture modelling, to examine the morphological differences between these two species. The findings suggest that the current taxonomic criteria are inadequate, and they propose updated species definitions based on more detailed and statistically supported morphological characteristics. This aligns with the following hypotheses:

1. How do the morphological traits, such as test size and shape, vary between these two species, and what implications do these variations have for their taxonomic classification?
2. Can quantitative morphometric analyses provide a more objective and reliable basis for species differentiation than the traditional qualitative descriptions?
3. What are the broader implications of these findings for taxonomy, particularly in addressing species with overlapping or ambiguous morphological traits in the fields of palaeoceanography and biostratigraphy?

Error! Reference source not found. investigates the long-term ecological dynamics governed by the interplay between biotic (living organisms) and abiotic (environmental) forces,

focusing on how these forces influence species extinctions. Specifically, the research examines 19 species extinctions of macroperforate planktonic foraminifera during the Plio-Pleistocene. Using new species abundance counts (richness), Hill numbers are used to calculate the evenness and dominance of 15,300 individuals across the 51 unique assemblages across three intervals of the individual species extinctions: pre-, imminent-, and post-extinction. These Hill numbers are used to correlate with the oxygen isotope record to detect changes in the relationship between diversity and the environment. The study's findings, enabled by an exceptionally resolved fossil record, offer insights into how ecological dynamics operate within communities in the context of ongoing extinctions. This approaches the following hypotheses:

1. How do biotic and abiotic factors interact to regulate long-term ecological dynamics, particularly during species extinctions?
2. What patterns can be observed in the relationship between global temperature and community metrics (e.g., species richness, evenness, dominance) before, during, and after extinction events?
3. How does the loss of climate control on community structure manifest during the imminent-extinction phase, and how does the community adjust post-extinction?

Chapter 4 explores analogous complex interactions between biotic and abiotic but focus on morphological trait diversity. While Error! Reference source not found. highlights the decoupling of abiotic controls on planktic foraminiferal communities during these events, the role of trait diversity in these processes, and whether there is a link from trait to community, remains unclear. Using morphometric data from over 15,000 specimens, the data demonstrates how dynamic changes in species size distributions affect key community metrics. By employing Gaussian Additive Mixture Modelling, the research underscores the importance of integrating trait diversity with species and community dynamics to better understand biodiversity changes on geological timescales. This approach provides a more nuanced interpretation of the complex interactions that drive biodiversity dynamics across different spatial and temporal scales and aligns with the following hypotheses:

1. How do environmental changes affect community diversity and functional traits in planktic foraminifera during individual extinction events?
2. How does trait diversity, particularly species size distributions, influence community composition and biodiversity dynamics during and after extinction events?
3. Can integrating trait diversity with species and community-level analyses provide a more comprehensive understanding of shifts in biodiversity on geological timescales?

Chapter 1 synthesises and concludes the discussion of the importance of accurate diversity measures and the biotic controls on planktic foraminifera during individual extinction events in the Plio-Pleistocene, which are explored in previous chapters. It presents the key findings and conclusions of the thesis and ideas for future work which could be undertaken.

Chapter 2 Updated species descriptions of the planktic foraminifera species *Menardella limbata* and *Menardella multicamerata* through quantitative analyses

Abstract

Taxonomy is how we identify species. However, current taxonomic definitions of many Neogene and Quaternary planktic foraminifera species are ambiguous and/or reliant on qualitative descriptions. While pragmatic approaches pivot on identifying gaps between inferred species, many taxonomic definitions blur the lines through overlapping descriptions. Such ambiguity makes species identification difficult and prone to arguments through subjective interpretation. Here, we use new quantitative analyses to explore potential overlaps in the morphospace of two such problematic species, *Globorotalia (Menardella) limbata* and *Globorotalia (Menardella) multicamerata*. The two species share many characteristics, and *Gr. (M.) multicamerata* is currently only distinguished from *Gr.* (*M.) limbata* by a more circular outline of the test, a deeper and more circular umbilicus, and overlapping number of chambers in the final whorl (6-8 and 8-10 for *Gr. (M) limbata* and *Gr. (M) multicamerata*, respectively). Species identification, therefore, relies on approximations of 'circular', especially for specimens with 8 chambers.

Using 2D images taken from light microscopy, we quantify 6 morphometric traits in 1000 specimens of *Gr (M.) limbata* and *Gr (M.) multicamerata*. Using Gaussian additive mixture modelling, which aggregates similar individuals into clusters without *a priori* classification, we show distinct morphological differences between the two species despite a greater overlap in the final-whorl chamber number, which is currently the basis for taxonomic differentiation. The test of *Gr (M.) limbata* is generally smaller and more elongated than that of *Gr (M.) multicamerata*. Additionally, we found significant differences in the final chamber size and shape, with *Gr (M.) limbata* having a proportionally larger and more circular final chamber than *Gr (M.) multicamerata*. Therefore, we update the definitions of these problematic species away from overlapping chamber numbers towards more comprehensive morphological descriptions and repeat calls for statistical investigation of inferred species differences.

2.1 Introduction

Taxonomy is the basis for accurate species identification, which is essential for scientific applications (Mayr, 1968; Elphick, 2008; Austen *et al.*, 2016), including conservation efforts

against ongoing biodiversity declines (Hopkins and Freckleton, 2002; Roberts, Elphick and Reed, 2010; Thomson *et al.*, 2018). In palaeoceanography, precise species identification allows researchers to accurately reconstruct past ocean conditions and climate changes by analysing microfossil records, as species-specific (Norris and Corfield, 1998; Gray and Evans, 2019; Boscolo-Galazzo *et al.*, 2024), and even sub-species-specific (Kearns *et al.*, 2023), geochemical signatures can impact paleo-reconstructions if specimens are incorrectly identified. In biostratigraphy, accurate taxonomic identification is critical for inferring an area's geological history through dating and correlating sediments (Wade *et al.*, 2011; BouDagher-Fadel, 2015; Fabbrini *et al.*, 2024). In evolutionary studies, taxonomy enables scientists to trace the lineage and evolutionary relationships of different species, providing insights into the processes of evolution over time (Pearson, 1998; Ezard *et al.*, 2011). Thus, taxonomy is a cornerstone of palaeoceanographic, biostratigraphic, and evolutionary research.

Species delimitation in the fossil record relies predominantly upon morphological analysis (Wiens, 2004), which involves examining the physical characteristics of the fossils to differentiate between species, and sometimes biostratigraphy and geochemical methods (Aze *et al.*, 2011). Morphological analysis can be challenging due to the often subtle and overlapping features between species, which may make accurate distinctions difficult. As an example, Tabachnick and Bookstein (1989) showed how intraspecific variation in Miocene *Globorotalia* spans the holotype differences of spiral geometry and the shape of the chambers and apertures, emphasizing the need to consider whether morphological features overlap across named species or whether gaps in morphospace separate those species. Distinguishing between two species exhibiting morphological similarities can be daunting, particularly when relying on outdated taxonomical descriptions that fail to differentiate the species adequately. Relying solely on type specimen images and descriptions and/or outdated or imprecise descriptions can lead to misidentifications and inaccuracies in species delineation (e.g., Fabbrini et al., 2021; Fayolle and Wade, 2021; Poole and Wade, 2019; Scott, 2011; Torres-Silva and Hohenegger, 2024), making taxonomic revisions and updates essential to incorporate the latest research and analytical techniques.

The menardii lineage of *Globorotalia* is comprised of 9 species of planktic foraminifera (**Figure 2.1)** which are notoriously difficult to distinguish due to the shared morphology of species within the group (e.g. a lenticular, trochospiral test with a prominent keel and smooth, densely perforate surface; Kennett and Srinivasan, 1983; Knappertsbusch, 2007; Mary, 2013; Mary and Knappertsbusch, 2013). Menardii-type *Globorotalia* are typically found in the open ocean thermocline of tropical water and have a biostratigraphic range of 16.27 Ma (within subzone M5b) to present (extant) (Kennett and Srinivasan, 1983; Aze, 2022). Here, we explore the morphological differentials between two species menardii-type species of the subgenus

Menardella (Bandy, 1972), *Globorotalia Gr. (Menardella M.) limbata* (Fornasini, 1902) (biostratigraphic range: 10.6 to 2.4 Ma; Wade *et al.*, 2011) and *Globorotalia Gr. (Menardella M.) multicamerata* (Cushman and Jarvis, 1930) (biostratigraphic range: 6.6 to 3.0 Ma; Wade *et al.*, 2011). While *Menardella* has previously been rejected as a genus/subgenus (Stewart, 2003; Brummer and Kučera, 2022), we will refer to the two species by *Menardella* from now on, under the guidance of the Neogene and Quaternary Planktic Foraminifera Working Group. Thus, *Globorotalia Gr. (Menardella M.) limbata* will be referred to as *Menardella (M.) limbata* and *Globorotalia Gr. (Menardella M.) multicamerata* as *Menardella (M.) multicamerata*. These two species highlight the challenges in Menardella taxonomy because the speciation of *M. Multicamerata* from *M. limbata* is widely used in both older and more recent biostratigraphic zonation schemes (Kennett and Srinivasan, 1983; Wade *et al.*, 2011). Despite their importance in these frameworks, they have traditionally been differentiated based on qualitative traits, such as the circularity of the test and the number of chambers in the final whorl (Kennett and Srinivasan, 1983). These traits often overlap significantly, making it difficult to reliably distinguish between species, even though accurate identification is critical for biostratigraphic dating.

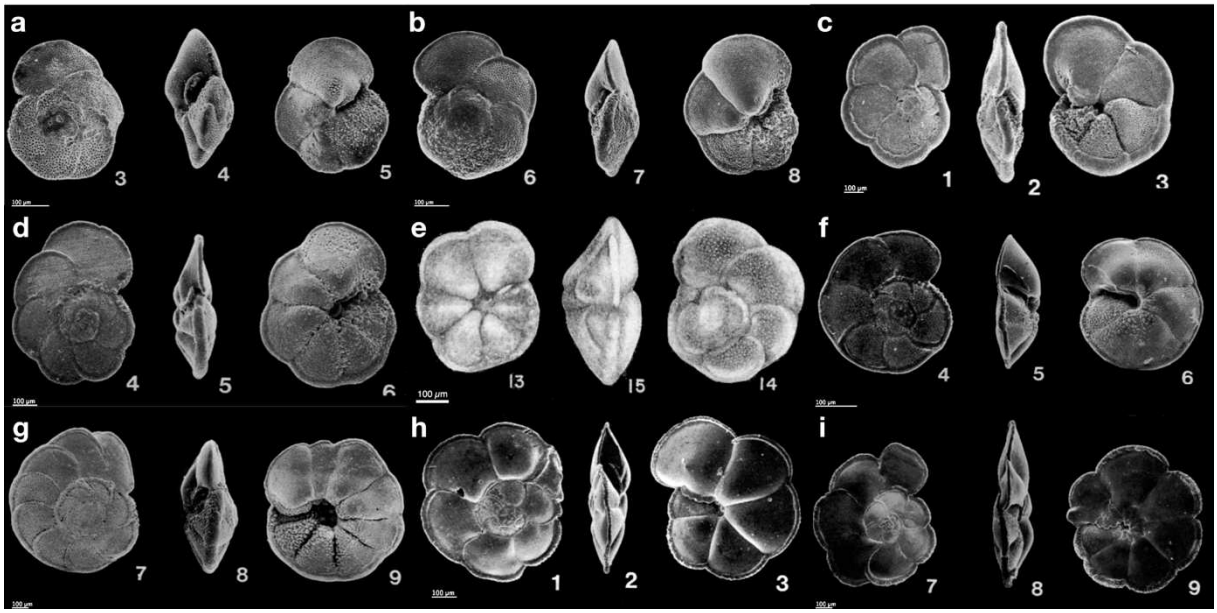

Figure 2.1 Type images of *Menardella* species **a)** *archeomenardii*, **b)** *praemenardii*, **c)** *menardii*, **d)** *limbate*, **e)** *pseudomiocenica*, **f)** *miocenica*, **g)** *multicamerata*, **h)** *exilis*, and **i)** *pertenuis*. **a-d** and **f-g** are from Kennett and Srinivasan (1983) and **f** is from Boli and Bermudez (1965).

Many of the features described for the species are, evidently, the same for both (e.g., single keel, low trochospiral chamber arrangement, limbate spiral sutures, depressed radial sutures, and uniformly and densely perforate wall texture), given that *M. limbata* is the proposed ancestor of *M. multicamerata* (Kennett and Srinivasan, 1983; Stewart, 2003). In the current Phylogenetic Atlas of Neogene planktic foraminifera (Kennett and Srinivasan, 1983), while some wording may differ slightly, the two species share similar descriptions of their morphology

(**Table 2.1**). For example, the test is described as "lenticular" in edge view with a "lobulate" outline for *M. limbata* but as "compressed" and "weakly lobulate" for *M. multicamerata* (Kennett and Srinivasan, 1983; **Table 2.1**). Likewise, the keel is also described as "pronounced" for *M. limbata* but "prominent" for *M. multicamerata,* while the spiral sutures are "recurved" in *M. limbata* and "curving backwards" in *M. multicamerata* (Kennett and Srinivasan, 1983; **Table 2.1**). The aperture is also ambiguously described as a "low arch with a distinct lip" for *M. limbata,* while *M. multicamerata* has a "low slit with a distinct lip" (Kennett and Srinivasan, 1983; **Table 2.1**). All these "diagnostic" features lack clear clarification of the difference in wording, if any, and without quantitative data, any difference between these descriptions is seemingly slight.

Using existing descriptions (Kennett and Srinivasan, 1983; **Table 2.1**), these two species are difficult to distinguish when looking at specimens under a microscope. Although the distinct difference in the size of the two species has previously been stated, with *M. limbata* at 300-400 µm and *M. multicamerata* at 500-700 µm (see: Stewart, 2003), recent studies on Miocene to Pliocene menardellids from tropical Indo-Pacific, Pacific and Atlantic oceans have shown a considerable size overlap (Stewart, 2003; Mary, 2013; Knappertsbusch, 2016), making it an unreliable trait for separating the two species. Similarly, the limbation of the spiral sutures is classically considered a key taxonomic feature in *M. limbata* (Blow, 1969; Kennett and Srinivasan, 1983). Yet, all degrees of limbation can be observed in all menardii-type specimens within the Pliocene, including *M. multicamerata* (Chaisson and Pearson, 1997; Pfuhl and Shackleton, 2004; Mary and Knappertsbusch, 2013).

The key features currently outlined in the current Atlas (Kennett and Srinivasan, 1983) as useful to differentiate between *M. limbata* and *M. multicamerata* is the number of chambers in the final whorl, with 6-8 and 8-10, respectively, the more "circular" outline of the test of *M. multicamerata* than *M. limbata*, and the difference in the umbilicus (Kennett and Srinivasan, 1983; **Table 2.1**). Recently, Mary (2013) noted that *M. multicamerata* might have 7-12 chambers in the final whorl, while Blow (1969) states 7-10 chambers are "usually" present, further highlighting the overlap in chamber numbers and raising questions about the effectiveness of the current descriptions (Kennett and Srinivasan, 1983). Although no studies have focused on the difference in the umbilicus of *Menardella* species*,* the specimens in this study have a wide range of umbilicus shapes across the two species, with various degrees of pustulose texture present in both. Therefore, circularity becomes the one feature, according to Kennett and Srinivasan (1983), that can be used to distinguish between the two species. Yet, this has not been quantified in the current descriptions, leaving room for misinterpretation.

Table 2.1 Species characteristics of *Globorotalia Gr. (Menardella M.) limbata* (Fornasini, 1902) and *Globorotalia Gr. (Menardella M.) multicamerata* (Cushman and Jarvis, 1930) from Kennett and Srinivasan (1983).

Traits / Species	*Globorotalia (Menardella) limbata*	*Globorotalia (Menardella) multicamerata*
test size	medium	large
test outline	lobulate	weakly lobulate
edge view shape	lenticular	compressed
keel	single, pronounced	single, prominent
chamber arrangement	low trochospiral	low trochospiral
umbilicus	extraumbilical-umbilical, narrow pit	extraumbilical-umbilical, circular pit
aperture	low arch bordered by a lip	low slit bordered by a distinct lip
final-whorl chambers	6-8	8-10
chamber growth	increasing slowly in size	increasing very slowly in size
spiral sutures	recurved, limbate, thickened at keel	limbate, curving backward to merge at keel
radial sutures	sinuous to radial, depressed	almost radial, depressed
wall texture	smooth, uniformly and densely perforate	pustulose near umbilicus, uniformly and densely perforate

The significant overlap between the taxonomic descriptions of *M. limbata* and *M. multicamerata* in the current Phylogenetic Atlas of Neogene planktic foraminifera (Kennett and Srinivasan, 1983) and the documented difficulty distinguishing the two species, likely arising from the ambiguous wording, is evidence that qualitative descriptions are insufficient. We need quantitative data and statistical analysis to better differentiate between the two species and update the taxonomic descriptions. Quantitative morphology has successfully been used to distinguish species within, for example, *Turborotalia* (Pearson and Ezard, 2014) and *Globigerina* (Fabbrini *et al.*, 2023) lineages. The confusion around species concepts in *Menardella* suggests a need to take a similar approach to this clade. This study provides quantitive evidence for updated species descriptions for both *M. limbata* and *M. multicamerata* from 2D morphometric trait data measured on Pliocene specimens from the tropical Atlantic Ocean.

2.2 Materials & Methods

2.2.1 Materials

Ocean Drilling Program (ODP) Site 925 is located on the Ceara Rise in the western Equatorial Atlantic (4°12.256'N, 43°29.349'W) at a water depth of 3040.6 meters (m) (Shipboard Scientific Party, 1995) (**Figure 1.3**). Foraminiferal material at this site is well preserved with no signs of severe dissolution, with mostly glassy preservation (see: Sexton, Wilson and Pearson, 2006), and includes large quantities of all species of the *Menardella* lineage (Chaisson and Pearson, 1997). Site 925 lies in the core of the biogeographic range of the species in this study, *M. limbata* and *M. multicamerata* (**Figure 2.2**), so the morphology of both species is unlikely to be affected by unusual shell shapes occurring at the range edges (Brombacher *et al.*, 2023). Two samples were taken from Hole 925C at 3.101 million years ago (Ma) and 3.402 Ma (following the age model by Wilkens et al (2017)) to ensure sufficient specimens for statistical analyses. These samples are far enough removed from the first occurrence of *M. multicamerata* (6.5 Ma (Aze et al., 2011)) to avoid species differentiation issues immediately following speciation (Kennett and Srinivasan, 1983) and not close to enough to the extinction of both species (2.55 Ma; Error! Reference source not found.) to encounter morphological changes such as pre-extinction dwarfing (e.g. Brombacher et al., 2017; Ferraro et al., 2020; Wade and Olsson, 2009; Weinkauf et al., 2014).

2.2.2 Methods

2.2.2.1 Measurements

Both samples were washed and dry-sieved to >150 µm. An initial pilot study of size and shape analysis was conducted on 90 Menardella specimens, across 4 time points (2.950, 3.101, 3.350 and 3.402 Ma) to test the species identification for this study (see **Appendix A.1**). Therefore, the specimens were picked following the species descriptions outlined in this study (see 2.5 **Species Descriptions**). We expanded the number of specimens included in the study to enhance the reliability of the data, ensuring more robust and reproducible results. Every specimen of the two potential species were picked until 250 specimens of each species were

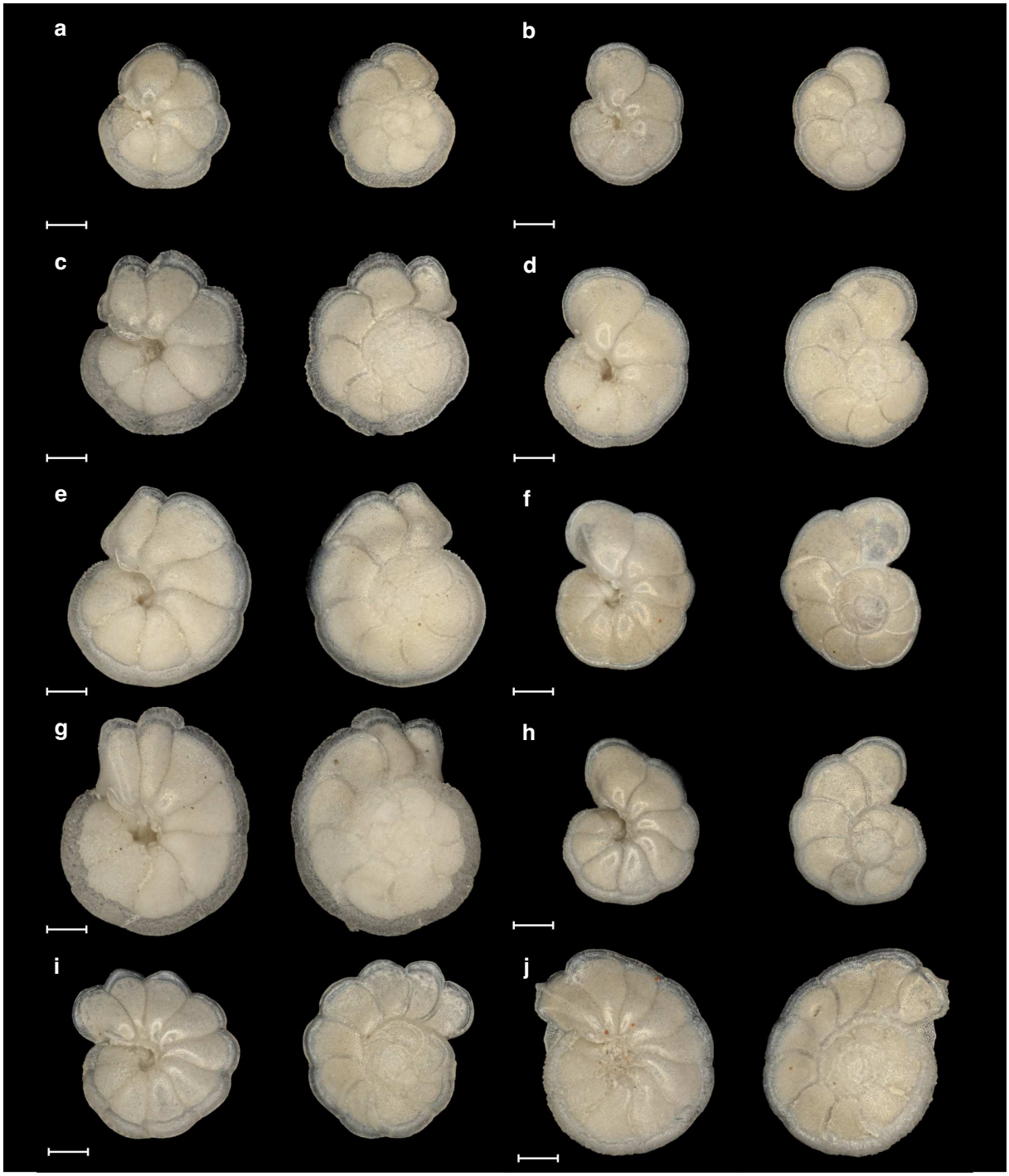

Figure 2.2 Proposed type specimens from this study of *Menardella multicamerata* **(a, c, e, g, i-j)** and *Menardella limbata* **(b, d, f, h)**. **a)** *M. multicamerata* and **b)** *M. limbata* – 6 chambers in final whorl, **c)** *M. multicamerata* and **d)** *M. limbata* – 7 chambers in final whorl, **e)** *M. multicamerata* and **f)** *M. limbata* – 8 chambers in final whorl, **g)** *M. multicamerata* and **h)** *M. limbata* – 9 chambers in final whorl, **i)** *M. multicamerata*– 10 chambers in final whorl, **j)** *M. multicamerata* – 11 chambers in final whorl. The scale bars are 200 µm.

picked from each sample at 3.1 and 3.4 Ma, resulting in 1,000 specimens in total (500 *M. limbata* and 500 *M.multicamerata*). The specimens picked for this study were mounted on a picking slide, umbilical side up, as all measurements can be measured on one side, and imaged using an Infinity 3 Lumenera camera mounted on an Olympus SZX10 light microscope. While using Scanning Electron Microscopes (SEM) for taxonomic assessment offers high-resolution details (Honjo and Berggren, 1967), it also presents several challenges. It requires specialised equipment and expertise, making it time-consuming and complex. Additionally, SEM studies often involve a limited number of specimens, leading to potential sampling bias, and results may be difficult to compare across different studies due to variations in imaging techniques. Moreover, the cost and limited accessibility of SEM equipment can restrict its use in routine taxonomic research. Therefore, light microscopy is better suited for the large datasets within this study because it is faster, more cost-effective, and allows for the examination of numerous specimens quickly. While it offers lower resolution than SEM, it is efficient for identifying broader morphological features across many samples without the need for complex preparation or specialised equipment.

The test area, aspect ratio, circularity (ratio between area and maximum ferret; **Equation 1**), roundness (ratio between perimeter and area; **Equation 2**) and lobulation (in this case, the degree of separation between chambers determined by the number of measurable areas between the test outline and smoothed outline, see **Figure 2.3f**) of the specimens were measured in Image-Pro Premier software, version 9.3.3 (Media Cybernetics, 2017; **Figure 2.3a-f**). This method has been shown to have an error of less than 5% (Brombacher *et al.*, 2017). The number of chambers in the final whorl was counted manually for each specimen. Scanning Electron Microscope (SEM) images of 2 hypotype specimens of *M. limbata* (Parker, 1973), in lieu of the lack of holotype specimens available for imaging, and 2 holotype specimens of *M. multicamerata* (Cushman and Jarvis, 1930) from the Miocene stored at the Smithsonian Museum of Natural History (see **Figure A.1**) were also measured in Image-Pro Premier following the same methodology to provide a reference point for size and shape of type specimens. Representative images of each final-whorl chamber number were taken on a VHX-700 Keyence Digital Microscope using a VHXE100 lens at 150 X magnification (**Figure 2.3**).

$$\text{Circularity} = \frac{4 \cdot Area}{\pi \cdot (MaxFeret)^2} \qquad \textbf{Equation 1}$$

$$\text{Roundness} = \frac{perimeter^2}{4\pi \cdot Area} \qquad \textbf{Equation 2}$$

For the final chamber analysis, the specimens were grouped by species and subdivided into groups based on the number of chambers in the final whorl, resulting in 9 groups in total. 15 specimens of each of these 9 groups were selected randomly, resulting in 135 specimens for analysis. The final chamber of each specimen was manually segmented and analysed for the

area (size) and aspect ratio (shape), much like the whole-test measurements in Image-Pro Premier (**Figure 2.3g-h**). Ten and 11 final-whorl chambered specimens of *M. multicamerata* were combined into one 10+ group, as there were insufficient numbers of 11 final-whorl chambered specimens for sufficiently powered statistical analyses. Using the area of the final chamber, the percentage size (% size) of the final chamber in relation to the whole test size was calculated. Kummerform chambers, where the final chamber(s) are much smaller and misshapen compared to the regular chambers of the foraminiferal test (Olsson, 1973), were present in 8 specimens. Typically, kummerform chambers are added just before death and often occur due to changes in ontogenetic growth, such as reducing buoyancy for increasing depth habitat while maintaining growth (Banerji, 1981), or environmental stress (Malmgren and Kennett, 1976). Although kummerform specimens have reached full adult size (Olsson, 1973), final chamber measurements in these specimens were taken on the penultimate chamber, with the area of the kummerform chamber subtracted from the whole test area measurement to reduce bias in the percentage size data.

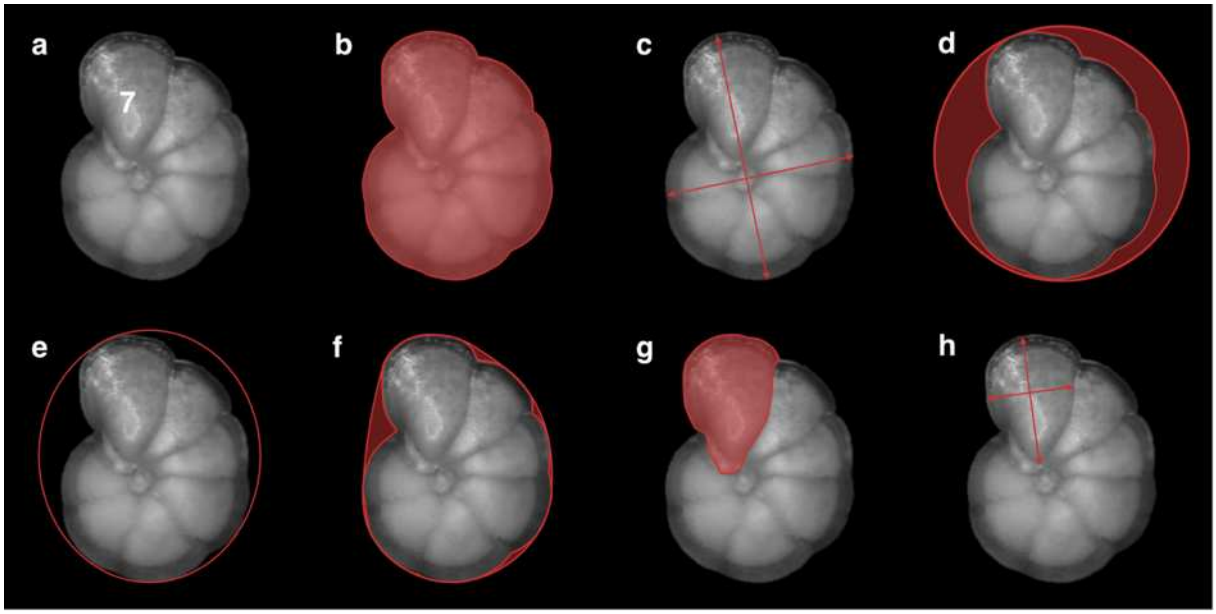

Figure 2.3 Analysed morphological traits on planktic foraminiferal whole tests **a-f)** and final chamber **g-h)**. Specimens were imaged umbilical side up. The final-whorl chamber number was counted manually **a)** and area **b)**, aspect ratio **c)**, circularity (determined by how close the shape is to a perfect circle, see **Equation 1**) **d)**, roundness (determined by how the test fits within an idealized circular shape, see **Equation 2**) **e)**, and lobulation (determined by the number of measurable areas between the test outline and smoothed outline) **f)** for the whole test and area **g)** and aspect ratio **h)** for the manually segmented final chamber were measured.err

2.2.2.2 Analysis

All calculations were performed in R version 4.3.2 (R Core Team, 2023) using the mclust package, version 6.0.0 (Scrucca *et al.*, 2016). We use a multivariate protocol to integrate the traits routinely used by stratigraphers and taxonomists to assign individuals to species, as

outlined in Ezard et al. (2010) and applied in Pearson & Ezard (2014). All eight measured traits were combined in a Principal Components Analysis (PCA) to identify a lower-dimensional space that defines enough of the observed variation across a smaller set of independent axes. Sufficiency is defined by established algorithmic stopping criteria to find a morphospace only containing axes that explain statistically significant amounts of variation (Peres-Neto, Jackson and Somers, 2005). Each dimension-reduced morphospace was then analysed using a Gaussian mixture model implemented in a Bayesian model-based methodology (Fraley and Raftery, 2002), which defines clusters by the volume, shape, and orientation of the data structure to test, for example, whether spherical clusters fit better than elliptical ones. Statistical support for all combinations of volumes, shapes, and orientations is assessed using a Bayesian (or Schwarz) Information Criterion, which is analogous to the more common Akaike Information Criterion (Burnham and Anderson, 2004) but with a different penalty for additional parameters (log(n) rather than 2 (Fraley and Raftery, 2002)). Both criteria provide a compromise between the variance explained and the number of parameters used.

2.3 Results

Gaussian Mixture Models of the dimension-reduced principal component morphospace indicate two distinct morphological groups (**Figure 2.4**) based on whole test traits. Area, aspect ratio and the number of final-whorl chambers are the major loadings onto PC1, which explains 30.2 % of the variation in the data, while circularity, roundness, and aspect ratio are the major loadings onto PC2, which explains 24.1 % of the variation. Age and lobulation are the major loadings onto PC3 and account for 14.9 % of the variance between the species. These PCAs suggest that shell size and aspect ratio, are driving the differences between the two morphological groups.

When identifying the species using the descriptions from Kennett and Srinivasan (1983), where differentiation predominantly relies on the number of chambers in the final whorl, there are 710 *Gr. (M.) limbata* and 290 *Gr. (M.) multicamerata* representatives, with no clear clustering (**Figure 2.5a**). Ambiguous 8-chambered specimens were identified based on the growth rate of chambers (**Table 2.1**) and, therefore, the final chamber size. The *non-priori* clustering via Gaussian Mixture Models, using only the whole test traits, suggests 246 *M. limbata* and 754 *M. multicamerata* representative morphotypes **Figure 2.5b**) with two clear clusters differentiated by size and shape. This switch in the number of each species is likely due to the high degree of similarity between the 2 species, with many specimens within the sample set that could be placed in either group. Species identification inclusive of final chamber trait data, based on the proposed suggested updates (see section **2.5 Species Descriptions**), splits the species evenly with 500 specimens each (**Figure 2.5c**). When not considering final chamber trait morphology,

this identification method creates greater morphological overlap between the two groups, making it difficult to identify between the two species based solely on whole chamber morphological traits.

The Gaussian Mixture Models PCA results for final chamber traits show 2 distinct morpho-groups (**Figure 2.6**). Final chamber circularity, aspect ratio and roundness are the major loadings onto PC1, which explains 65.3 % of the variation in the data. Area, with some influence from roundness, is the major loading onto PC2, which explains 19.4 % of the variation. Percentage size and roundness are the major loadings onto PC3 and account for 7.9 % of the variance between the species. These PCAs suggest that the final chamber shape is the main trait driving the differences between the two morphological groups.

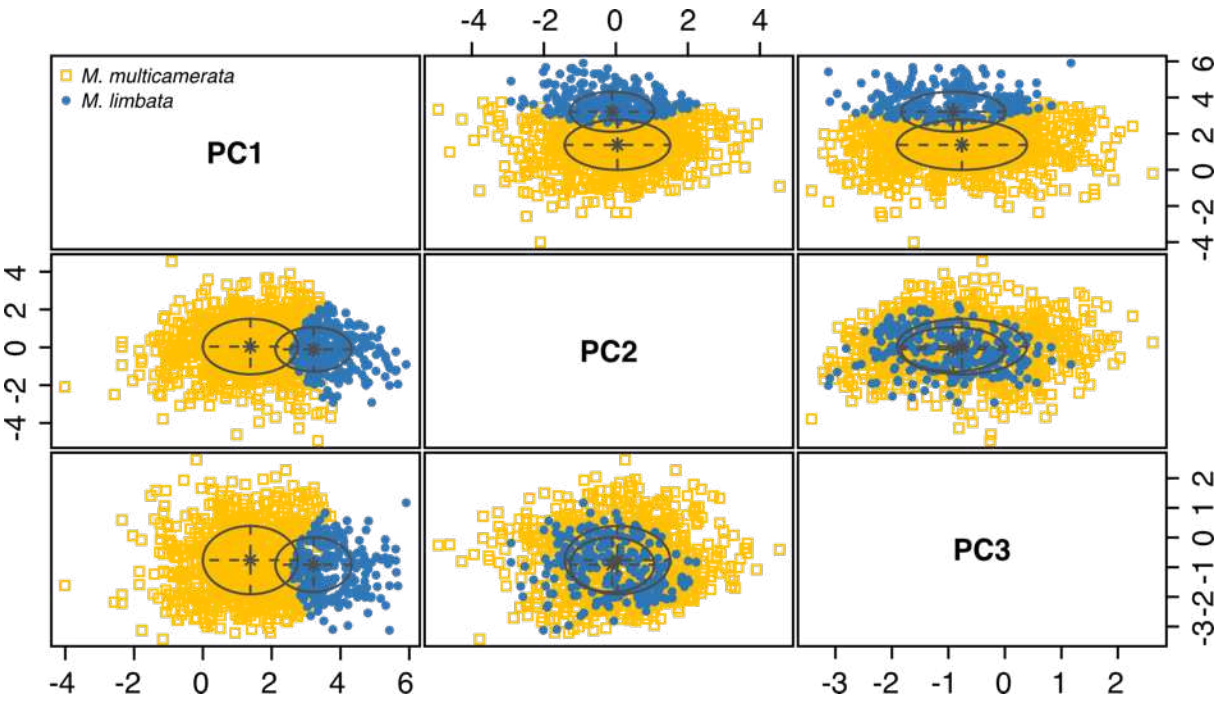

Figure 2.4 Principal component analysis (PCA) of whole test morphological measurements in *Menardella* specimens. The first 3 PCAs explain 69.2% of the variance. **PC1** = area (size), number of final-whorl chambers, aspect ratio, and explains 30.2 % of the variance. **PC2** = circularity, roundness, aspect ratio, and explains 24.1 % of the variance. **PC3** = age and lobulation and explains 14.9 % of the variance. Closed blue circles = *Menardella limbata* representatives and open yellow squares = *Menardella multicamerata* representatives.

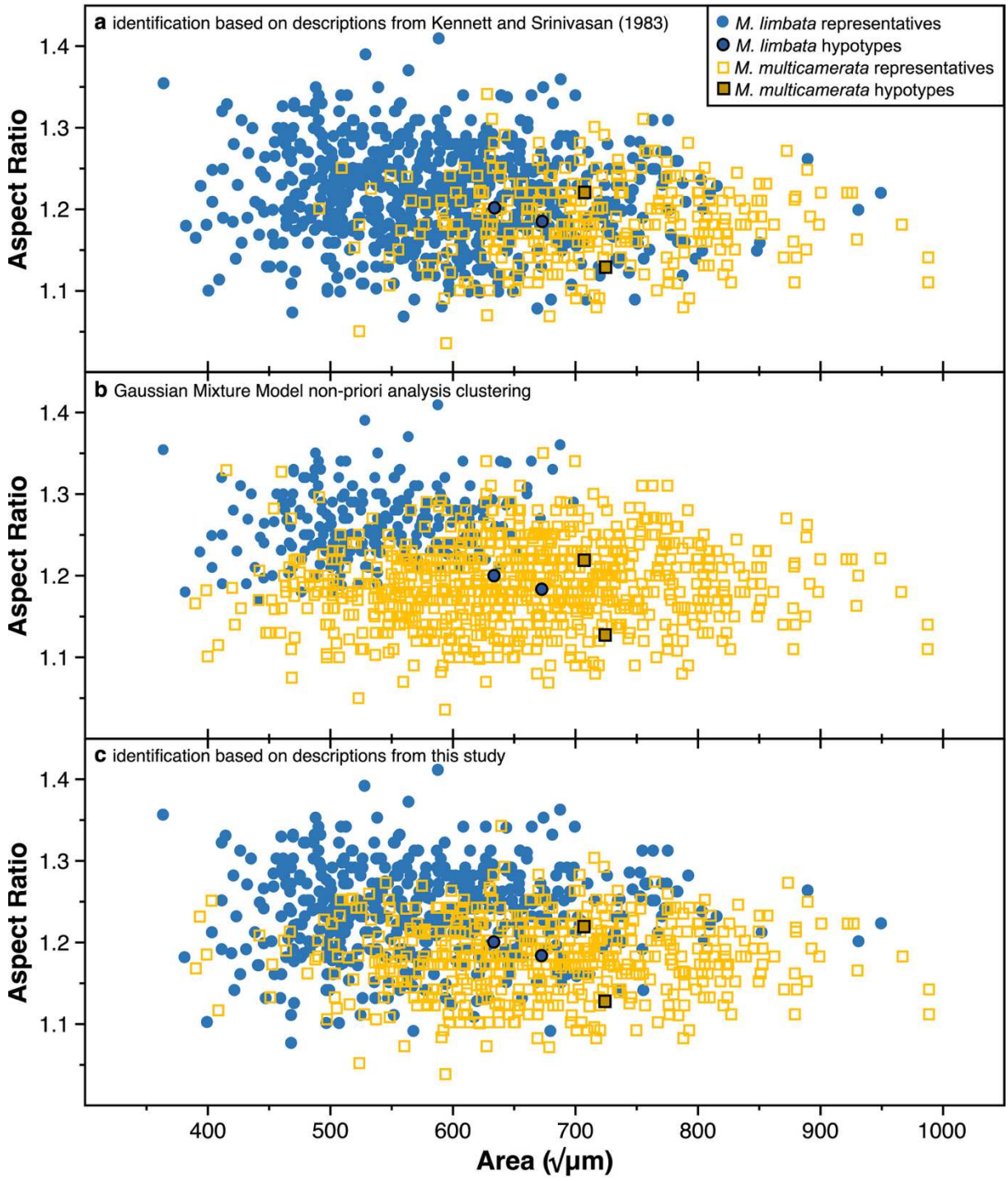

Figure 2.5 Whole test trait based species clusters at 3.101 and 3.402 Ma combined, distinguishing between *M. multicamerata* and *M. limbata* via **a)** Kennet and Srinivasan (1983) species descriptions, **b)** Gaussian Mixture Model analysis with non-priori clustering, and **c)** suggested updated descriptions from this study. Closed blue circles = *Menardella limbata* representatives and open yellow squares = *Menardella multicamerata* representatives. Solid blue circle with black outline = *Menardella multicamerata* holotypes, and solid yellow squares with black outline = *Menardella limbata* hypotypes.

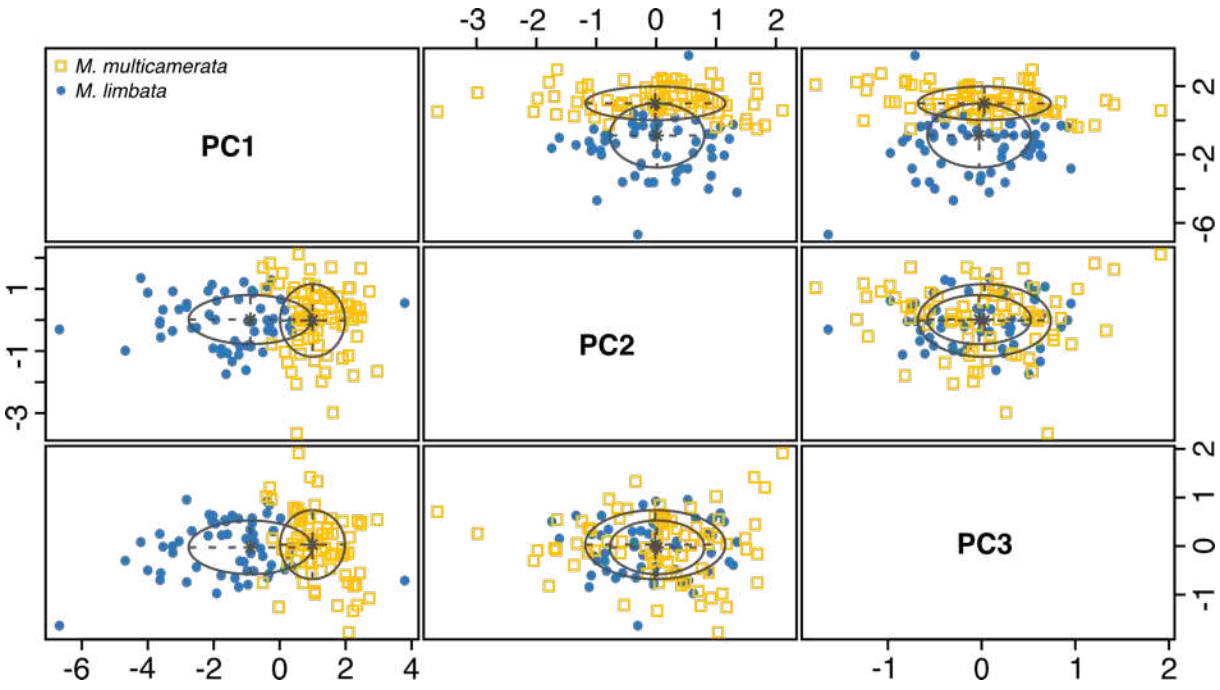

Figure 2.6 Principal component analysis (PCA) of final chamber +morphological measurements in *Globorotalia (Menardella)* specimens. The first 3 PCAs explain 92.6% of the variance. **PC1** = circularity, aspect ratio and roundness, and explains 60.3 % of the variance. **PC2** = area and roundness and explains 19.4 % of the variance. **PC3** = percentage size and roundness and explains 7.9 % of the variance. Closed blue circles = *Menardella limbata* representatives and open yellow squares = *Menardella multicamerata* representatives.

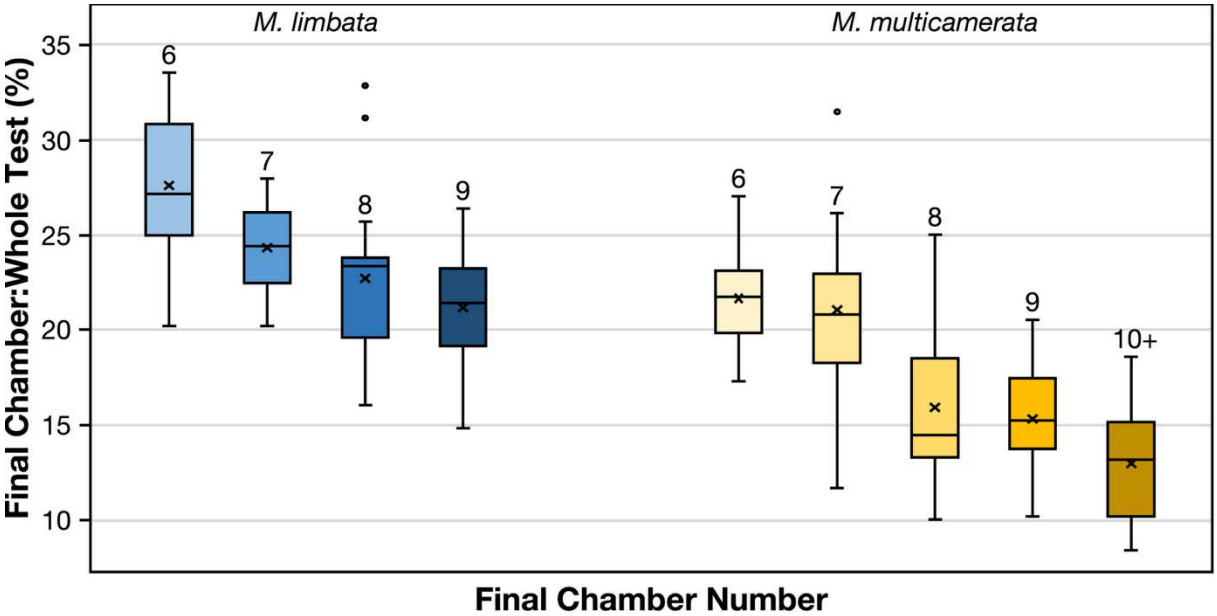

Figure 2.7 Final chamber size in relation (%) to the whole test size in *Menardella limbata* (light to dark blue) and *Menardella multicamerata* (light to dark yellow) across all final-whorl chamber numbers.

However, *M. limbata* has a larger final chamber compared to the whole test across all final-whorl chamber numbers (mean % size = 23.95% ± 0.04) than *M. multicamerata* (mean % size: 17.41% ± 0.05) (**Figure 2.7**). The aspect ratio of the final chamber of *M. limbata* (1.276 ± 0.15) is marginally lower than the final chamber aspect ratio of *M. multicamerata* (1.449 ± 0.24). The difference in the size, and consequently percentage area, and aspect ratio of the final chamber

between the two species translates to a larger, wider final chamber in *M. limbata*, which appears more lobate than a smaller, narrower, and more compact final chamber observed in *M. multicamerata*. The *non-priori* clustering via Gaussian Mixture Models, using only the final chamber traits, suggests 58 *M. limbata* and 77 *M. multicamerata* representative morphotypes (**Figure 2.8a**) with two clear clusters differentiated by size and aspect ratio. Manual identification based on the proposed suggested updates (see section **2.5 Species Descriptions**) splits the specimens into 60 *M. limbata* and 75 *M. multicamerata*, and while some specimens differ from the GMM predictions (**Figure 2.8b**), the groupings are more similar than the whole test trait-based data.

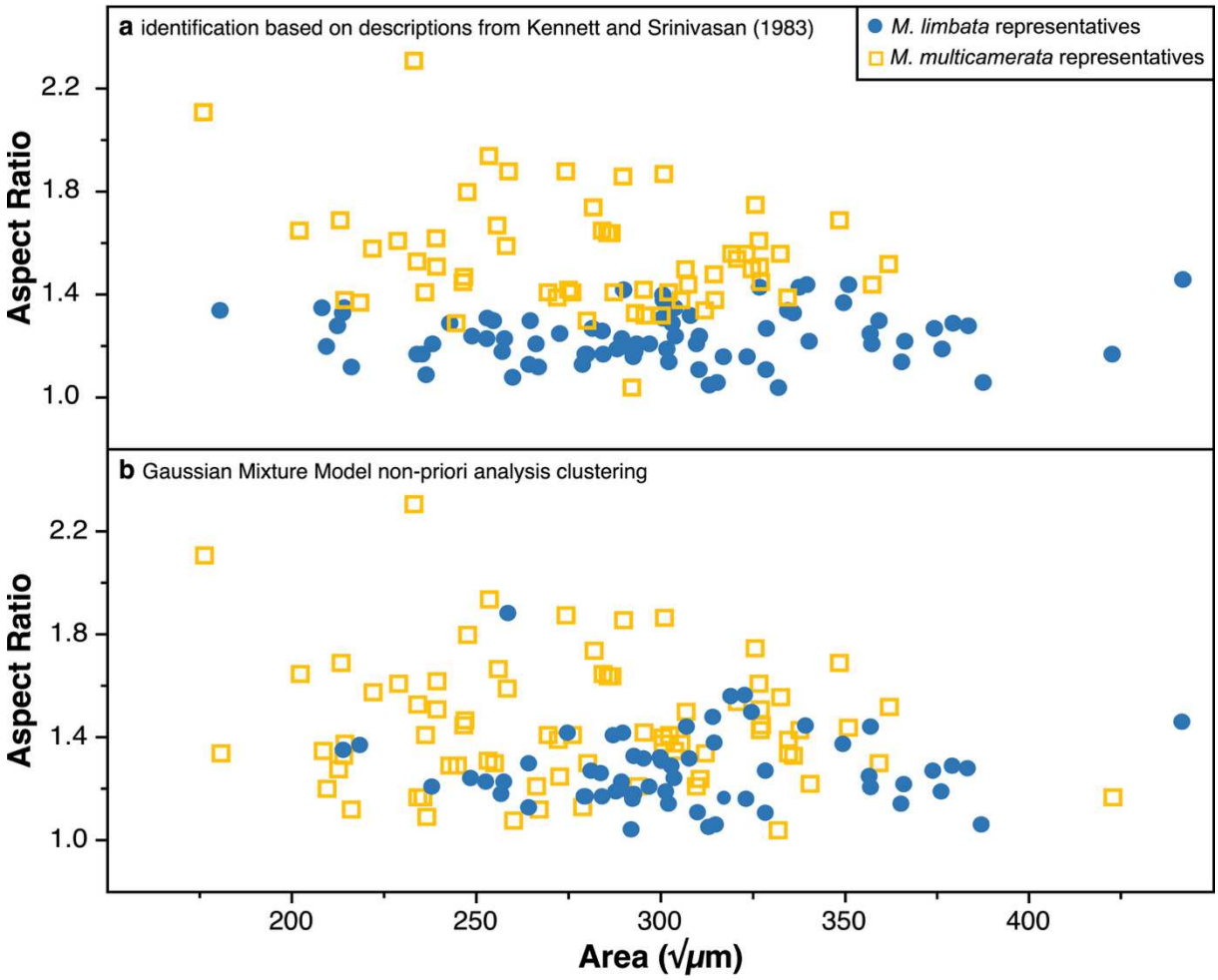

Figure 2.8 Final chamber trait-based species clusters at 3.101 and 3.402 Ma combined, distinguishing between *M. multicamerata* and *M. limbata* via **a)** Gaussian Mixture Model analysis with non-priori clustering and **b)** suggested update description from this study. Closed blue circles = *Menardella limbata* representatives and open yellow squares = *Menardella multicamerata* representatives.

The differences between the species final chamber and the whole test traits are consistent through time from 3.4 to 3.1 Ma. However, from 3.4 to 3.1 Ma, the average size of both *M. limbata* (569.98, *s.e.* = 77.65, 95% CI = 0.41 and 594.78, *s.e.* = 105.52, 95 % CI = 0.42, respectively) and *M. multicamerata* (633.36, *s.e.* = 91.55, 95% CI = 0.36 and 671.36, *s.e.* = 103.19, 95 % CI = 0.39, respectively) increases, with increased variability in size in both (**Figure**

A.2, Table A.1). Additionally, from 3.4 to 3.1 Ma, the number of chambers in the final whorl decreases in specimens with 6 chambers in *M. limbata* and *M. multicamerata* (loss of 38 % and 2% respectively) and specimens with 7 chambers in *M. multicamerata* (37 % loss), subsequentially with an increase in 7+ chambered *M. limbata*, 8+ chambered *M. multicamerata* specimens (**Figure A.3**).

2.4 Discussion

The results of our study highlight the significant morphological overlap and challenges associated with the traditional qualitative taxonomy of *Menardella* species *M. limbata* and *M. multicamerata*. Traditional methods, relying heavily on qualitative descriptions of test size and shape and the number of chambers in the final whorl, prove insufficient for reliable species differentiation. Our approach, utilizing quantitative morphometric analysis and Gaussian Mixture Models, provides a more objective and statistically robust method for species identification, revealing clearer distinctions between these two closely related species. Our findings corroborate previous studies that have reported substantial overlap in these traits (Mary, 2013; Knappertsbusch, 2016), rendering reliance on such traits insufficient for species separation. The application of quantitative morphometric analysis in this study has identified statistically significant differences between *M. limbata* and *M. multicamerata*.

As with all fossil approaches, the approach assumes that different biological species are morphologically distinct. While molecular studies are valuable for defining extant species of planktic foraminifera (Darling *et al.*, 1996; Morard *et al.*, 2024), this method cannot be applied to extinct species (Darling and Wade, 2008) because molecular techniques that rely on DNA and/or other molecular markers cannot be used on fossils where such materials are no longer preserved. We acknowledge that discrimination of closely similar taxa may be problematic, and any morphologically invisible ‘‘cryptic’’ speciation may have occurred. Genetic studies of modern planktic foraminifera (e.g., Huber et al., 1997; De Vargas et al., 1999; Darling and Wade, 2008) suggest that cryptic genotypes are abundant in the modern ocean, although this is not true of all morphospecies (André *et al.*, 2014). Importantly, cryptic genetic variation has thus far been confined within more inclusive morphological definitions (Brummer and Kučera, 2022; Morard *et al.*, 2024). Hence, morphological differences are indicative of some degree of taxonomic differentiation in planktic foraminifera.

The conventional taxonomic criteria used to differentiate *M. limbata* and *M. multicamerata*, as outlined in the Phylogenetic Atlas of Neogene planktic foraminifera (Kennett and Srinivasan, 1983), demonstrate considerable overlap between the two species. Characteristics such as test size and shape are subject to considerable variation and are influenced by multiple factors,

including ontogenetic stage, environmental conditions and evolutionary trends (De Villiers, 2004; Schmidt, Thierstein and Bollmann, 2004; Schmidt, Vautravers and Spero, 2006; Kucera, 2007; Lombard *et al.*, 2009; Todd *et al.*, 2020; Brombacher *et al.*, 2022), which compromise their reliability as diagnostic traits. For example, while both species increase in size from 3.4 to 3.1 Ma, with an increase in size variation in the younger specimens, and *M. multicamerata* is consistently larger than *M. limbata* through time, *M. multicamerata* has a greater increase in size, and variation, than *M. limbata* (**Figure A.2, Table A.1**). These changes in size over time suggest that it is an inconsistent trait for species delimitation and that it might be more effective for distinguishing between the two species in younger samples (e.g., Knappertsbusch, 2007) and may not be a reliable diagnostic feature for identifying species throughout their appearance in the fossil record. Furthermore, the number of chambers in the final whorl increases over time (**Figure A.3**). This shift to a greater number of final-whorl chamber numbers further away from the speciation further demonstrates the unreliability of using this feature as a diagnostic for identifying species.

The morphological variability within planktic foraminifera can complicate the reliability of holotypes, limiting their utility in precisely defining species and understanding evolutionary relationships. Despite being Miocene of age, the type specimens of *M. limbata* (hypotypes) and *M. multicamerata* (holotypes) plot within their species ranges based on both the current species descriptions (**Figure 2.5a**) and the suggested updated descriptions (**Figure 2.5c**). However, all specimens have 7 chambers in the final whorl, which further supports the inclusion of *M. multicamerata* having less than 8 chambers in the final whorl in the species descriptions. While planktic foraminiferal holotypes are designated as the type for describing a new species, they are often unreliable as a reference for identifying specimens for several reasons. First, they represent only one individual, which may not capture the full range of morphological variability within the species, as demonstrated in this study (**Figure 2.2**; **Figure 2.5**). This can lead to misidentifications or overemphasis on traits that are not consistent across the population (Scott, 2011). Additionally, holotypes are sometimes poorly preserved or inadequately documented, making it difficult to compare them accurately with other specimens, as is the case for *M. limbata* with no image of the specimen holotype and the lectotype is a drawing of a broken specimen (Banner and Blow, 1960).

While the PCAs give two distinct morphotypes (**Figure 2.4**), we still see a large overlap between the species when considering the updated descriptions based solely on whole test measurements (**Figure 2.5c**). This includes an increasing overlap of final-whorl chamber number, with *M. limbata* having 6-9 chambers (previously 6-8) and *M. multicamerata* having 6-11+ (previously 8-10) chambers in the final whorl. However, the size (area) and shape (aspect ratio) of the final chamber are critical metrics for distinguishing these species (**Figure 2.6**).

Specifically, *M. limbata* exhibits a larger and more lobate final chamber than *M. multicamerata*, which has a smaller and more compact final chamber. Yet, *M. multicamerata* has higher lobulation overall (mean = 3.31, *s.e* = 1.39, 95% confidence interval = 0.12) than *M. limbata* (mean = 2.36, *s.e* = 1.19, 95% confidence interval = 0.10). This differentiation in lobulation is seemingly due to the greater degree of curvature of the spiral sutures, especially in the final chambers, in *M. multicamerata* than in *M. limbata,* which appears to have "strongly-curved" rather than "recurved" sutures (see Figure 6.3: Stewart, 2003) as suggested in the current description (Kennett and Srinivasan, 1983). This observation of stronger recurved spiral sutures in *M. multicamerata*, which may result from increased chamber number in the final whorl, presents as the distinct and often more "angular" shape frequently observed in the final chambers of the species (see **Figure 2.2**).

Regardless of speculative observations, the measurable final-chamber quantitative traits are consistent and reproducible, providing a more reliable basis for species identification than traditional qualitative descriptors. With the final chamber becoming the pivotal diagnostic feature, it is important to note that the occurrence of kummerform chambers is not factored into the analysis, with measurements being taken on the penultimate chamber of specimens with kummerform chambers (see section **2.2.2**).

Given the results, there are important implications for biostratigraphy when using *M. multicamerata* as a bioevent marker (Wade *et al.*, 2011). The updated species descriptions, incorporating quantitative morphometric analysis, enhance differentiation but still reveal significant morphological overlap. This suggests that bioevent markers based solely on qualitative traits may introduce uncertainty in biostratigraphic correlations. However, the refined morphometric approach mitigates some of this uncertainty by providing a more objective and statistically supported method for species identification, ultimately strengthening confidence in bioevent placement. Importantly, these updates do not alter the speciation or extinction dates for either species.

The distinction between *M. limbata* and *M. multicamerata* is most reliable in younger samples (e.g., ~3.1 Ma), where *M. multicamerata* is significantly larger (**Figure A.2**). Differentiation is most challenging near their speciation event, where morphological overlap is greatest (see pilot study, Appendix…), and towards their extinction, as both species converge in size (**Figure A.2**). However, the shape and size of the final chamber remain relatively stable diagnostic traits over time, aiding in species distinction despite broader test-size variability.

From a palaeoceanographic perspective, distinguishing these taxa is less critical, as their ecological preferences and functional roles, although poorly constrained, are thought to be largely similar (Mary and Knappertsbusch, 2013). Nonetheless, improving species classification

enhances the accuracy of biostratigraphic frameworks, which are essential for refining geological timelines and paleoenvironmental reconstructions. While the quantitative approach significantly improves species differentiation, challenges remain, particularly in the earliest and latest phases of their stratigraphic range. Yet, the refined classification outlined below reduces error and increases confidence in species identification.

2.5 Species Descriptions

The purpose of this study is not to define new species but re-define and update the current species descriptions in accordance with the quantitative morphological data presented. As such, we suggest the following, with the original genus descriptions from Kennett and Srinivasan (1983) and species description updates following this study:

Order Foraminiferida d'Orbigny, 1826

Superfamily Globigerinidae Carpenter, Parker and Jones, 1862

Family Globigerinidae Carpenter, Parker and Jones, 1862

Genus Globorotalia

Synonyms: *Globorotalia (Menardella)* (Bandy, 1972); *Menardella* (Bandy, 1972)

Type species: *Pulvinulina menardii* (Parker, Jones, and Brady, 1865)

Type of wall: Non-spinose, smooth (Kennett and Srinivasan, 1983; Aze *et al.*, 2011)

Test morphology. Characterised by compressed, lenticular, trochospiral tests, with a prominent keel and smooth, densely perforate surfaces (after Kennett and Srinivasan, 1983, p.120).

Remarks. The subgenus *Menardella*, proposed by Bandy (1972) for the Globorotalia *praescitula-archeomenardii-praemenardii-menardii* evolutionary lineage, remains an important element of Late Neogene planktic foraminiferal assemblages of tropical to warm-subtropical waters. The subgenus *Globorotalia*, which includes the *Globorotalia lenguaensis-plesiotumida-tumida* lineage, has many characteristics in common with *Menardella*, but they are phylogenetically unrelated.

Although *Globorotalia praescitula* originally evolved in the temperate areas, it subsequently migrated to the tropics and gave rise to *Menardella* during the late Early Miocene. Although the earliest representative of *Menardella archeomenardii* first appeared within Early Miocene Zone N8, the lineage did not become dominant among the tropical globorotaliids until the extinction of *Fohsella* at 12.4 Ma. Members of *Menardella* during the Pliocene and Quaternary exhibit a

wide range of variation, especially with respect to the strength of the keel, the number of chambers in the final whorl, coiling mode, and bending of the final chamber (after Kennett and Srinivasan, 1983, p.120).

Range. Early Miocene Zone N8 to present [extant] (Kennett and Srinivasan, 1983).

Menardella limbata (d'Orbigny in Fornasini, 1902)

Figure 2.2b, d, f, h

Basionym. *Rotalia limbata* (Cushman and Jarvis, 1930)

Synonyms. Rotalia limbata (d'Orbigny 1826); Globorotalia (Menardella) limbata (Fornasini 1902)

Test morphology. Test medium-large, compressed/lenticular, biconvex, low trochospiral, medium lobulation of periphery, axial periphery acute with prominent keel. Chambers on umbilical side slightly more highly vaulted and inflated than on spiral side. Six to nine chambers in the final whorl, slowly increasing in size as added, with a large lobate final chamber. Sutures on spiral side are strongly-curved to recurved, limbate and thickened where merging into the keel. Sutures on umbilical side are sinuous to radial and depressed. The surface is smooth and densely perforate, sometimes pustulous near umbilicus. The umbilicus is a narrow to circular pit and the aperture is interiomarginal, umbilical-extraumbilical, and a low-arched slit with a lip (after Aze et al., 2011; Kennett and Srinivasan, 1983).

Size. Hypotype maximum diameter 780 µm.

Remarks. *Gr. (M.) limbata* evolved from *Gr. (M.) menardii* and is the ancestor of *Gr. (M.) multicamerata*. Like *Gr. (M.) menardii* but distinguished by the uniformly increasing chambers in the final whorl and spiral sutures, which are nearly straight for most of their length but become sharply curved near the periphery, giving a hockey-stick shape (Blow, 1969) (after Kennett and Srinivasan, 1983).

Range. Middle Miocene Zone N14 to Late Pliocene Zone N21. Tropical to warm subtropical (Kennett and Srinivasan, 1983).

Menardella multicamerata (Cushman and Jarvis, 1930)

Figure 2.2a, c, e, i, j

Basionym. *Globorotalia menardii var*. *multicamerata* (Cushman and Jarvis, 1930)

Synonyms. *Globorotalia (Menardella) multicamerata* (Cushman and Jarvis, 1930)

Test morphology. Test medium-large, compressed/lenticular, biconvex, low trochospiral, lobulation of periphery, axial periphery acute with prominent keel. Chambers on umbilical side slightly more highly vaulted and inflated than on spiral side. Six to twelve chambers in the final whorl, very slowly increasing in size as added, with a compact and often angular final chamber. Sutures on spiral side are recurved, limbate and thickened where merging into the keel. Sutures on umbilical side are sinuous to radial and depressed. The surface is smooth and densely perforate, often pustulous near umbilicus. The umbilicus is a sub-circular to circular pit and the aperture is interiomarginal, umbilical-extraumbilical, and a low-arched slit with a lip (after Aze et al., 2011; Kennett and Srinivasan, 1983).

Size. Holotype maximum diameter 890 µm.

Remarks. Like *Gr. (M.) limbata* but differs by an increased number of final-whorl chambers overall (usually six to twelve), more circular outline of the test, and by its small and narrow, often angular, final chambers. A continuous morphological intergradation exists between typical *Gr. (M.) limbata* and *Gr. (M.) multicamerata*, and the distinction between these species is somewhat difficult to recognise, especially in Late Miocene Zone N17B. The evolution of *Gr. (M.) multicamerata* from *Gr. (M.) limbata* is a useful biostratigraphic datum within Zone N17 (after Kennett and Srinivasan, 1983).

Range. Late Miocene Zone N17B to Late Pliocene Zone N21. Tropical to warm subtropical.

2.6 Conclusion

The main findings of this study are that *Menardella (M.) multicamerata* differs from *Menardella (M.) limbata* by having a lower aspect ratio and higher lobulation. The final chamber in *M. multicamerata* is smaller, more compact and often more angular than the larger, lobate, final chamber of *M. limbata*. Contrary to previous species descriptions, the size, sutures, and umbilical shape are not distinguishing features. This study underscores the limitations of traditional qualitative taxonomic methods and demonstrates the efficacy of quantitative morphometric analysis in resolving species distinctions within the *Menardella* lineage. By providing clear, statistically supported criteria for differentiating *M. limbata* and *M. multicamerata*, our findings pave the way for more accurate and reliable species identification in paleontological and biostratigraphic research. Accurate species identification is crucial for reconstructing past oceanographic conditions and correlating sedimentary sequences across different geographic regions. This, in turn, can enhance our understanding of past climate changes and the evolutionary dynamics of planktic foraminifera through more accurate palaeoceanographic reconstructions and refined biostratigraphic frameworks.

Chapter 3 Extinction unravels climate controls on community composition

Abstract

The interplay between biotic and abiotic forces regulates long-term ecological dynamics. Over the longest time scales, extinctions have been linked more strongly to climate perturbations but obtaining sufficient data to explore biotic dynamics spanning populations, species, and communities is challenging. Replicating randomised sampling protocols across 19 species' extinctions during the Plio-Pleistocene, we use the exceptionally resolved fossil record of planktonic foraminifera to show the loss of climate controls on community structure spanning pre-, imminent- and post-extinction phases. The positive correlations between global temperature and species richness, community evenness and dominance unwind through the imminent-extinction phase. There is no detectable correlation in the post-extinction phase as the community adjusts to the loss of one of its constituents, but the positive correlations re-emerge before the next extinction. The unprecedented resolution of our results fills a key gap in how ecological dynamics span species to communities in the presence of ongoing extinctions.

3.1 Introduction

Biodiversity regulates many ecosystem processes and provides goods and services essential for humanity (Cardinale *et al.*, 2012). Environmental change, which includes temperature, carbon dioxide (CO_2) levels, salinity, and ocean circulation, is known to impact global biodiversity (Condamine, Rolland and Morlon, 2013). With rapid environmental changes predicted by the Intergovernmental Panel on Climate Change (IPCC) for the next 30-80 years (IPCC, 2021; **Figure 1.1**), environmental changes are expected to further negatively impact current biodiversity loss through increasing rates of extinction (Urban, 2015). Biodiversity has the potential to buffer itself against abiotic impacts through the functional diversity of ecosystems, but identifying how this resilience is achieved is non-trivial.

Different diversity measures capture various aspects of biodiversity, providing key insights into the structure, functioning, and health of ecosystems. For example, high species richness (**Figure 3.1a**), one of the most basic indicators of biodiversity, allows for community stability due to differential species' responses and tolerances to environmental changes (Ives, Klug and Gross, 2000; Loreau *et al.*, 2001). Likewise, the evenness of an assemblage (a measure of how equally individuals are distributed among species in a community, where the abundance of individuals in proportion to their frequency; **Figure 3.1a**) is indicative of community stability: high evenness is often associated with greater resilience to environmental changes because the ecosystem is not overly reliant on a particular species (Cusson *et al.*, 2015). Conversely, high dominance (a measure of the degree to which one or a few species exert control over a community, where the frequency of abundant species is considered and rare species are discounted; **Figure 3.1a**) can lead to a reduction in overall biodiversity, as other species may be suppressed or excluded (Cusson *et al.*, 2015). While common taxa are generally easily detectable and can be informative of diversity drivers as influential components of ecosystems (Lennon *et al.*, 2004; Gaston, 2008; Hannisdal *et al.*, 2017), less is known about the functional role of the rare species in ecosystems (Lyons *et al.*, 2005) that could act as "ecosystem canaries" in providing early warning signals of ecosystem collapse (Doncaster *et al.*, 2016). Since biodiversity is not univariate and encompasses genetic diversity, species interactions, ecosystem processes, and functional roles that contribute to ecosystem stability and resilience, broad representations of community composition are beneficial for predicting how assemblages will respond to environmental change.

The most complete documentation of extinction comes from the fossil record, which provides a long-term perspective on biodiversity changes across geological time scales. The study of extinction requires a paleontological approach because investigations restricted to extant species struggle to distinguish between multiple competing hypotheses for how the interplay

between biotic and abiotic variation shapes diversity dynamics (Quental and Marshall, 2010; Louca and Pennell, 2020). While mass extinctions are important for studying macroevolutionary trends (Jablonski, 2005), the majority of extinctions in marine organisms occur during intervals of "background" extinction rates (Harnik *et al.*, 2012; Lowery *et al.*, 2020). Background extinctions are useful when studying different past scenarios of climate-driven extinction, as background extinctions can provide insights into natural fluctuations in biodiversity over time.

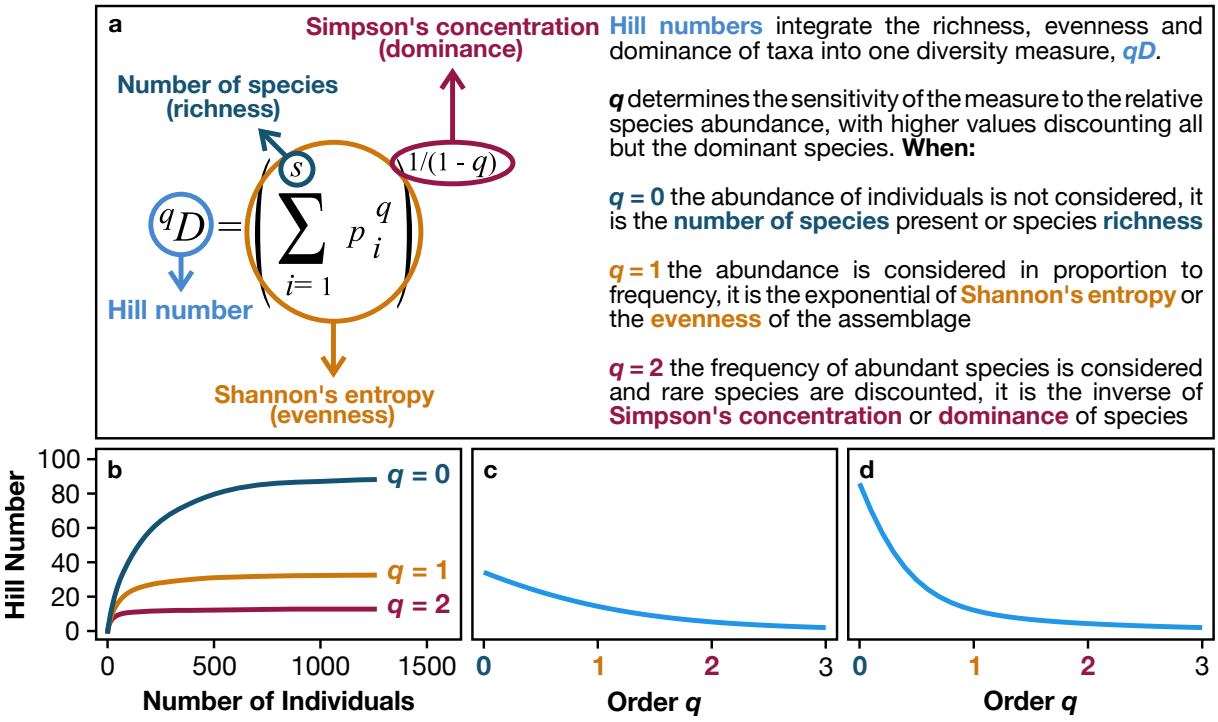

Figure 3.1 **a)** Schematic explanation of Hill numbers, including equation (Chao *et al.*, 2014) **b)** sample-sized based diversity accumulation curves; **c)** example of an even assemblage diversity curve; **d)** example of an uneven assemblage diversity curve.

Planktic foraminifera represent a model paleontological system for understanding biodiversity due to their high abundance across a large timespan, as well as their wide biogeographical cover and good taxonomic resolution (Aze *et al.*, 2011; Yasuhara *et al.*, 2017; Fenton *et al.*, 2023; Swain *et al.*, 2024). Using the exceptional fossil record of planktic foraminifera from the last 5 million years (Myr), we can explore the effects of individual extinctions on community dynamics. Contemporary planktic foraminiferal species richness generally decreases from the tropics to the poles, peaking at the mid-latitudes (Rutherford, D'Hondt and Prell, 1999; Fenton *et al.*, 2016). It is suggested that sea surface temperature, linked to the strength of ocean stratification, is the strongest predictor of large-scale diversity changes (Rutherford, D'Hondt and Prell, 1999; Fenton *et al.*, 2016) and the steady decline in foraminiferal diversity over the last 5 Myr (Aze et al., 2011; Ezard et al., 2011; **Figure 1.2**). Many individual background extinctions have also been linked to temporal climate fluctuations (Banerjee and Boyajian, 1997; Abramovich *et al.*, 2010; Peters, Kelly and Fraass, 2013; Fraass, Kelly and Peters, 2015;

Weinkauf *et al.*, 2019). While changes in oxygen isotope ($\delta^{18}O$) levels, indicative of temperature, are an important predictor of extinction in the context of standing biological diversity (Fraass, Kelly and Peters, 2015; Woodhouse *et al.*, 2023), far less is known about how community composition co-occurrences influence these extinctions.

Hill numbers (Hill, 1973), or "the effective number of species" (Chao *et al.*, 2014), are used to characterise either the taxonomic, phylogenetic, or functional diversity of an assemblage (Chao *et al.*, 2014) by integrating richness, evenness and dominance of taxa (Hill, 1973), and are ideal for extracting biologically meaningful signals from species assemblage counts (**Figure 3.1a**). Hill numbers require adequate sample sizes (**Figure 3.1b**) to be useful. Therefore, using abundant foraminiferal fossil assemblages to plot Hill number profiles of assemblage counts across extinction events allows a more in-depth, comparative look at complex communities with a high degree of diversity and interdependence among species (Yasuhara *et al.*, 2020; Kearns *et al.*, 2021).

Here, we apply Hill numbers to fossil planktic foraminifera communities undergoing repeated extinctions to provide a comprehensive way of representing community composition and then measuring if community dynamics change as the constituent species go extinct. We use oxygen isotopes ($\delta^{18}O$) from benthic foraminifera as a paleoclimate proxy, representative of temperature, salinity, and ice levels (Lisiecki and Raymo, 2005). $\delta^{18}O$ describes the ratio of ^{18}O to ^{16}O in a sample, with a higher $\delta^{18}O$ indicative of lower temperatures and more continental ice, thus glacial conditions, due to greater evaporation of the lighter ^{16}O, and vice versa (Lea, 2014).

3.2 Materials and Methods

3.2.1 Materials

1,123 samples from Ocean Drilling Program (ODP) Site 925, located on the Ceara Rise in the Equatorial Atlantic, were used for this study (**Figure 1.3**). Samples are from Holes 925B (4°12.248'N, 43°29.349'W, water depth: 3041.1 meters below sea level (mbsl)), 925C (4°12.256'N, 43°29.349'W, water depth: 3040.6 mbsl) and 925D (4°12.260'N, 43°29.363'W, water depth: 3040.5 mbsl) (Shipboard Scientific Party, 1995). This site and samples were selected due to the diverse planktic foraminifera species content and an accurate age model (Wilkens *et al.*, 2017) to create a more precise record of species extinctions and assemblage changes. The age model for Site 925 (Wilkens *et al.*, 2017) is tuned to the Lisiecki and Raymo (2005) LR04 stack (high-resolution benthic $\delta^{18}O$ compilation). All samples are within the range of 0.5 to 5.1 million years ago (Ma), with a temporal resolution between samples of ~4 thousand years (kyr) (min = 0.246, max = 90.000, median = 3.612).

Oxygen isotope ($\delta^{18}O$) data as a representative environmental record (glacial vs interglacial) were taken from the Lisiecki and Raymo (2005) LR04 stack, and each sample was mapped to the nearest environmental reconstruction (maximum offset = 2.3 kyr, i.e. less than the sample resolution).

3.2.2 Methods

3.2.2.1 Extinction dates

28 individual species extinctions were identified at Site 925 within this study's time frame (Chaisson and Pearson, 1997) and were used to assess the extinction events (i.e., before, during and after the extinction). 19 species extinctions were selected for this study due to the availability of specimens within the sample, meaning the species were abundant or taxonomically distinct enough prior to the extinction for the extinction to be detected within the samples. Extinction dates from both the shipboard observations (Chaisson and Pearson, 1997) and global (Aze *et al.*, 2011) records were used to predict the last occurrence (LO) of 19 species from Site 925 samples (**Table B.1**). For each of the species' extinctions, the samples around the predicted extinction dates were split to ~1000 specimens and manually checked for the extinct-going species. The final specimen of the extinct-going species defines the LO within Site 925 in this study, with the lack of specimens within the subsequent 20 samples suggesting local extinction.

Recognising whether a species' disappearance at Site 925 reflects local or global extinction is essential for interpreting the broader significance of these extinction events. Global extinction, which occurs when a species disappears entirely from the fossil record and no longer exists anywhere on Earth, is significant for understanding broad-scale biodiversity crises, such as mass extinctions (Jablonski, 2005). In contrast, local extinction (extirpation) happens when a species disappears from a specific region but may persist elsewhere, driven by environmental changes, oceanographic shifts, or migration rather than true species extinction (Woodruff, 2001; Yasuhara *et al.*, 2009). Since this study focuses on the impacts of paleoenvironmental change within a single ecosystem across time, identifying extirpation patterns remains crucial for reconstructing past oceanographic conditions and ecological dynamics.

The ecogroups and morphogroups of the 19 extinct-going species are assigned according to Aze et al. (2011; **Table B.1**). The ecogroups in this study include ecogroup 1 (open ocean mixed layer tropical/subtropical, with symbionts), ecogroup 2 (open ocean thermocline), and ecogroup 4 (open ocean sub-thermocline). The morphogroups in this study include morphogroup 3 (spinose, globular with supplementary apertures), morphogroup 7 (non-spinose, globular),

morphogroup 14 (non-spinose, globorotaliform, keeled), and morphogroup 16 (non-spinose, globorotaliform, non-keeled).

The LO dates in this study follow the Site 925 age model (Wilkens *et al.*, 2017) and are referenced with the $\delta^{18}O$ LR04 stack (Lisiecki and Raymo, 2005) to see when each extinction occurred in relation to glacial-interglacial cycles (**Figure 3.2**).

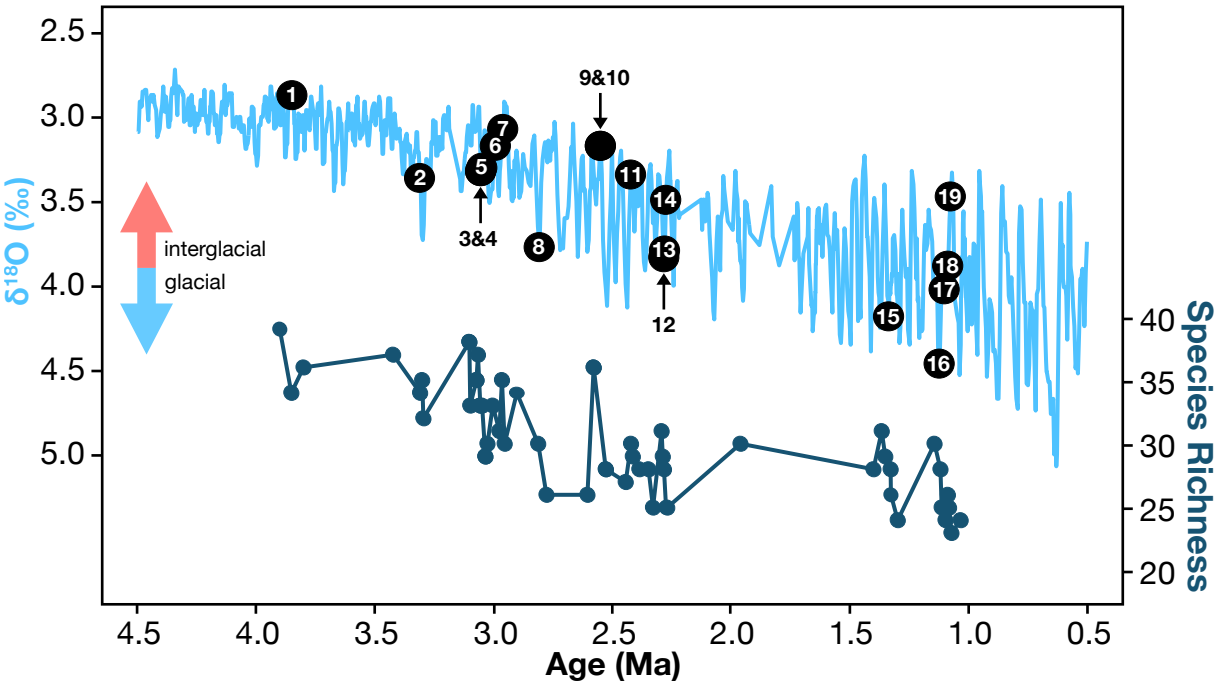

Figure 3.2 Extinction dates (Site 925 last occurrences for each species, dark numbered circles), LR04 benthic foraminifera oxygen isotope compilation $\delta^{18}O$ (‰) (Lisiecki and Raymo, 2005) (where higher values of $\delta^{18}O$ mean lower temperatures and more continental ice, and vice versa (blue line)), and the number of species (dark blue line) through time (millions of years ago (Ma)) according to the Wilkens et al. (2017) age model. Species: **1)** *Hirsutella margaritae*, **2)** *Sphaeroidinella kochi*, **3)** *Dentoglobigerina baroemoenensis*, **4)** *Dentoglobigerina venezuelana*, **5)** *Dentoglobigerina altispira*, **6)** *Sphaeroidinellopsis seminulina*, **7)** *Sphaeroidinellopsis paenedehiscens*, **8)** *Hirsutella cibaoensis*, **9)** *Menardella limbata*, **10)** *Menardella multicamerata*, **11)** *Globoconella puncticulata*, **12)** *Menardella miocenica*, **13)** *Menardella pertenuis*, **14)** *Menardella exilis*, **15)** *Globigerinoidesella fistulosa*, **16)** *Neogloboquadrina humerosa*, **17)** *Neogloboquadrina acostaensis*, **18)** *Globigerinoides extremus*, **19)** *Globigerinoides obliquus*.

Preliminary counts of the species facing extinction were taken during this process (see https://doi.org/10.5258/SOTON/D3228). The LO date and preliminary counts of each species were then used to choose 3 samples for assemblage counts: one sample where the species were abundant (pre-extinction), one sample where the species were in decline before the LO sample (imminent extinction) and the third sample as soon as feasible after the last occurrence of the species (post-extinction) (**Figure 3.3**). These three markers define the extinction event for each species in this study. Assemblage counts were conducted for these 3 extinction markers across the 19 selected individual species extinctions at Site 925, following the sampling method

outlined in **3.2.2.2**, giving the species richness. The pre-extinction sample was determined to be when abundance was "high" for the given species; the imminent-extinction samples were within 30.01 kyr before the sample with the last occurrence (LO) of the extinct-going species, and the post-extinction samples were within 44.90 kyr of the LO sample (**Figure 3.3**; **Table C.1**; see Error! Reference source not found.). *D. baroemoenensis* and *D. venezuelana* share an extinction date and thus share pre-, imminent-, and post-extinction samples for assemblage measurements, as do *M. limbata* and *M. multicamerata* (**Table B.1**), resulting in 17 unique extinction events and 51 samples for assemblage counts.

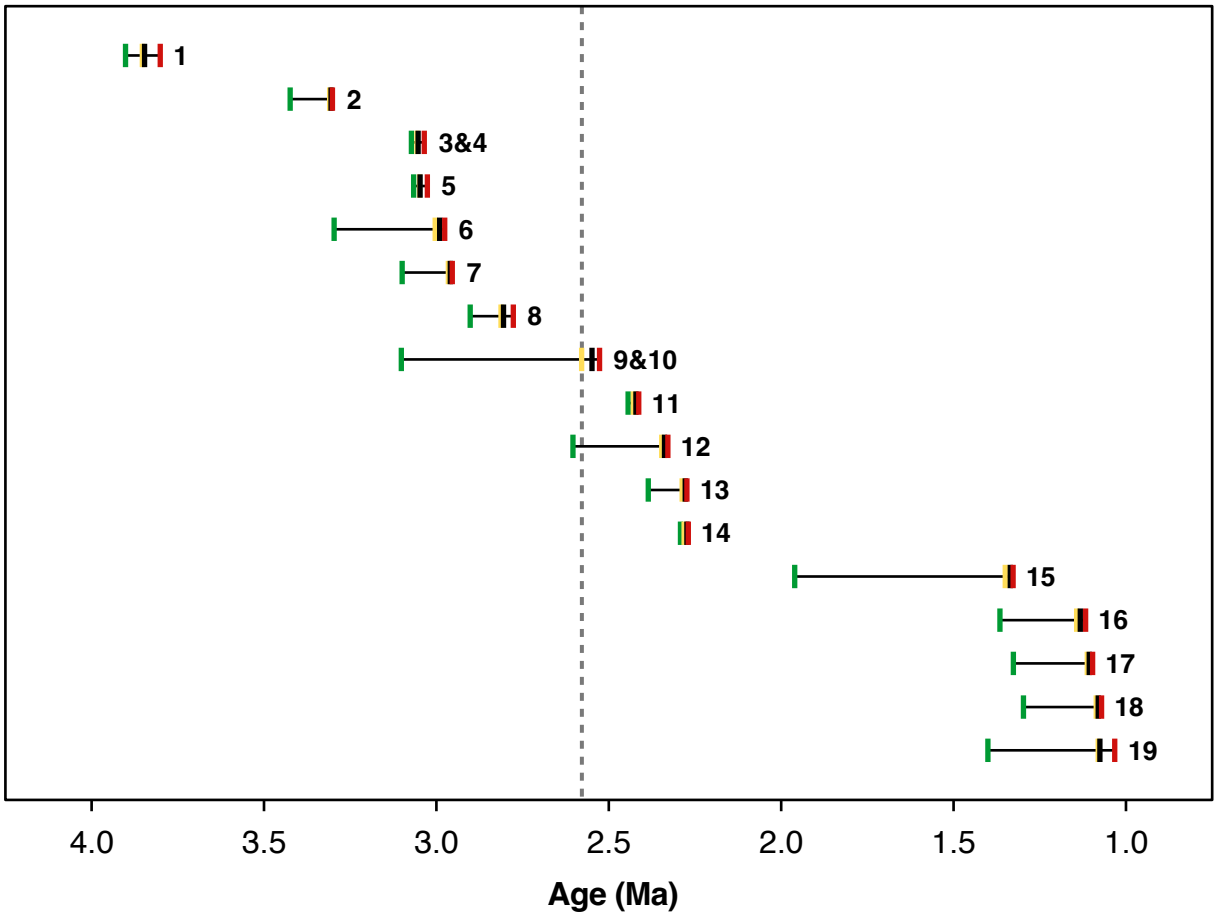

Figure 3.3 Sample ages for the LO sample (black line), pre-extinction (green line), imminent-extinction (yellow line), and post-extinction (red line) See **Figure 3.2** for species 1-19. The Grey dashed line represents the Pliocene-Pleistocene boundary and the onset of the 41-kyr glacial-interglacial cycles.

3.2.2.2 Assemblage Counts and Sample Repeatability

300 specimens is the commonly cited figure to faithfully measure relative abundance in planktic foraminifera, but this total was determined using Recent assemblages (Al-Sabouni, Kucera and Schmidt, 2007) and not in a formal rarefaction framework. We, therefore, used repeated counts of increasing numbers of specimens to determine an adequate number to assess assemblage diversity. To measure assemblage count repeatability, one sample at 2.4285 Ma was sieved at

>125 µm to maximise the chance of all species being present (Al-Sabouni, Kucera and Schmidt, 2007) and then re-sampled repeatedly to generate a rarefaction curve of species richness as a function of sample size. Individuals in the subsamples were identified at the species level according to published taxonomy (Kennett and Srinivasan, 1983; Aze *et al.*, 2011). Species abundance counts were conducted on 10, 30, 50, 100, 300, and 500 specimen splits to determine how many individuals need to be counted to represent community composition accurately. The repeated sample counts supported the choice of 300 specimens as a sufficient sample to represent biodiversity (**Figure 3.4**), as the number of species present does not change detectably after this point (**Table B.2**).

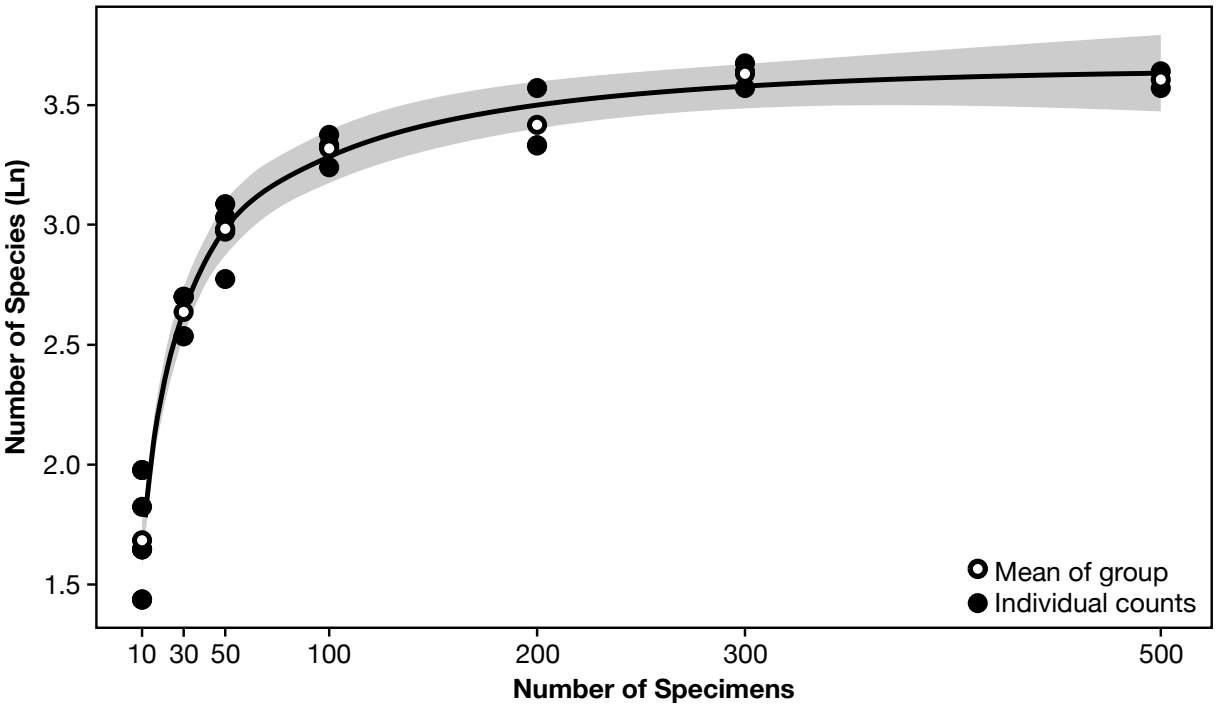

Figure 3.4 The number of species per sample on a natural log (ln) scale; the fitted line is a non-linear semi-log line with a 95% confidence interval.

While planktic foraminiferal samples are typically sieved at >125 µm for assemblage studies (Al-Sabouni, Kucera and Schmidt, 2007), in the case of Site 925, which is situated in a tropical location, the use of a larger sieve size (>150 µm) is unlikely to have resulted in the exclusion of any species from the assemblage count. This is due to the generally larger test sizes of foraminifera in tropical regions (Schmidt, Renaud, and Bollmann, 2003). Although species specimens are present at <150 µm, smaller sieve fractions may lead to the misidentification of smaller and juvenile individuals (Huber et al., 1999; Al-Sabouni, Kucera, and Schmidt, 2007). Thus, all samples were washed and dry-sieved to >150 µm for abundance counts of 300 specimens and further analysis.

3.2.2.3 Community composition

Hill numbers (^qD) are used to calculate diversity as a curve (Hill, 1973) (**Figure 3.1a**). Two curves are calculated: one is based on the observed species richness in the samples, and the other is an estimated value influenced strongly by the number of single occurrences of taxa as a proxy for the "dark diversity" missing from the sample to reduce potential sampling bias (Chao and Jost, 2015) (**Figure 3.1b**). The slope of the curve is used to understand the evenness of an assemblage: a flat diversity curve shows an even assemblage with an equal number of taxa (**Figure 3.1c**), whereas a high gradient curve which plateaus shows an uneven assemblage with few dominant taxa and a high number of rare taxa (**Figure 3.1d**). The observed diversity values typically underestimate "true" species richness as some species go undetected in samples (Chao and Jost, 2015). The estimated diversity profiles (**Figure B.3-3**) are the estimated values and reduce any sampling bias (Chao and Jost, 2015), in this case, any species that may not have been counted in the sample size of 300 (see **3.2.2.2**). All empirical diversity profiles at $q = 0$ ($q0$, species richness), $q = 1$ ($q1$, ln-transformed Shannon's entropy index, or the evenness of the assemblage, and $q = 2$ ($q2$, inverse of Simpson's concentration index, or dominance within the assemblage; **Figure 3.1a**) are below the estimated values (**Figure B.3-3**), although the difference is minimal for $q1$ and $q2$ (**Table B.3**). 95% confidence intervals were generated for each diversity curve by bootstrapping 1,000 times.

Linear regressions were compared for both observed (**Figure 3.5**) and estimated (**Figure B.6**) diversity values ($q0$, $q1$, and $q2$) to $\delta^{18}O$ (‰) using mixed-effect models. However, the results and discussion focus on the observed values, as the estimated values were used to assess uncertainty around the observed data, and the observed values fall within the estimated confidence bands (**3.3 Results** and **Figure B.3-3**). Therefore, we conducted statistical analysis only on observed values to avoid adding additional layers of uncertainty by reanalysing estimates, which already incorporate assumptions. This approach ensures that our conclusions are based on actual data rather than potentially misleading additional statistical modelling.

3.3 Results

There is a decline in species richness between the oldest and youngest samples (**Figure 3.2**), with a detectable relationship between the number of species and the global $\delta^{18}O$ record (**Figure B.1**). The number of species present (richness) decreases with increased $\delta^{18}O$ and thus increased glacial conditions ($\beta = -0.237$, s.e = 0.0420, $p < 0.001$). The coefficient of determination (r^2) indicates that climate explains 38.7% of the variation in species counts.

Analysis of extinction percentages by ecogroup, morphogroup, and the combined ecogroup-morphogroup classifications reveals distinct patterns. Among ecogroups, ecogroup 3

experienced the highest extinction percentage (63.16 %), followed by ecogroup 1 (21.05 %) and ecogroup 4 (15.79 %). In terms of morphogroups, group 7 exhibited the highest extinction percentage (47.37 %), followed by group 14 (31.58 %), group 3 (15.79 %), and group 16 (5.26 %). When eco-groups and morpho-groups are considered together (**Figure B.2**), the highest extinction rate was observed in ecogroup 3-morphogroup 7 (36.84 %), followed by ecogroup 3-morphogroup 14 (26.32 %). Additionally, ecogroup 1-morphogroup 3, and ecogroup 4-morpho-group 7 each contributed 5.26 % of extinctions.

The diversity profiles (**Figure B.3-5**) are based on observed species richness from the assemblage counts conducted in this study. At $q0$, 11% of the observed values sit outside the confidence bands of the bootstrapped empirical values, whereas all $q1$ and $q2$ observed values are within the proposed value confidence bands (**Figure B.3-5**). This suggests that this study's methodology for assemblage counts satisfactorily captures community richness.

Using mixed-effect models, partitioning the overall temporal sequence into phases by extinction state reveals context-dependent relationships between the abiotic and biotic drivers of biodiversity change (**Figure 3.5**, **Figure B.6**). Although there are differences in absolute values between $q0$, $q1$ and $q2$, the relationships between $\delta^{18}O$ and these biodiversity metrics are consistent.

Increasing temperature, as invoked by decreasing $\delta^{18}O$, increases species richness ($q0$) in the pre-extinction phase (β = -0.307, s.e = 0.059, $p < 0.001$). Although the coefficient weakens in the imminent-extinction phase, there is no detectable difference from pre-extinction (difference from pre-extinction β = 0.028, s.e = 0.100, $p > 0.05$) and examining this imminent-extinction phase in isolation supports a detectable relationship between $\delta^{18}O$ and biodiversity (β = -0.278, s.e = 0.067, $p < 0.001$, **Figure 3.5**). There is however a detectable difference from pre- to post-extinction (difference from pre-extinction: β = 0.202, s.e = 0.087, $p < 0.05$). These two coefficients effectively cancel each other out, which is also visible by examining the post-extinction phase in isolation where no systemic correlation exists (β = -0.104, s.e = 0.081, $p > 0.05$, **Figure 3.5**).

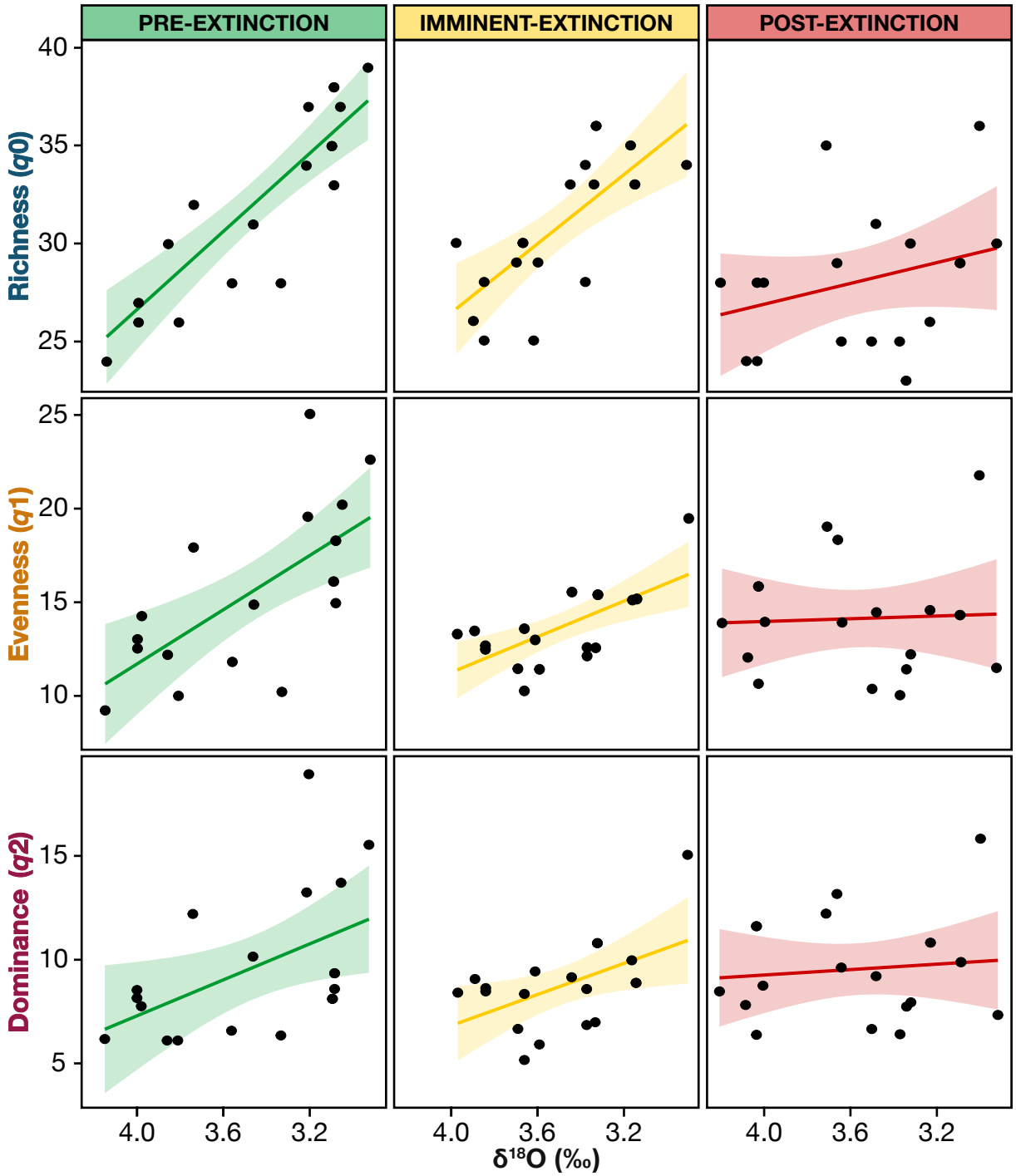

Figure 3.5 Change in regression slopes and strengths for observed diversity values (*q*0, *q*1, and *q*2) and oxygen isotopes ($\delta^{18}O$ (‰)) (Lisiecki and Raymo, 2005) for pre- (green), imminent- (yellow), and post-extinction (red) intervals, with 95% confidence interval bands from linear regressions.

Increasing temperature increases evenness (*q*1) in the pre-extinction phase (β = -0.502, s.e = 0.120, $p < 0.001$). Although the coefficient weakens in the imminent-extinction phase, there is no detectable difference from pre-extinction (difference from pre-extinction β = 0.185, s.e = 0.205, $p > 0.05$) and examining this imminent-extinction phase in isolation supports a detectable relationship between $\delta^{18}O$ and biodiversity (β = -0.317, s.e = 0.092, $p < 0.01$, **Figure 3.5**). There is, however, a detectable difference from pre- to post-extinction (difference from pre-extinction: β = 0.452, s.e = 0.173, $p < 0.05$). These two coefficients effectively cancel each

other out, which is also visible by examining the post-extinction phase in isolation where no systemic correlation exists (β = -0.050, s.e = 0.149, p > 0.05, **Figure 3.5**).

In the pre-extinction phase, dominance (*q*2) has a relationship with $\delta^{18}O$, with increasing temperature increasing dominance (β = -0.057, s.e = 0.018, p < 0.01). The coefficient weakens in the imminent-extinction phase, with no detectable difference from pre-extinction (difference from pre-extinction β = -0.007, s.e = 031, p > 0.05) and examining this imminent-extinction phase in isolation supports a detectable relationship between $\delta^{18}O$ and biodiversity (β = -0.437, s.e = 0.179, p < 0.05, **Figure 3.5**). There is no detectable difference from pre- to post-extinction (difference from pre-extinction: β = -0.044, s.e = 0.025 p > 0.05), and by examining the post-extinction phase in isolation, no systemic correlation exists (β = -0.116, s.e = 0.175, p > 0.05, **Figure 3.5**).

In summary, in species richness (*q*0) and dominance (*q*1), the abiotic environment structures biodiversity in the pre-extinction phase. This structuring weakens during the approach to extinction (note the reduced gradient and increased uncertainty in the middle column of **Figure 3.5**) and then dissipates further to become not detectable in the immediate aftermath of species loss (right column of **Figure 3.5**). Across the full time-series of all 19 extinctions, there is a detectable linear change between *q*0 and *q*1 through time (species richness and evenness; β = 0.079, s.e. = 0.267, p < 0.01), between *q*0 and *q*2 (species richness and dominance; β = 0.89, s.e. = 251, p < 0.001) and between *q*1 and *q*2 (evenness and dominance; β = 0.120, s.e.=0.036, p < 0.01). Inspecting patterns using a non-linear generalised additive model reveals a drop in diversity from around 3.25 to 2.50 Ma at q1, *q*0-*q*1, *q*0-*q*2, *q*1-*q*2 **Figure 3.6d-f**). There is a stronger signal in *q*0-*q*2 and *q*1-*q*2 than in *q*0-*q*1 **Figure 3.6d-f**). In species richness, the decline is from 3.9 to ~2.5 Ma, whereas in evenness and dominance, the decline ends closer to ~2.75 Ma (**Figure 3.6a-c**). As the difference between species richness and dominance and the difference between evenness and dominance decreases towards the modern, the more recent communities consist of fewer species but the same overall dominance levels.

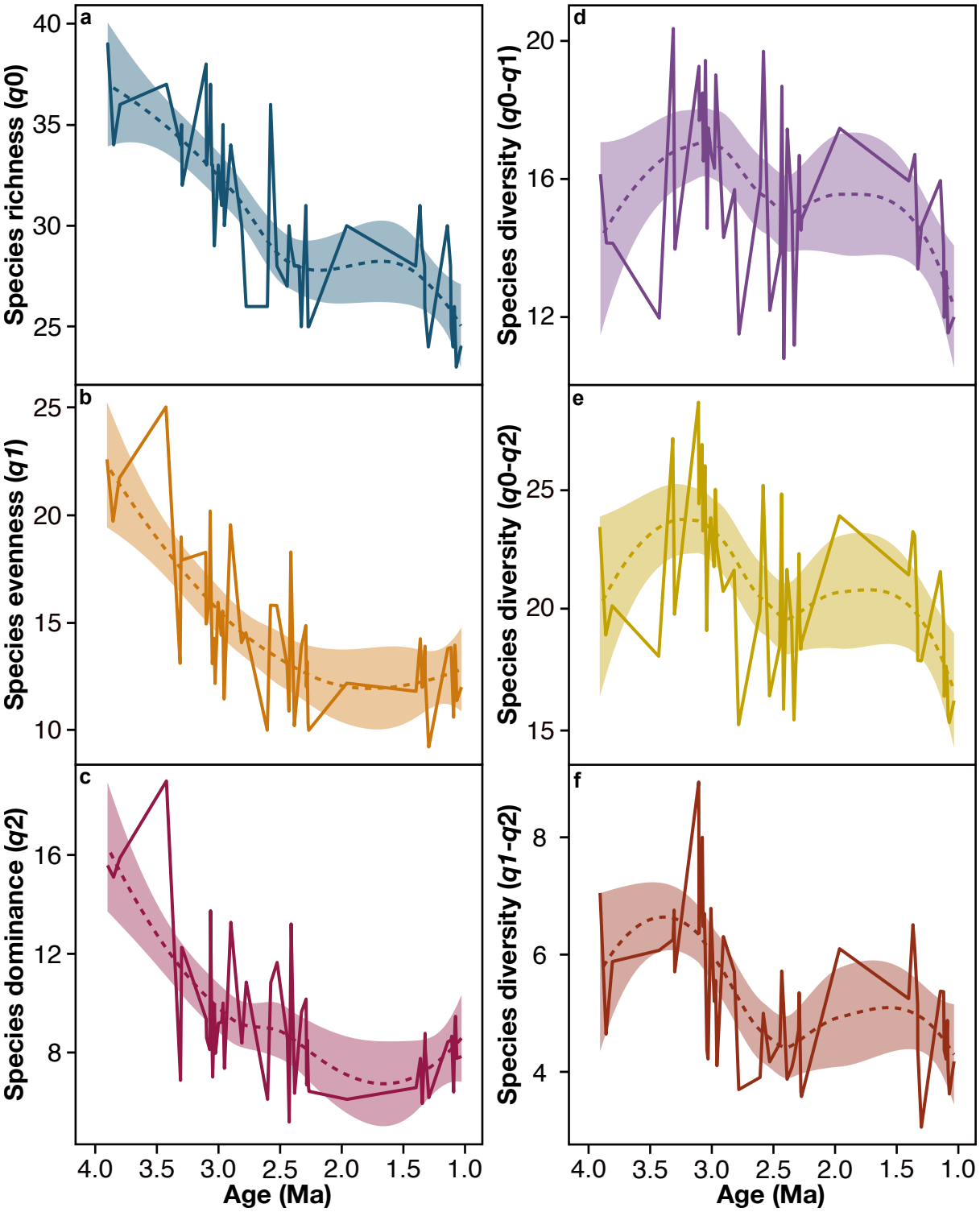

Figure 3.6 Diversity profiles for **a)** *q*1, **b)** *q*2, **c)** *q*2, and differences between **e)** *q*0-*q*1), **f)** *q*0-*q*2, and **g)** *q*1-*q*2 with 95% confidence interval bands from generalised additive models.

3.4 Discussion

Hill number curves support the inference from rarefaction for capturing richness in assemblages (**Figure 3.4**), providing a more comprehensive view of biodiversity trends. However, our repeated sampling of community dynamics across species extinctions shows a weakening of climatic regulation of the Hill Number representation of community structure: the

regression between the $\delta^{18}O$ signal is strong and statistically significant in the pre-extinction phase, becoming more marginal as extinction becomes imminent before being lost post-extinction (Figure 4). As there are repeated cycles of the 3-phase extinction events across the whole temporal sequence (Figure 3), it is suggested that between the extinctions, abiotic controls resume, as in the next pre-extinction phase, the community has a strong relationship with $\delta^{18}O$. Detecting changes from one extinction event to the next was not the purpose of our experimental design, and thus we did not seek to measure the time taken for communities to recover to pre-extinction states, but this might be possible if sampling resolution could be increased further.

The observed decline in species richness at Site 925 in the last 5 Ma (Figure 3; Table S3) follows the global trend of decreasing planktic foraminiferal species richness throughout the Plio-Pleistocene (Aze *et al.*, 2011; Ezard *et al.*, 2011; **Figure 1.2**). Although planktic foraminiferal samples are generally sieved at >125 µm for assemblage studies (Al-Sabouni, Kucera and Schmidt, 2007), as site 925 is in a tropical location, it is unlikely that a larger sieve size of >150 µm has excluded any species from the assemblage count as the test size is generally larger in the tropics (Schmidt, Renaud and Bollmann, 2003) and smaller size fractions can lead to incorrect identification of smaller and juvenile individuals (Huber *et al.*, 1999; Al-Sabouni, Kucera and Schmidt, 2007). This suggests that the community profiles reported in this study represent broader trends. The multifaceted nature of Hill Numbers provides a more thorough representation of biodiversity than any single measure (Hill, 1973; Chao *et al.*, 2014; Chao and Jost, 2015) and reveals abiotic structuring onto $q0$, $q1$ and $q2$ through each pre-, imminent- and post-extinction phase (**Figure 3.5**), despite the accumulating loss of species during individual extinction or extirpation events (**Figure 3.4**).

The extinction patterns observed in ecogroups and morphogroups provide further insight into the vulnerability of specific functional and morphological traits to environmental changes (see Chapter **4**). Ecogroup 3 experienced the highest extinction rate, suggesting that species within this ecological category were particularly susceptible to shifting environmental pressures. Similarly, morphogroup 7 dominated extinction events, implying that certain morphological adaptations may have been disadvantageous during this period. When analysed together (**Figure B.2**), the highest extinction frequencies occurred in ecogroup 3 combined with morphogroup 7, reinforcing the idea that both ecological function and morphology jointly influenced survival likelihood. These findings indicate that extinction events were not random but were structured by ecological and morphological characteristics, highlighting the selective pressures acting on planktic foraminiferal communities. Morphological traits, such as test size, shape, spine presence, and symbiotic relationships, play a crucial role in the resilience of planktic foraminifera to environmental stressors (see Chapter **4**). For example, *Trilobatus*

sacculifer exhibited morphological stabilisation before extinction, while the morphology of *Orbulina universa* diversified prior to extinction, suggesting differing adaptive responses to increasing stress (Weinkauf *et al.*, 2019). The selective pressures on specific ecogroups and morphogroups indicate that certain functional traits were less adaptable to environmental changes, resulting in higher extinction rates. Understanding these trait-based vulnerabilities provides deeper insight into the mechanisms driving extinction patterns in planktic foraminiferal communities.

While climate changes are clear across the duration of our sampling window, the community appears to adjust to them in a way that maintains its inherent stability. Our failure to detect any accumulating impact of species extinction, as might be seen by a non-linear alteration of the relevant biodiversity metric with time (see Figure 3: Reich et al., 2012) or a shift in the strength of the abiotic correlation with community metrics over time, (see Figure 4: Reich et al., 2012) does not necessarily mean it is unimportant, given that non-linear feedback can accelerate extinctions and provoke a loss of ecosystem function (Cardinale *et al.*, 2012). The non-linear decline in the differences between species richness, evenness, and dominance in the assemblage of planktic foraminifera (**Figure 3.6**) likely reflects a shift in ecosystem structure over time.

Throughout the late Pliocene to the start of the Pleistocene, there is a decrease in the variation between all diversity profiles, followed by a plateau during the Pleistocene itself (**Figure 3.6**). This trend suggests a homogenisation of species presence, indicating a loss in diversity as certain species become more dominant under changing climate conditions. Simultaneously, species richness, evenness, and dominance all decline from the Pliocene to the Pleistocene, eventually stabilising during the Pleistocene (**Figure 3.6**). Within the predominantly warm Pliocene was a short-lived glaciation (3.285 - 3.305 Ma) within marine isotope stage (MIS) M2 (3.26 - 3.31 Ma; De Schepper et al., 2013; Dowsett et al., 2015). This climatic disturbance coincides with the onset of the decline in differences among the diversity profiles (**Figure 3.6**), suggesting that the observed community restructuring could be a response to this environmental shift. The decreasing differences between species richness, evenness, and dominance suggest that the early stages of climate cooling and glaciation, around MISM2, triggered a fundamental restructuring of communities and the onset of ecological homogenisation. However, despite the general decline in species richness, evenness, and dominance during the warm Pliocene, diversity stabilises in the cooler Pleistocene, although there is greater climatic variability (**Figure 3.2**). Thus, increased temperatures appear to drive biodiversity loss over the increased amplitude of climate change.

Yet, there are still clear fluctuations in diversity throughout the Plio-Pleistocene, and understanding the mechanisms of how communities recover after each extinction necessitates higher resolution geochemical work to disentangle the depth optima of individual species' niches (Pearson *et al.*, 2001; Rohling *et al.*, 2004) from various seawater properties, such as temperature and salinity (Lea, 2014) that are interwoven in the $\delta^{18}O$ proxy but homogenised in the LR04 stack (Lisiecki and Raymo, 2005). The lack of other applicable high-resolution environmental data (e.g. pCO_2 for ocean acidification, Mg/Ca for sea surface temperature) limits the ability to untangle the precise environmental driver of the decline in species number during this time. The results do, however, support previous findings (Ezard *et al.*, 2011) that $\delta^{18}O$ can be used to predict extinction threats to planktic foraminifera by tracking declines in local diversity. The association between the abiotic state and the biotic structure of the community (**Figure 3.5**) regulates evolutionary dynamics (Ezard *et al.*, 2011). While the relationship with $q2$ is not statistically significant at the 95% level when analysed in isolation, it follows the same qualitative patterns as $q0$ and $q1$. Sampling further extinctions would increase statistical power, and thus the likelihood of detecting an effect that is there or an analysis that treats all parts of the Hill Number curve rather than simply the touchpoints of $q0$, $q1$ and $q2$ are two routes to obtaining that statistically significant result. Given the similarity in profiles across $q0$, $q1$ and $q2$, all diversity profiles are discussed as species diversity.

While $\delta^{18}O$ is correlated with species diversity in the pre-extinction phase, it becomes less so during the imminent-extinction phase, and there is a decoupling of the relationship between $\delta^{18}O$ and species diversity in the post-extinction phase. This suggests that biotic controls might drive community dynamics after an extinction event and buffer against abiotic changes, allowing for biodiversity to recover somewhat (e.g., (Cardinale *et al.*, 2012; Marshall, 2017; Pires, Srivastava and Farjalla, 2018). The clearest evidence for the re-establishment of biotic controls on biodiversity comes in the aftermath of mass extinctions (Marshall, 2017) after periods of transient volatility in which biological function is restored on faster timeframes than taxonomic counts suggest (Alvarez *et al.*, 2019). The average resolution between the nine samples that have pre-extinction samples directly following post-extinction is 24.4 kyr (min = 4.64, max = 51.65, std = 17.08, 95% confidence interval = 11.63), which is above our sampling resolution. Therefore, detecting the return to the pre-extinction phase community dynamics may be possible if the sampling resolution is increased to <4 kyr. Although mass extinctions and background extinctions are said to have similar recovery rates (e.g., Kirchner and Weil, 2000)

, this study suggests that community dynamics recover within thousands of years compared to that of millions of years following mass extinctions (Alroy, 2008; Barnosky *et al.*, 2011). The variability in recovery times also reflects the dynamic interplay between abiotic factors, such as climate, and biotic factors, including species interactions, that mediate biodiversity recovery.

The faster recovery observed after background extinctions suggests that while abiotic factors set the stage for extinction, biotic interactions may play a more crucial role in shaping the speed and direction of community recovery. This time-dependence of the speed of biotic response reinforces the need for multifaceted representations of biodiversity dynamics to link extinction events to their community context.

3.5 Conclusion

Our study reveals a decoupling of abiotic controls on planktic foraminifera communities across repeated extinction events, shedding light on the interplay between climate, community structure, and biodiversity. The resetting of the community after each extinction prevents cumulative destabilisation, with the consistent structure in each extinction phase suggesting resilience to ongoing climate changes and some form of biotic stability. The high extinction rates in specific a ecogroup and morphogroup suggests that both ecological function and morphology influenced survival, with certain traits proving disadvantageous under environmental stress. Our findings underscore the importance of considering the interplay of biotic and abiotic variation in understanding long-term biodiversity patterns and highlight how work spanning individuals and communities can reveal nuances in how biodiversity resists the challenges of a changing climate.

Chapter 4 Do size dynamics result from environmental changes or shifts in community composition?

Abstract

Diversity is multifaceted and encompasses various dimensions within ecosystems, including taxonomy, community, and species traits. Diversity is difficult to measure in deep time as we typically cannot directly observe biotic interactions in dynamic abiotic settings changing at a higher frequency than sedimentation typically reveals. Community dynamics, i.e., the number of species present and their relative abundances within their communities, influence and are influenced by many factors. These communities comprise individual species, each characterised by a unique set of traits that contribute to species' ecological roles within their respective habitats. The spatially, biogeographically, and taxonomically comprehensive fossil record of Plio-Pleistocene planktic foraminifera allows high-resolution studies of long-term eco-evolutionary change within ecosystems over time. In this chapter, I merge the individual, species, and community resolution described previously with morphometric data from >15,000 specimens to demonstrate how dynamic size distributions correlate with key community composition metrics. While the strongest effect on planktic foraminiferal size species identification, climate is a stronger predictor than biodiversity for trait changes through time. However, while species richness has little effect on size change in planktic foraminifera, evenness and dominance play a key role. Given the interconnectedness among trait, species and community dynamics, this research highlights how palaeontologists can benefit from integrating the concept of trait diversity with species and community shifts to better understand biodiversity dynamics on the longest time scales.

4.1 Introduction

The variety and abundance of different species within a community (community diversity) is crucial for understanding an ecosystem's health, stability and functioning (Ives, Klug and Gross, 2000; Ives and Carpenter, 2007). Environmental change, including temperature and atmospheric carbon dioxide (pCO_2) levels, is known to impact global biodiversity (Condamine, Rolland and Morlon, 2013). With unprecedented environmental changes predicted by the Intergovernmental Panel on Climate Change for the next 30-80 years (IPCC, 2021; **Figure 1.1**), there is a necessity for accurate predictions of community diversity and, thus, ecosystem health, stability and functioning (Loreau *et al.*, 2001).

The different measures of community diversity, such as species richness, evenness and dominance, all play a role in community diversity (Ives, Klug and Gross, 2000; Loreau *et al.*, 2001; Cusson *et al.*, 2015). Yet, communities are comprised of individuals and species, each characterised by a unique set of traits that contribute to species' ecological roles within their respective habitats, known as functional diversity (Petchey and Gaston, 2006). Measuring functional diversity is crucial for understanding how ecosystems respond to long-term environmental change and its ability to adapt to changing conditions (Tilman, Isbell and Cowles, 2014; Goswami *et al.*, 2017). Functional diversity links species' traits directly to ecosystem processes (Tilman, Isbell and Cowles, 2014), allowing the prediction of changes in species composition driven by environmental pressures. Ecosystems with a diverse range of functional traits may be more resilient to environmental changes, as different traits allow species to respond differently to stressors (e.g. Elmqvist *et al.*, 2003; Mouillot *et al.*, 2013). Therefore, ecosystems with high biodiversity tend to resist disturbances more effectively than less stable, low-biodiversity ecosystems (Goswami *et al.*, 2017; Hackett *et al.*, 2024).

Morphological trait change, as an alternative measure of biodiversity, offers a complementary approach to assessing ecosystem stability. Unlike species richness, which primarily counts the number of species, morphological traits focus on the underlying mechanisms of persistence within communities, emphasising the functional aspects of biodiversity rather than taxonomic distinctions (**Chapter 3**; Loreau *et al.*, 2001; Stachowicz, Bruno and Duffy, 2007; Laureto, Cianciaruso and Samia, 2015; Swain *et al.*, 2024). In this way, morphological trait change provides a direct link to functional diversity and ecosystem resilience and, in principle, focuses more directly on the mechanisms of persistence rather than the politics and peculiarities of taxonomy.

However, measuring very long-term functional diversity requires fossil record studies, and very few records allow for such reconstructions. Databases, such as The Paleobiology Database (Uhen *et al.*, 2023), Triton (Fenton *et al.*, 2021) and NOW (The NOW Community, 2024), provide

long-term fossil data but are largely taxon counting. Phenomes10K is a fossil database for traits (Goswami, 2015), but we need the interconnectedness of traits from individuals, species, and communities to determine the important links that determine biodiversity patterns across scales. Planktic foraminifera provide an exceptional 200 million year (Myr) fossil record with a good taxonomic resolution for understanding morphological changes through time (Fraass, Kelly and Peters, 2015; Yasuhara *et al.*, 2017) within the context of mature (Aze et al. 2011) and evidence-based (**Chapter 2**) taxonomic understanding and the capacity to assess multidimensional community change (Error! Reference source not found.).

When applied across individuals, size measurements of planktic foraminifera can be used to make comparisons across species and populations, aiding in monitoring ecosystem dynamics (Schmidt, Thierstein and Bollmann, 2004; Kucera, 2007). The growth of calcareous planktic foraminifera tests is controlled by many environmental factors, including ocean acidification, temperature, salinity, light, oxygen levels, nutrients, and food availability (Kucera, 2007). The general trend in foraminiferal size is larger tests in warm tropical/subtropical zones with a decrease towards the poles (Kucera, 2007) due to a combination of environmental parameters: carbonate ion saturation, faster metabolic rates, higher light intensity and greater niche diversity due to stronger stratification (Schmidt, Renaud, *et al.*, 2004; Lombard *et al.*, 2010). This size trend is complicated by the close correlation with salinity, where strongly reduced salinity hinders calcification in some species (Weinkauf *et al.*, 2013, 2019), plus the increase in size with more food and nutrient availability (Kucera, 2007; Aldridge, Beer and Purdie, 2012), such as in upwelling regions. Furthermore, each species has differing optimum growth conditions (Darling and Wade, 2008; Lombard *et al.*, 2009, 2010), outside of which growth decreases and reproduction ceases (Schmidt *et al.*, 2006), ultimately resulting in extinction if the environmental conditions are outside the optimum throughout the species' habitat.

Despite many variables influencing the size of planktic foraminifera, it is a key morphological trait commonly used to record evolutionary trends (Arnold, Kelly and Parker, 1995; Schmidt, Thierstein and Bollmann, 2004), changes in ecological niche occupation (Kearns *et al.*, 2021; Woodhouse *et al.*, 2021) and response to environmental change (Schmidt, Renaud and Bollmann, 2003; Schmidt *et al.*, 2016; Brombacher *et al.*, 2017). The "Lilliput Effect" is often observed following mass extinctions, where the surviving species tend to be smaller in size as a response to stressful environmental conditions, such as lower food availability and changes in temperature (Keller and Abramovich, 2009). However, dwarfing in planktic foraminifera has been proposed as a common stress-induced reaction in extinct-going species before their disappearance (Schmidt *et al.*, 2006; Wade and Olsson, 2009). Yet, Abramovich *et al.* (2010) observed this effect as a possible result of increased reproduction during the late Maastrichtian warm event. Dwarfed species with very low abundance pre- and post-extinction events became

more abundant during the warming, whereas those species that retained their 'normal' size saw a drop in abundance (Abramovich *et al.*, 2010).

While the planktic foraminifera fossil record suggests that net diversification (speciation - extinction) is strongly controlled by competition among species (Ezard *et al.*, 2011), there is no evidence of competition in extant planktic foraminifera species (Rillo *et al.*, 2019), as there are too few living individuals within an ecological space to feasibly limit resources (Rillo *et al.*, 2019). Mass extinctions are strongly linked to abiotic rather than biotic factors (e.g., Abramovich *et al.*, 2010; Aze, 2022), as are individual "background" extinctions, which have also been linked to temporal climate fluctuations (Banerjee and Boyajian, 1997; Abramovich *et al.*, 2010; Peters, Kelly and Fraass, 2013; Fraass, Kelly and Peters, 2015; Weinkauf *et al.*, 2019). Ezard *et al*. (2011) show that changes in oxygen isotope ($\delta_{18}O$) levels (indicative of temperature, salinity and continental ice levels (Shackleton, 1977; Shackleton and Vincent, 1978)) are an important predictor of extinction.

Little is known, however, about how these individual "background" extinctions influence community dynamics. Losing species with unique morphological traits can reduce functional diversity in planktic foraminifera communities (Kucera, 2007), impacting ecosystem functions such as nutrient cycling, carbon sequestration, and energy transfer within marine food webs (Hull and Norris, 2011; Lombard *et al.*, 2011). Planktic foraminiferal species richness has declined in the last 5 Myr (Aze *et al.*, 2011; Ezard *et al.*, 2011; **Figure 1.2**) and has been linked predominantly to climate change (Banerjee and Boyajian, 1997; Abramovich *et al.*, 2010; Peters, Kelly and Fraass, 2013; Fraass, Kelly and Peters, 2015; Weinkauf *et al.*, 2019). More specifically, the decline in planktic foraminifera diversity observed during the Pliocene and Quaternary is likely a result of both large-scale palaeoceanographic fluctuations, beginning ~6 million years ago (Ma), and high-frequency climate oscillations related to the 41-thousand year (kyr) glacial-interglacial cycles that began ~ 2.5 Ma (Wei and Kennett, 1986; Peters, Kelly and Fraass, 2013; Fraass, Kelly and Peters, 2015). What remains unclear, however, is if the links between levels of biodiversity from trait to individual to community are associated with the extinction dynamics and decline in species richness through the study interval.

Given these hypotheses and observations, we analyse ODP Site 925, which sees a decline in species richness from 39 to 25 in the Plio-Pleistocene between 4 and 1 Ma across the climate transition (**Figure 4.1**). From what is already known about planktic foraminifera test growth, we expect to see dwarfing and less variation in test size within the extinction-going species just before the extinction event. However, we will also explore whether we observe the Lilliput Effect post-extinction in the remaining community across the individual species extinctions. Measuring morphological trait changes throughout the exceptional fossil record of planktic

foraminifera could, therefore, be useful in understanding the role of functional diversity and community dynamics during individual extinction events.

4.2 Materials & Methods

4.2.1 Materials

51 samples from ODP Site 925 on the Ceara Rise in the tropical Equatorial Atlantic were used in this study. The samples are from Holes 925B (4°12.248'N, 43°29.349'W, water depth: 3041.1 meters below sea level (mbsl)), 925C (4°12.256'N, 43°29.349'W, water depth: 3040.6 mbsl) and 925D (4°12.260'N, 43°29.363'W, water depth: 3040.5 mbsl) (Shipboard Scientific Party, 1995, p. 925), from 3.900 to 1.032 Ma. Site 925 has good sample availability, well-preserved calcareous material, and no signs of severe dissolution or reworking (Chaisson and Pearson, 1997). Site 925 also has high species richness, with continuous extinction throughout the study period (**Figure 4.1**). The 51 samples were selected following the sampling method in Error! Reference source not found.. The age model for Site 925 (Wilkens *et al.*, 2017) is tuned to the Lisiecki and Raymo LR04 high-resolution benthic oxygen isotope ($\delta^{18}O$ (‰)) compilation (LR04 stack) (Lisiecki and Raymo, 2005).

4.2.2 Methods

4.2.2.1 Study species

We focus on 19 species extinctions: *Hirsutella margaritae*, *Sphaeroidinella kochi*, *Dentoglobigerina baroemoenensis*, *Dentoglobigerina venezuelana*, *Dentoglobigerina altispira*, *Sphaeroidinellopsis seminulina*, *Sphaeroidinellopsis paenedehiscens*, *Hirsutella cibaoensis*, *Menardella limbata*, *Menardella multicamerata*, *Globoconella puncticulata*, *Menardella miocenica*, *Menardella pertenuis*, *Menardella exilis*, *Globigerinoidesella fistulosa*, *Neogloboquadrina humerosa*, *Neogloboquadrina acostaensis*, *Globigerinoides extremus*, and *Globigerinoides obliquus*. The samples represent the pre-, imminent-, and post-extinction assemblages of 19 species-level local extinction events throughout the Plio-Pleistocene at ODP Site 925. Each species extinction has a pre-, -imminent, and post-extinction sample (see Error! Reference source not found.).

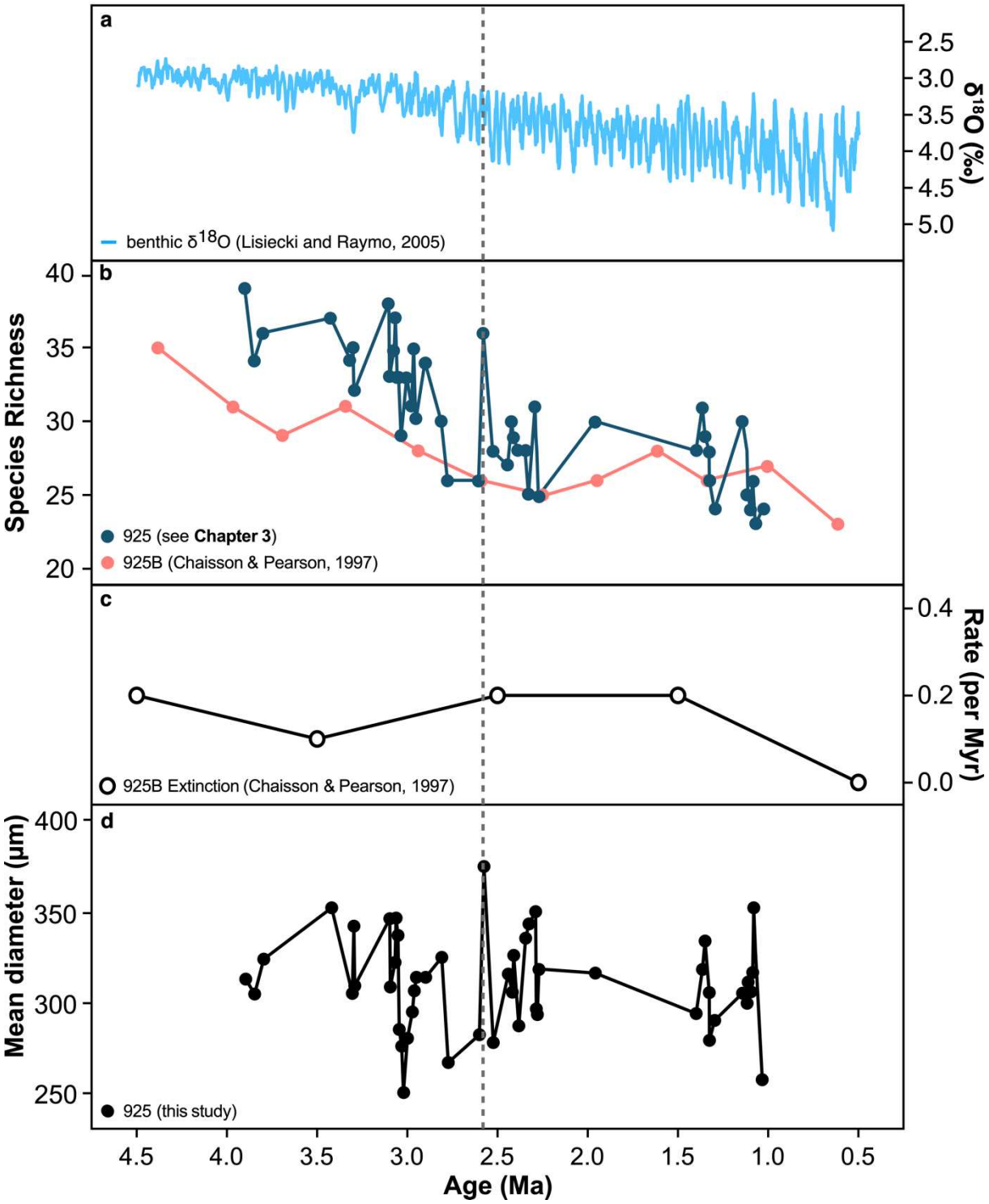

Figure 4.1 **a)** LR04 high-resolution benthic oxygen isotope ($\delta^{18}O$ (‰)) compilation (Lisiecki and Raymo, 2005) as a representative of environmental change (light blue) with **b)** species richness of planktic foraminifera from **Chapter 3** (dark blue) and Chaisson and Pearson (1997), **c)** extinction rate of planktic foraminiferal species as species per 0.5 million years (Rate (per .5Myr); black line with open circles, and **d)** mean diameter (µm) per assemblage from this study (black line with closed circles) from ODP site 925 between 4.5 and 0.5 Myr. The vertical grey dashed line represents the boundary between the Pliocene and the Pleistocene, at 2.58 Ma, and the onset of the 41 kyr glacial-interglacial cycles.

4.2.2.2 Morphological Traits

All samples were washed and dry-sieved to >150 µm. Three hundred specimens (see Error! Reference source not found.) from each sample were identified at the species level according to published taxonomy (Kennett and Srinivasan, 1983; Aze *et al.*, 2011; Wade *et al.*, 2011), resulting in ~15,300 specimens in total. The specimens were mounted on a picking slide, with each species orientated in umbilical view and imaged using an Infinity 3 Lumenera camera mounted on an Olympus SZX10 light microscope. The maximum diameter (referred to as diameter from now on) was measured in Image-Pro Premier software, version 9.3.3 (Media Cybernetics, 2017) (**Figure 4.2**).

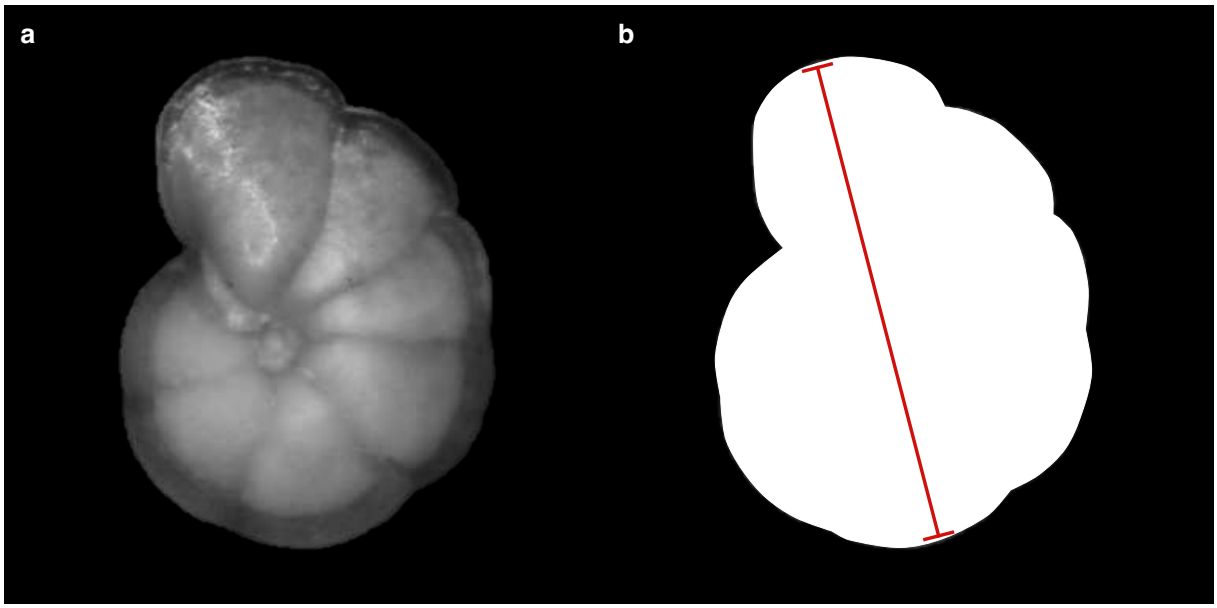

Figure 4.2 Analysed morphological traits on planktic foraminiferal tests: **a)** specimens were imaged in umbilical view, and **b)** maximum diameter was measured on the extracted two-dimensional representation.

4.2.2.3 Community Change

We use the Hill numbers calculated in Error! Reference source not found. for each sample to represent different diversity measures. *q*0 is the number of species counted (species richness), *q*1 is the ln-transformed Shannon's entropy index (evenness of the assemblage), and *q*2 is the inverse of Simpson's concentration index (dominance within the assemblage) (see Error! Reference source not found.).

4.2.2.4 Environmental Change

The Pliocene (5.3 to 2.6 Ma) is often used as a model for future climate scenarios because its global temperatures were 2-3°C warmer than pre-industrial levels (Dowsett and Caballero Gill, 2010), similar to projections for the next century under high emissions (see **Chapter 1**; **Figure 1.1**). This makes it valuable for studying potential ecosystem and climate responses to similar

warming. In contrast, the Pleistocene (2.6 Ma to 11.7 ka) was cooler but marked by significant climate variability with 41-kyr glacial and interglacial cycles, providing insights into how rapid climate changes might impact ecosystems. The Plio-Pleistocene period is well-documented, with the LR04 stack (a high-resolution benthic $\delta^{18}O$ compilation) offering precise age control and insights into glacial-interglacial climate changes, aiding in the study of climate impacts on extinction events.

4.2.2.5 Statistical Analysis

All calculations were performed in R version 4.3.2 (R Core Team, 2023) using generalised least squares and mixed effects models in the nlme package, version 3.1.166 (Pinheiro *et al.*, 2024), to compare the impact of species identification as the random effect. Species identification (ID) is included as a random effect and is assessed by comparing a generalized least squares (GLS) model without a random effect to a full model incorporating ID as a random factor. The fixed effects in the linear mixed-effects (LME) models include Climate (represented by $\delta^{18}O$), extinction intervals (Intervals), the three Hill numbers (*q*0, *q*1, *q*2), and the interaction between Climate and Interval. This approach allows for evaluating the influence of climatic variability and extinction phases on diversity while accounting for species-specific differences (**Figure 4.5**). We use species ID as the random effect, as even though we are not interested in predicting species size changes per se (some of the species recovered are very rare and below relevant sample sizes for that purpose), we do want to know how much species' composition contributes to overall trait change at the community/assemblage level, particularly in assessing within-taxon controls on species diameter. Comparing amongst models quantifies the influence of each term using the difference in Akaike Information Criterion (AIC) scores of the full model to an alternative model with each of the fixed effects removed. The AIC provides a compromise between model complexity and variance explained, providing a metric of the quality of each model fit relative to the other models considered. Prior to analysis, all variables were scaled to have mean zero and standard deviation one to ensure comparability of effect size for variables measured on different scales. Linear regressions were used to compare the mean assemblage diameter and mean species diameter to the $\delta^{18}O$ (‰) and diversity measures to calculate the relationship of size to environmental change, and ecogroup/morphogroup relationships to size changes (

Table C.1). Here we report r, rather than r^2, to indicate the positive or negative change in trait in relation to $\delta^{18}O$ (‰).

4.3 Results

There is a marginal decline in the mean diameter of the assemblage across all 51 samples (mean assemblage diameter), from the oldest sample (3.901 Ma) to the youngest sample (1.032 Ma) (**Figure 4.1**). There is a detectable relationship with the global $\delta^{18}O$ record ($r = -0.279$, $p < 0.05$, **Figure C.1**) and with the first differences in $\delta^{18}O$ and first differences in the mean assemblage diameter ($r = -0.357$, $p < 0.01$), where mean assemblage diameter increases when $\delta^{18}O$ decreases and thus planktic foraminiferal size is larger in interglacial (warmer) conditions, and vice versa. There is a significant relationship between the mean assemblage diameter and the biodiversity at *q*0 ($r = 0.423$, $p < 0.001$), *q*1 ($r = 0.374$, $p < 0.05$), and *q*2 ($r = 0.270$, $p < 0.05$), with the mean assemblage diameter increasing with increased diversity **Figure C.2**).

Separating the studied time interval into the phases based on extinction states (as in Error! Reference source not found.) uncovers analogous context-dependent relationships between the abiotic and biotic factors driving trait changes. When taking the mean diameter of each of the assemblages within the pre-, imminent-, and post-extinction intervals, the assemblage size is smaller post-extinction (299.9 µm) than in the pre-extinction (316.4 µm) and imminent-extinction (319.9 µm) phases. Temperature, as invoked by $\delta^{18}O$, exhibits a statistically significant correlation in the pre-extinction phase ($r = -0.539$, $p < 0.05$), but this is not detectable in the imminent-extinction ($r = -0.218$, $p = 0.371$) nor the post-extinction ($r = -0.063$, $p = 0.799$) phases with the mean assemblage diameter (**Figure C.3**). There is a significant relationship between the mean diameter of the assemblage in the pre-extinction phase and the biodiversity at $q0$ ($r = 0.759$, $p < 0.001$), $q1$ ($r = 0.070$, $p < 0.001$) and $q2$ ($r = 0.552$, $p < 0.05$), but not at the imminent- ($p = 0.514$, 0.174, 0.267, respectively) or post-extinction phase ($p = 0.629$, 0.440, 0.628, respectively) (**Figure 4.3**).

When extracting the extinct-going species from the assemblages, there is a significant relationship between the remaining community assemblage mean diameter and the environment at the pre-extinction phase ($r = -0.5455$, $p < 0.05$) but not at the imminent-extinction phase ($r = -0.1983$, $p = 0.4156$), with the post-extinction phase remaining unchanged as there are no species being removed from the data (**Figure 4.4**, top panel). There is a greater decrease in size from pre-extinction (312.95 µm) to the imminent-extinction (318.18 µm) phase, with the extinct-going species removed from the community assemblages.

Although there is a small reduction in size in the extinct-going species from pre- (479.81 µm) to imminent-extinction (457.16 µm), there is no relationship with environment at the pre- ($r = -0.316$, $p = 0.594$) or imminent-extinction phases ($r = -0.038$, $p = 0.8778$) (**Figure 4.4**, bottom panel), At species-level, 8 species decrease in size from pre- to imminent-extinction with an average size decrease of 17.7 % (range = 2.8 to 26.7 %), while 11 species increase in size across prior to the extinction with a size increase of 21.3% (range = 5.4 to 54.9 %) (**Figure C.1**). There is a significant relationship between the diameter of individual species in 4 of the 19 extinct-going species and $\delta^{18}O$: *N. acostaensis* ($r = -0.142$, $p < 0.0001$), *G. extremus* ($r = -0.139$, $p < 0.01$), and *Gs. fistulosa* ($r = 0.524$, $p < 0.001$) all decreased in size prior to their extinction, while *S. seminulina* ($r = 0.463$, $p < 0.05$) increased in size before its extinction. *N. acostaensis* and *G. extremus* both have negative relationships with $\delta^{18}O$, meaning that their size decreases as $\delta^{18}O$ increases, suggesting warmer temperatures, while *Gs. fistulosa* and *S. seminulina* both have a positive relationship with $\delta^{18}O$, meaning they increase in size with increased $\delta^{18}O$ or cooler temperatures.

The analysis of size change trends across ecogroups (see **Table C.1**) reveals notable differences, though these variations are not statistically significant. Ecogroup 1 exhibited an average size increase (mean = +21.78 µm, std = 109.00 µm), whereas ecogroups 3 and 4 showed an overall decrease in size (ecogroup 3: mean = -27.62 µm, std = 109.45 µm; ecogroup 4: mean = -16.51 µm, std = 100.06 µm). While these trends suggest that species from certain eco-groups may be more prone to size reduction before extinction, an ANOVA test (F = 0.313, p = 0.736) indicates that the differences in size change among ecogroups are not statistically significant. Similarly, the analysis of size change trends across morphogroups (see **Table C.1**) highlights variation in body size shifts before extinction. Morphogroup 3 exhibited an average size increase (mean = +14.63 µm, std = 132.35 µm), while morphogroup 7 showed a much smaller change (mean = +1.26 µm, std = 81.21 µm). Morphogroup 14 experienced a notable size decrease (mean = -74.66 µm, std = 116.31 µm), whereas morphogroup 16 had the largest size increase (mean = +98.89 µm) but lacked sufficient data for a standard deviation calculation. Despite these differences, an ANOVA test (F = 1.232, p = 0.320) indicates that the variations in size change among morphogroups are also not statistically significant. This is supported by highlighting the 4 species that have a statistically significant correlation with climate. While *N. acostaensis* and *S. seminulina* are in the same ecogroup (3) and morphogroup (7) (see **Table C.1**), they have differing responses to changes in climate. Likewise, *G. extremus* and *Gs. fistulosa* also share an ecogroup (1) and morphogroup (3) and have differing responses to changes in climate (see **Table C.1**).

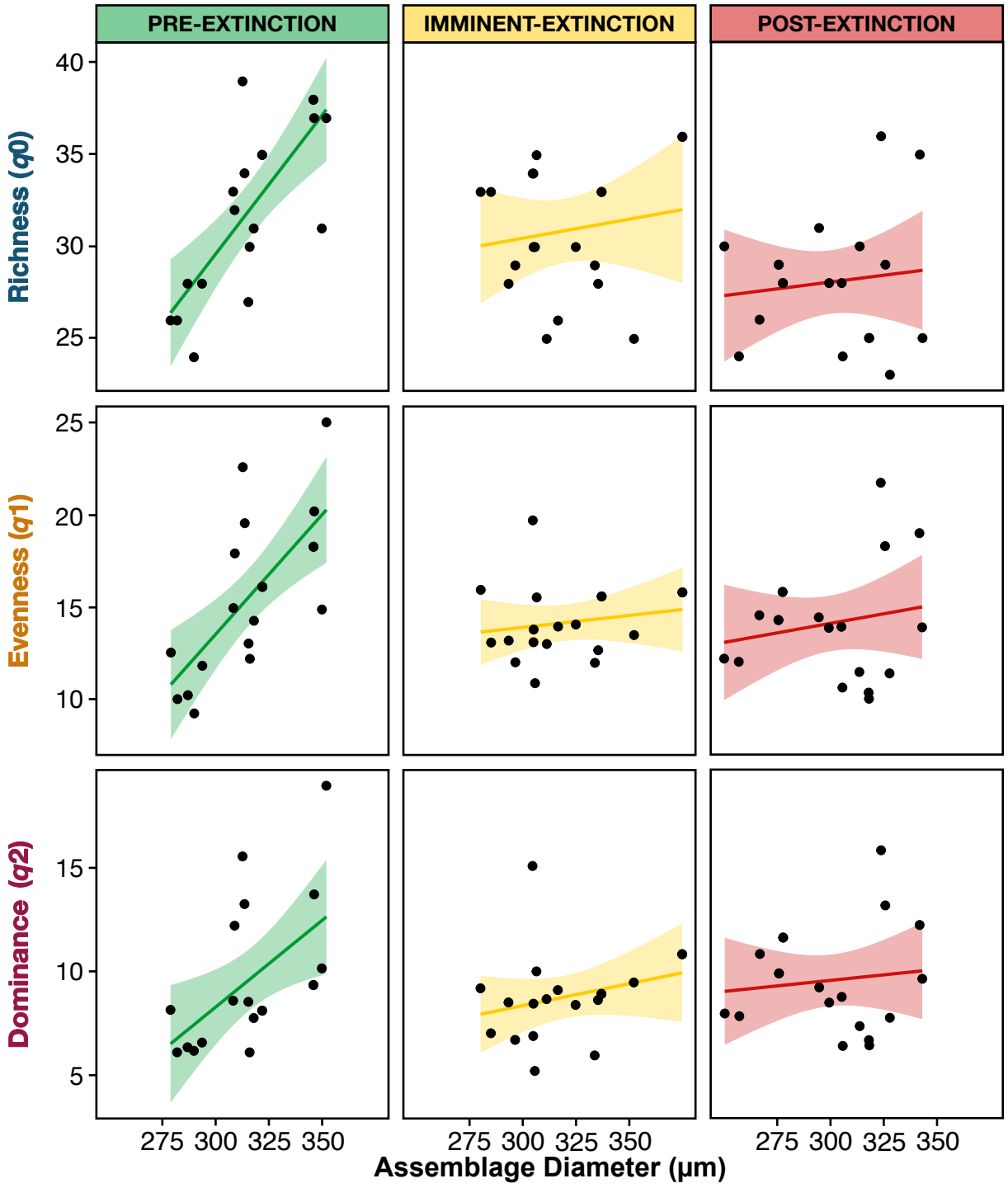

Figure 4.3 Change in regression slopes and strengths for mean assemblage diameter (µm)and diversity profiles (*q*0, *q*1, and *q*2) for pre- (green), imminent- (yellow), and post-extinction (red) intervals, with 95% confidence interval band from linear regressions.

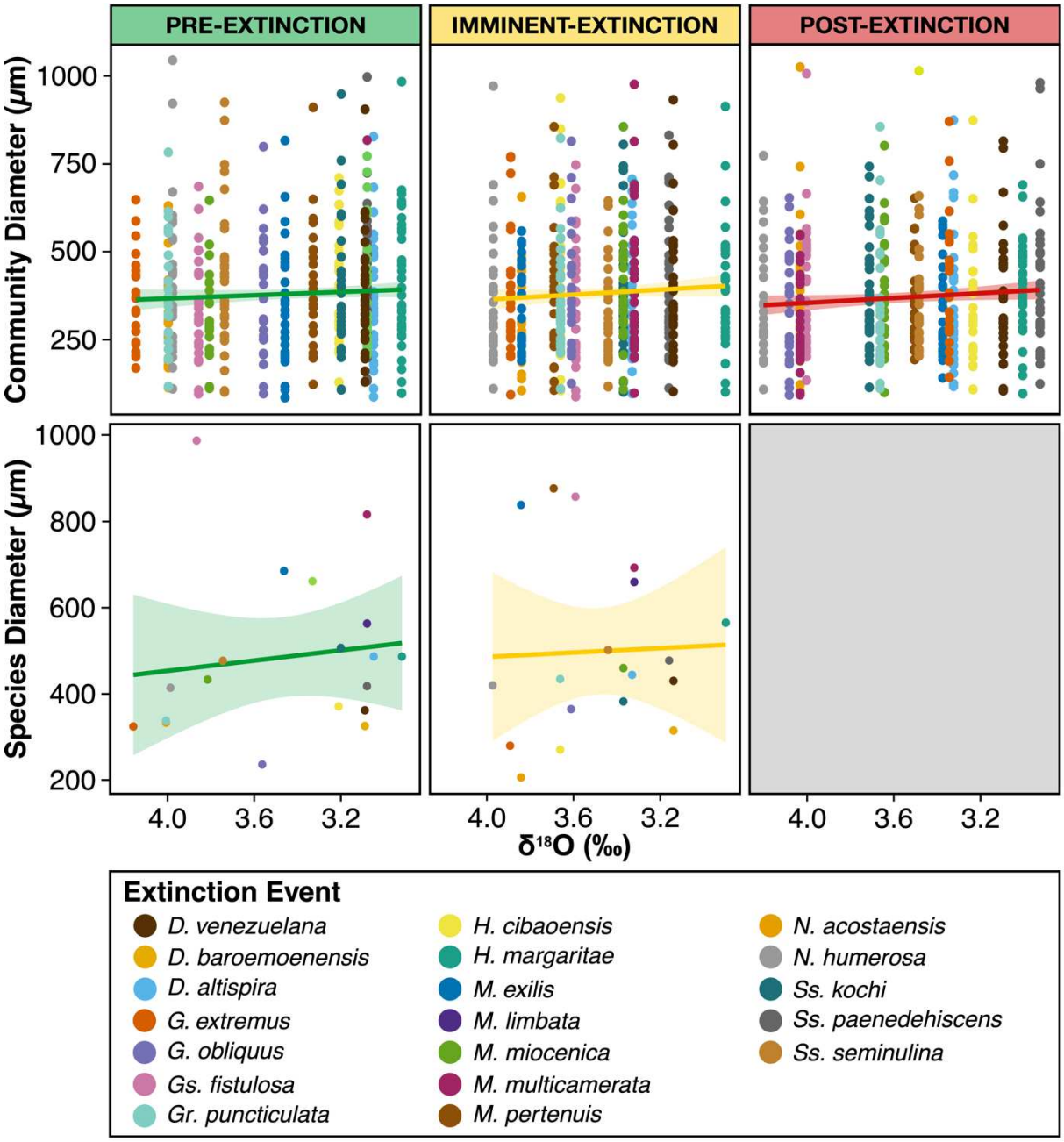

Figure 4.4 Change in regression slopes and strengths for community assemblage diameter (μm; top panel) and extinct-going species diameter (μm; bottom panel) with diversity oxygen isotopes ($\delta^{18}O$ (‰); Lisiecki and Raymo, 2005) for pre- (green), imminent- (yellow), and post-extinction (red) intervals, with 95% confidence interval bands from linear regressions. Each colour (see key) represents each of the 19 species extinction events, with each point in the community assemblage representing a different species and each colour in the species diameters representing the extinct-going species.

The community level results above demonstrate clear trends through time but cannot pinpoint whether those changes are due to individual species getting larger or smaller or due to the whole assemblage changing consistently. The variation in foraminiferal size and species-specific results (**Figure 4.4**) indicates a clear scope for different responses amongst species. As such, the community-level analysis was followed up with a mixed-effect model that controls for differences amongst species as a random effect.

The mixed effects models show the fundamental importance of species differences in understanding trait dynamics. The difference in AIC scores, a combination of model likelihood and a penalty for model complexity, between models of maximum diameter with and without Species ID is largest (AIC = 20063.43), followed by climate ($\delta^{18}O$; AIC = 40), dominance (*q*2; AIC = 22), and the interaction between climate the extinction phases (AIC = 19) (**Figure 4.5**). Unlike in Error! Reference source not found., where the intervals are the strongest control on biodiversity, here climate and q2 are better models for trait change. Although taxon counts such as species richness (*q*0) are a common form of biodiversity metric, *q*0 is a much weaker predictor of changes in maximum diameter than either *q*1 (evenness) or *q*2 (dominance).

Figure 4.6 shows the regression coefficients of each fixed effect in the final linear mixed model, which were scaled to allow for easier comparison, as the variables are measured on different scales. Here we analyse climate, *q*0, *q*1, *q*2, and the interactions between the slope/gradient of the climate relationship from the imminent- to pre-extinction phase (Climate:Imm -> Pre) and from imminent- to post-extinction phase (Climate:Imm -> Post). Climate is ranked second on model influence (**Figure 4.5**) but has a smaller scaled coefficient (coef = -0.013, s.e. = 0.008), albeit with a tighter 95% confidence interval than *q*1 (coef = 0.040, s.e. = 0.020) or *q*2 (coef = -0.035, s.e. = 0.015) (**Figure 4.6**). As with the influence analysis (**Figure 4.5**), the scaled coefficient for species richness (*q*0; coef = -0.010, s.e. = 0.010) is less influential than either *q*1 or *q*2 (**Figure 4.6**). In summary, the results reinforce the centrality of differences amongst species for trait dynamics and the role of climate changes in shaping trait dynamics through extinctions, but also suggest a role for community composition, as represented by *q*1 and *q*2, in determining the size of individual foraminifera within assemblages.

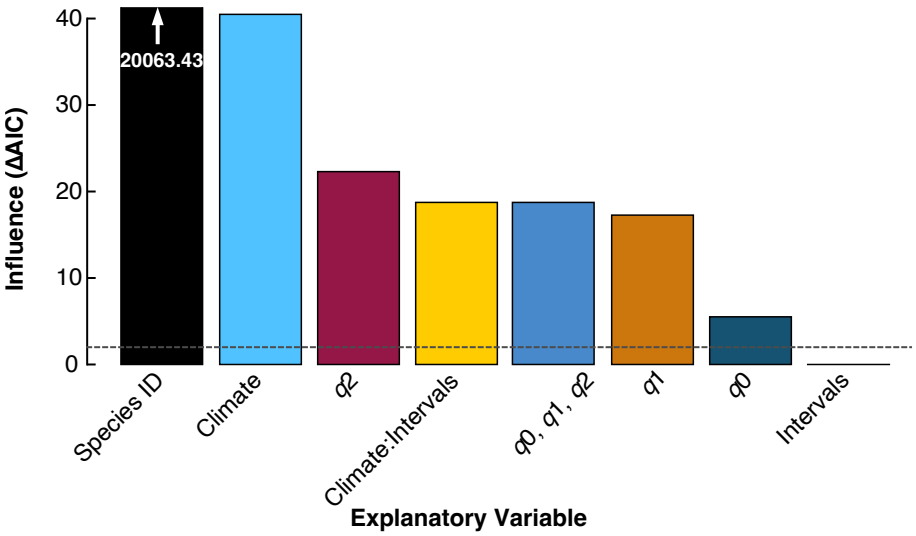

Figure 4.5 Comparison of the difference in Akaike Information Criterion (AIC) values between the full model and the model with the named term removed; the height of the bar is the difference in AIC scores and thus the change in model likelihood and associated penalty for model complexity due to the named term (a bigger difference implies the term is more influential, and vice versa). Species identification (ID) is the random effect and is measured by comparing a generalised least square (GLS) without random effect to the full model, with Climate (represented by $\delta^{18}O$), extinction intervals (Intervals), each of the Hill numbers (*q*0, *q*1, *q*2) and the Climate: Interval interaction as fixed effects compared within linear mixed effect (LME) models. Both GLS and LME comparisons were made in the nlme package (Pinheiro et al., 2024).

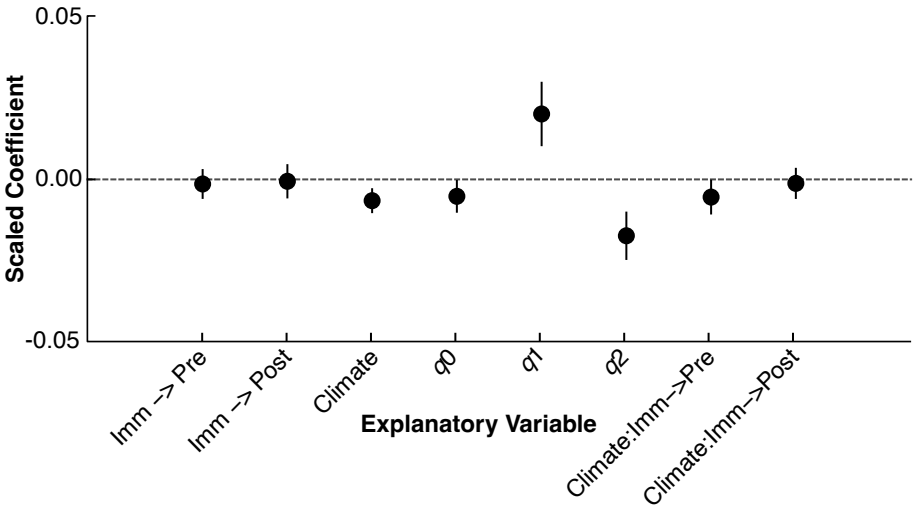

Figure 4.6 Scaled regression coefficients of each fixed effect in the final linear mixed model. Coefficients were scaled to facilitate comparison, given the different measurement scales. Arrows denote the term associated with a shift from imminent- to pre-extinction phase (Imm -> Pre) and imminent- and post-extinction phase (Imm -> Post). The interactions, indicated using colons, show the difference between the slope/gradient of the climate relationship from the imminent- to pre-extinction phase (Climate:Imm -> Pre) and from imminent- to post-extinction phase (Climate:Imm -> Post). Error bars show 95% confidence intervals and highlight that while climate has the strongest influence on model fit (**Figure 4.5**), a proportional change in *q*1 or *q*2 can have a proportionally larger effect size on mean size.

4.4 Discussion

Since planktic foraminiferal growth is influenced by environmental fluctuations, size changes are often closely tied to extinction events, making morphological analysis a key tool for understanding these dynamics. This study reveals that while species differences are crucial for understanding trait dynamics, as indicated by the largest difference in AIC scores (**Figure 4.5**), climate ($\delta^{18}O$), evenness (*q*1), and dominance (*q*2) also significantly influence trait changes. Species richness (*q*0) is less predictive of changes in planktic foraminiferal size, reinforcing that community composition and species-specific responses, along with environmental factors, are key in shaping size dynamics across extinction phases. The observed decline in species diversity and the relationship between test maximum diameter and environmental variables largely match the trends previously observed at a temporal level. However, the relationship breaks down across extinctions with species-specific responses to climate change.

The assumption that planktic foraminifera are invariably stressed in the interval preceding extinction events is a prevalent notion in palaeoecological studies; however, its universal applicability warrants scrutiny. While environmental stressors such as climate change, ocean acidification, and shifts in nutrient availability often precede extinction events, leading to observable stress indicators in foraminiferal assemblages, this pattern is not consistent across all species or events (Keller and Abramovich, 2009). Some foraminiferal species exhibit resilience or even thrive temporarily due to ecological release or adaptive advantages (Weinkauf et al., 2019).Moreover, the fossil record is subject to biases, including sampling and preservation biases, which can influence the detection and interpretation of stress indicators (Lloyd *et al.*, 2012). Therefore, while stress is a plausible factor leading to extinction, it should not be assumed as a universal precursor without supporting evidence from multiple lines of data, including stable isotope analysis, population dynamics, and sedimentological context.

The analysis of planktic foraminiferal size dynamics in response to environmental factors reveals important insights into extinction processes and community restructuring over time. The marginal decline in mean assemblage diameter from 3.9 to 1.0 million years ago correlates with fluctuations in the global $\delta^{18}O$ record, demonstrating that foraminifera tend to grow larger during warmer interglacial periods, where $\delta^{18}O$ values are lower (**Figure 4.1**). This suggests that warmer conditions, associated with greater food availability and metabolic efficiency (Kucera, 2007; Lombard *et al.*, 2010), promote larger test sizes in foraminifera in the Plio-Pleistocene. This observation aligns with previous studies linking climate fluctuations to changes in foraminiferal size, particularly in periods of environmental stress like glacial-interglacial cycles (Keller and Abramovich, 2009).

Interestingly, the relationship between assemblage size and environmental variables weakens as extinction events approach (as in Error! Reference source not found. with biodiversity). The strong correlation between the mean assemblage size and climate during the pre-extinction phase diminishes in the imminent- and post-extinction phases (**Figure 4.3**), suggesting the assemblage's sensitivity to environmental changes becomes less pronounced, potentially due to the selective pressure on species with less optimal growth conditions, which could lead to the extinction of those species with narrower ecological niches. Species with narrower ecological niches, e.g., those more specialised and less adaptable to changing environments, are typically more vulnerable to extinction, whereas generalist species, which can tolerate a broader range of environmental fluctuations, tend to persist longer (e.g., Colles, Liow and Prinzing, 2009). For example, environmental stressors in marine ecosystems, such as increased ocean temperatures and decreased pH levels, disproportionately affect species with narrow habitat preferences (Payne and Finnegan, 2007; Harnik *et al.*, 2012). Ultimately, as environmental conditions deviate further from the optimum, specialised species decline, with increased function redundancy, reduced biodiversity and an increase to the risk of ecosystem collapse (Canadell and Jackson, 2021).

The species-specific responses to climate further highlight the complexity of extinction dynamics. The analysis of individual species shows a complex pattern, with some species exhibiting a decrease in size before extinction, potentially as a response to environmental stressors, while others increased in size. The species-specific responses to $\delta^{18}O$ indicate that different species had varying tolerances to temperature changes, which could reflect their differing ecological roles and adaptive strategies. For instance, species like *N. acostaensis* and *G. extremus* showed a decrease in size with increasing temperatures, suggesting that warmer conditions were detrimental to their growth (**Figure 4.3**). Conversely, species such as *Gs. fistulosa* and *S. seminulina* increased in size with cooling, indicating a preference for or better adaptation to cooler conditions (**Figure 4.3**). This variability suggests that not all species respond uniformly to environmental stressors, and the observed dwarfing effect (e.g., Wade and Olsson, 2009) is not a universal response among extinct-going species. This not only highlights the complexity of extinction dynamics but also raises important questions about the role of trophic state in shaping foraminiferal size patterns. Understanding how nutrient availability and metabolic efficiency influence test size is crucial for interpreting the adaptive strategies of foraminifera, particularly in the context of past oceanographic changes observed at ODP Site 925.

The trophic state at Site 925 is shaped by surface productivity, nutrient availability, and ocean circulation, impacting planktonic foraminifera (Chaisson and Pearson, 1997). Geochemical proxies like $\delta^{13}C$ and $\delta^{15}N$, along with assemblage shifts, indicate trophic fluctuations (Adebayo *et al.*, 2023). Nutrient availability directly regulates foraminiferal growth, test size, and

population dynamics (Schiebel and Hemleben, 2017), but species-specific responses complicate the size-trophic state relationship with metabolic efficiency influences foraminiferal size (Tyszka *et al.*, 2017). Larger foraminifera face surface-to-volume ratio challenges, while smaller ones, with higher ratios, enhance nutrient uptake, particularly in oligotrophic conditions (Grigoratou *et al.*, 2019).Smaller sizes also lower metabolic demands and enable faster reproduction, offering survival advantages (Schmidt *et al.*, 2006). Therefore, trophic state shifts influence size distributions, with smaller foraminifera potentially thriving in nutrient-poor settings. This could explain the community size variation at Site 925, as not just a stress response but an adaptation to trophic fluctuations. This complexity in size in response to environmental change underscores the importance of species-specific ecological roles and adaptive strategies in determining survival outcomes during extinction events.

The role of ecogroups and morphogroups in extinction dynamics further reinforces species-specific trends, highlighting the complexity of extinction processes. While ecogroup and morphogroup classifications provide valuable ecological and functional context, they were not strong predictors of size change before extinction, despite some groups showing tendencies toward increasing or decreasing test size. This suggests that ecological function alone does not determine size responses and that species-level traits, including individual adaptations and environmental tolerances, may be more influential. The lack of statistical significance in these classifications further indicates that morphological traits such as test shape, chamber arrangement, or ornamentation did not uniformly dictate extinction risk, reinforcing the idea that species-specific characteristics played a greater role. However, narrow ecological niches are more susceptible to extinction, even if species exhibit adaptive niche migration in response to environmental changes (Woodhouse *et al.*, 2021). This increased susceptibility is attributed to the limited adaptability of specialist species to rapid or extreme environmental fluctuations, underscoring that niche specialisation can heighten extinction risk despite adaptive behaviours. Here, we see the disappearance of nine species within morphogroup 7 (non-spinose, globular forms) and six species of morphogroup 8 (non-spinose, keeled globorotaliforms), which are often within proximity of each other. This suggests that these groups were unable to adapt to environmental changes, reinforcing the claim that niche specialisation can increase extinction risk.

A key implication of these findings is the role of functional redundancy in ecosystem stability. High redundancy within ecogroups may help buffer against species loss, whereas low redundancy could make ecosystems more fragile to environmental perturbations (Laliberté *et al.*, 2010; Mouillot *et al.*, 2014). Additionally, species with morphological plasticity may have been better able to adapt to environmental changes, while highly specialized traits may have increased extinction risk (Finnegan *et al.*, 2015; Payne *et al.*, 2016). The weak correlation

between morphogroup classification and size change suggests that morphology alone does not dictate extinction outcomes. Instead, survival likely depended on a combination of functional traits, ecological strategies, and physiological tolerances, further supporting the idea that extinction is not random but is shaped by evolutionary and ecological factors, often favouring generalists over specialists (Jablonski, 2005; Harnik *et al.*, 2012).

The consequences of these extinction dynamics become even more apparent when considering the post-extinction community structure. The post-extinction reduction in the remaining community assemblage size (**Figure 4.3**) suggests that the selective pressures acting on pre-extinction species not only influenced individual survival but also shaped the functional diversity of the ecosystem. As species with unique morphological traits were removed, the overall assemblage size declined, indicating a potential loss of functional diversity within foraminiferal communities(Hull and Norris, 2011; Lombard *et al.*, 2011). The Lilliput Effect (Keller and Abramovich, 2009), commonly observed after mass extinctions, supports the notion that surviving species are typically smaller and less functionally diverse. Such a shift towards a simplified ecosystem may have long-term implications, as reduced functional diversity can make communities more vulnerable to subsequent environmental perturbations (MacDougall *et al.*, 2013; Biggs *et al.*, 2020). The link between pre-extinction species-specific responses and post-extinction community restructuring highlights the importance of understanding extinction not only as an event of species loss but as a driver of broader ecological and evolutionary change.

Additionally, while climate undoubtedly plays a significant role in shaping foraminiferal size, community composition and biodiversity metrics such as evenness and dominance also exert a considerable influence. Mixed-effects models indicate that species evenness ($q1$) and dominance ($q2$) are strong predictors of size variation (**Figure 4.5**, **Figure 4.6**), reinforcing the idea that community structure and diversity impact how individual species respond to environmental pressures. This aligns with the "optimum-size hypothesis," which suggests that planktic foraminifera reach their maximum size under optimal environmental conditions, typically when species diversity and abundance are high (Schmidt *et al.*, 2004; Moller, Schulz and Kucera, 2013). Thus, the mixed effects models and scaled coefficients emphasise the importance of both species-specific traits and environmental factors in shaping foraminiferal size.

However, isolating biotic factors from environmental influences on planktic foraminiferal size remains challenging due to several factors. Planktic foraminifera have complex life cycles, with various growth stages and reproductive strategies (Hemleben, Spindler and Anderson, 1989; Schiebel and Hemleben, 2017), making it difficult to pinpoint specific biotic influences on size. Furthermore, testing for competition in planktic foraminifera is challenging, as there is not

enough ecological knowledge to explicitly test for it in their fossil record (Rillo, 2019), and modern planktic foraminifera show no evidence of resource limitation and thus competition at high densities (Rillo *et al.*, 2019). Environmental fluctuations like changes in temperature and nutrient availability indirectly affect these biotic factors (Kucera, 2007), making it hard to isolate their specific impacts. Moreover, evolutionary adaptations over millions of years, shaped by both biotic and abiotic pressures (Norris, 1991; Schmidt, Thierstein, *et al.*, 2004; Rillo *et al.*, 2019), complicate the task of disentangling the specific biotic factors that regulate size. This highlights the need for more comprehensive studies integrating abiotic and biotic factors to better understand trait dynamics in planktic foraminifera across geological timescales.

4.5 Conclusions

This study demonstrates that while species differences are crucial in understanding trait dynamics, environmental factors such as climate and biodiversity, particularly evenness and dominance, significantly influence planktic foraminiferal size. Maximum test sizes correspond with peak abundance and optimal temperatures, supporting the "optimum-size hypothesis." However, this correlation weakens during extinction events, suggesting a decreased sensitivity to climate changes as extinctions approach. Additionally, species-specific responses to temperature fluctuations vary, with some species decreasing in size in warmer conditions and others increasing in size during cooler periods. The presence of the Lilliput Effect, where extinction events lead to smaller post-extinction community sizes, points to a potential reduction in functional diversity, which could result in less resilient ecosystems. Furthermore, while ecogroups and morphogroups offer useful ecological and functional context, they do not fully explain species' extinction risk or size changes. The observed variability suggests that broader classifications may overlook species-specific traits that influence survival. These findings emphasize the challenges in isolating biotic influences due to the complex life cycles of foraminifera, limited competition evidence, and the impact of long-term evolutionary adaptations. Instead, a trait-based approach, integrating morphology, ecology, and physiology, may provide a clearer framework for assessing extinction selectivity.

In conclusion, these findings highlight the complexity of species-specific responses to climate change and the need for more species-specific studies to better predict future biodiversity loss amid ongoing climate change. The varied responses among planktic foraminifera suggest that future climate shifts may have diverse impacts on marine communities, with some species more susceptible to extinction depending on their ecological traits and adaptability. Future research should focus on linking species-specific traits to extinction vulnerability, particularly in the context of climate change and environmental instability. Understanding the functional roles

of species will be essential to enhancing predictions of biodiversity loss and understanding ecosystem resilience in the face of rapid environmental change.

Chapter 5 Conclusion

5.1 Synthesis

This thesis explores the interrelated links across traits, species and communities in planktic foraminifera during the Plio-Pleistocene climate change**.**

Chapter 2 explores the challenges and importance of precise taxonomic classification in the study of planktic foraminifera. The research underscores the limitations of relying solely on outdated taxonomic descriptions and proposes a shift toward quantitative morphometric analysis to update species descriptions. By applying statistical methods like Principal Component Analysis (PCA) and Gaussian Mixture Models (GMM), the study provides a more objective way to differentiate these species based on specific traits. The findings reveal that *Menardella limbata* and *Menardella multicamerata* exhibit subtle yet statistically significant differences in the shape and size of their final chambers. These quantitative methods represent a significant advancement in the field, enabling clearer, more reliable species identification, which in turn enhances our understanding of evolutionary relationships.

Error! Reference source not found. focuses on the broader impact of environmental changes on biodiversity, particularly examining the relationship between climate fluctuations over the past 4 million years with tighter sampling through species' extinction events. Although direct measurements of past foraminiferal density are unavailable, making it difficult to assess biotic competition, sediment core accumulation rates may provide indirect insights into relative abundance trends and potential competitive interactions over time. This chapter's detailed analysis of species assemblages demonstrates that biodiversity declines in cooler, glacial periods, with lower temperatures correlating with reduced species richness. However, it also highlights the resilience of marine ecosystems. Functional diversity, particularly species evenness, is key in buffering communities against environmental disturbances. High evenness, where species are more equally represented, leads to greater stability, whereas dominance by a few species can reduce overall resilience. This balance between species richness and evenness offers insights into how ecosystems have historically responded to climate change and provides a framework for understanding future biodiversity trends under predicted warming scenarios.

Furthermore, the chapter's use of Hill numbers, which integrate richness, evenness, and dominance, provides a nuanced view of community structure. These metrics allow researchers to capture complex dynamics across extinction events and examine how communities reorganise as they lose or gain species. The chapter underscores the critical need for

multifaceted biodiversity measures to predict how assemblages might respond to ongoing climate changes.

Chapter 4 takes a closer look at extinction events and their effects on planktic foraminiferal size during individual species extinctions of the past 4 million years. The analysis reveals a decoupling of abiotic controls (such as temperature) on community structure during extinction phases. Prior to extinction, abiotic factors like changes in oxygen isotope levels (reflecting temperature and ice volume) strongly correlate with size. However, this correlation weakens as extinction approaches (as in Error! Reference source not found.), suggesting that biotic interactions, such as functional redundancy, could be taking over in regulating community dynamics. In the post-extinction phase, the community shows resilience, with biodiversity stabilising and species composition reorganising in response to the loss of species. Yet, there are weaker predictive powers of species richness on trait dynamics but stronger roles of dominance and evenness. This biotic-driven recovery process ensures that ecosystems are not permanently destabilised by extinction events.

One key insight from this chapter is that while species richness declines during extinction events, the overall stability of the community's relationship with climate appears to remain relatively intact. The community appears to adjust to environmental changes, maintaining a level of resilience through shifts in dominance and evenness. The chapter concludes that while climate changes are a major driver of biodiversity loss, ecosystems have inherent mechanisms that allow them to buffer against these changes, re-establishing equilibrium after periods of volatility.

Together, these findings have significant implications for understanding how marine ecosystems respond to environmental changes over geological timescales. The insights gained from these studies can also inform predictions about how current and future climate change might impact biodiversity, particularly in terms of species extinctions and the resilience of ecosystems. By advancing both the methodologies used to study species and understanding how species interact with their environments, this research contributes to the broader goal of reconstructing past oceanographic conditions and predicting the future impacts of climate change on marine life.

Beyond this thesis, the dataset produced has broader applications in identifying patterns in species distributions and reconstructing ecosystem changes over geological timescales, particularly in relation to species abundance and size dynamics. It can also be utilised to explore which species or functional groups are most vulnerable to climate change; an aspect briefly addressed in Chapter **4** but not the primary focus of this study. Additionally, it provides an opportunity for a more detailed examination of individual species' responses to extinction

events, offering deeper insights into the mechanisms driving biodiversity loss and ecosystem resilience.

5.2 Future work

Building on these findings, future work could deepen our understanding of taxonomy, climate-driven biodiversity shifts, and extinction dynamics within planktic foraminifera.

1. **Further Development of Quantitative Taxonomy:** While this research highlights the success of quantitative methods in distinguishing species like *Menardella limbata* and *M. multicamerata*, future studies should refine and expand these methods across a broader range of taxa. Integrating machine learning algorithms and 3D morphometric analyses could offer faster, even more precise species identification and reduce subjectivity. Beyond morphology, incorporating functional and life history traits such as growth rates and ecological roles (e.g., Brombacher *et al.*, 2022; Mulqueeney *et al.*, 2024), could provide a more comprehensive understanding of the differentiation between species. Expanding these methods to understand taxa could resolve taxonomic ambiguities and improve reconstructions of evolutionary and environmental changes over time. These advancements will enhance taxonomy's role in palaeoceanography and climate science.

2. **Linking Environmental Proxies with Species-Specific Responses:** While this research correlates general environmental factors such as temperature and salinity (Kucera, 2007) with biodiversity and size in planktic foraminifera, future studies should focus on linking other specific environmental proxies (e.g., Mg/Ca for sea surface temperature and pCO_2 for ocean acidification) to species-specific responses in planktic foraminifera size (e.g., Todd *et al.*, 2020; Kinoshita *et al.*, 2022). Especially as size variation in planktonic foraminifera cannot be consistently explained by temperature across different species (Chapter 4; Rillo *et al.*, 2020). High-resolution geochemical and isotopic analyses combined with species-specific morphometrics (e.g., Kearns *et al.*, 2021) could provide more detailed insights into how individual species adapt or perish in response to environmental stressors.

3. **Investigating Post-Extinction Community Recovery:** The resilience of marine ecosystems after extinction events is a key finding in this research with its novel sampling focus through and around particular extinction events. Future work should focus on understanding the mechanisms of post-extinction recovery in more detail (e.g., BSc project on *Gs. fistulosa* – on which I supervised). Specifically, identifying which traits or species interactions contribute to community stability after species loss could offer

insights into how ecosystems might recover from future extinctions (Simmons *et al.*, 2020; She *et al.*, 2023). Additionally, long-term studies tracking the recovery and reorganisation of species assemblages after modern extinction events could provide valuable real-time data.

4. **Assessing the Impact of Future Climate Scenarios:** With the rapid pace of current climate change (IPCC, 2021), future studies should model how predicted environmental changes might affect planktic foraminiferal biodiversity and extinction rates. By integrating paleoenvironmental data with modern climate projections, researchers could better predict biodiversity loss, ecosystem shifts and species resilience. Using Earth system models and species-environment correlations, future research can assess changes in species distributions, extinction risks, and potential refugia. Additionally, studying biotic interactions under future climate conditions will help determine whether stabilizing mechanisms like functional redundancy can maintain ecosystem resilience. These insights will be crucial for informing conservation strategies and predicting marine ecosystem responses to climate change.

By pursuing these avenues, future research can build upon the foundations laid by this work, providing a more detailed and predictive understanding of how species and ecosystems respond to both gradual environmental changes and sudden extinction events.

5.3 Concluding remarks

This thesis investigates the impact of biotic and abiotic controls on extinction and community dynamics in planktic foraminifera during the climatic fluctuations of the Plio-Pleistocene. The findings provide important insights into long-term biodiversity dynamics and ecological shifts. It emphasises the need for more precise, quantitative methods in species identification, as traditional approaches fall short in distinguishing closely related species. Furthermore, the findings highlight the resilience of marine ecosystems, showing that functional diversity and biotic interactions play vital roles in stabilising communities in the face of environmental shifts and extinction events.

Looking forward, the proposed future works suggest several key areas for expanding this research. Refining quantitative taxonomy and integrating more environmental proxies with species responses are essential next steps. Additionally, modelling the impacts of future climate scenarios and studying post-extinction recovery processes could offer predictive insights into how marine ecosystems might adapt or collapse under ongoing climate pressures. Together, this thesis and future directions offer a comprehensive framework for addressing

pressing questions about biodiversity, climate change, and extinction, with implications for both palaeoecological research and modern conservation efforts.

Appendix A Supplementary Material for Chapter 2

A.1 Pilot study for Chapter 2

Four samples from ODP Site 925 were selected for the pilot study at 2.950, 3.101, 3.251, and 3.402 Ma, ensuring even distribution throughout the study period while avoiding proximity to extinction events (see **2.2.1 Materials**). For each sample, all available specimens of suspected *Menardella (M.) limbata* and *Menardella (M.) multicamerata*, based on the original descriptions (see **Chapter 2**), were picked until a total of 15 specimens each were selected from the 2.95 Ma and 3.25 Ma samples, and 30 specimens each from the 3.10 Ma and 3.40 Ma samples, yielding a total of 90 specimens. The two former samples had fewer well-preserved and distinguishable specimens and were therefore excluded from the final study.

Following the methodology outlined in Chapter **2** (**2.2.2 Methods**), the specimens were mounted, imaged and analysed. Based on the original species descriptions (see **Chapter 2**) 59 specimens were identified as *M. limbata* and 31as *M. multicamerata*, though no clear clustering was observed (**Figure A1.1a**). The non-priori clustering via Gaussian Mixture Models, without prior species assignment, divides the specimens into 45 of each representative morphotype (**Figure A1.1b**). Despite the lack of distinct clustering, these results indicated that M. multicamerata may be more abundant than previously suggested by traditional descriptions.

Based on this, other studies (e.g., (Blow, 1969; Mary, 2013) and specimen observations within the samples, I hypothesised that *M. multicamerata* may be more abundant than previously suggested by traditional descriptions, with specimens having fewer chambers than 8 in the final whirl. As discussed in **Chapter 2**, this complicates the descriptions further and highlights the need for a more reliable distinguishing feature. Given the increasing overlap in final whorl chamber counts, I proposed that the key differentiating trait lies in the shape and size of the final chamber relative to the overall test. Applying this identification method resulted in 37 classified as *M. limbata* and 63 as *M. multicamerata* (**Figure A1.1c**), resulting in more *M. multicamerata*. While there is no clear clustering, there are slightly stronger trends in both species. To validate this hypothesis, the study was expanded to 1,000 specimens, and additional measurements and more in-depth analysis of morphological traits were incorporated to enhance species differentiation.

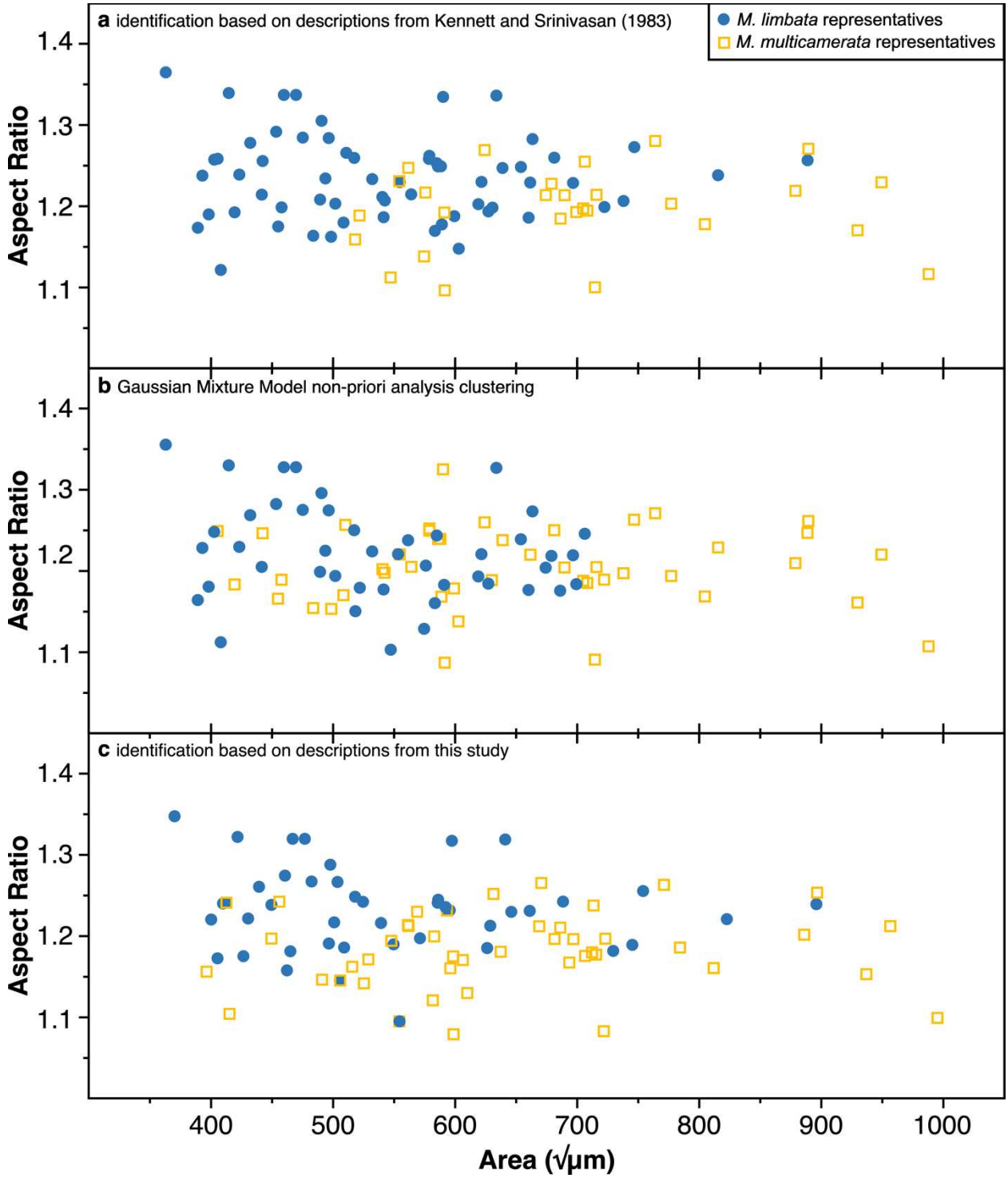

Figure A1.1 Whole test trait based species clusters at 2.950, 3.101, 3.251 and 3.402 Ma combined, distinguishing between *M. multicamerata* and *M. limbata* via **a)** Kennet and Srinivasan (1983) species descriptions, **b)** Gaussian Mixture Model analysis with non-priori clustering, and **c)** hypothesised morphological differences from this study. Closed blue circles = *Menardella limbata* representatives and open yellow squares = *Menardella multicamerata* representatives.

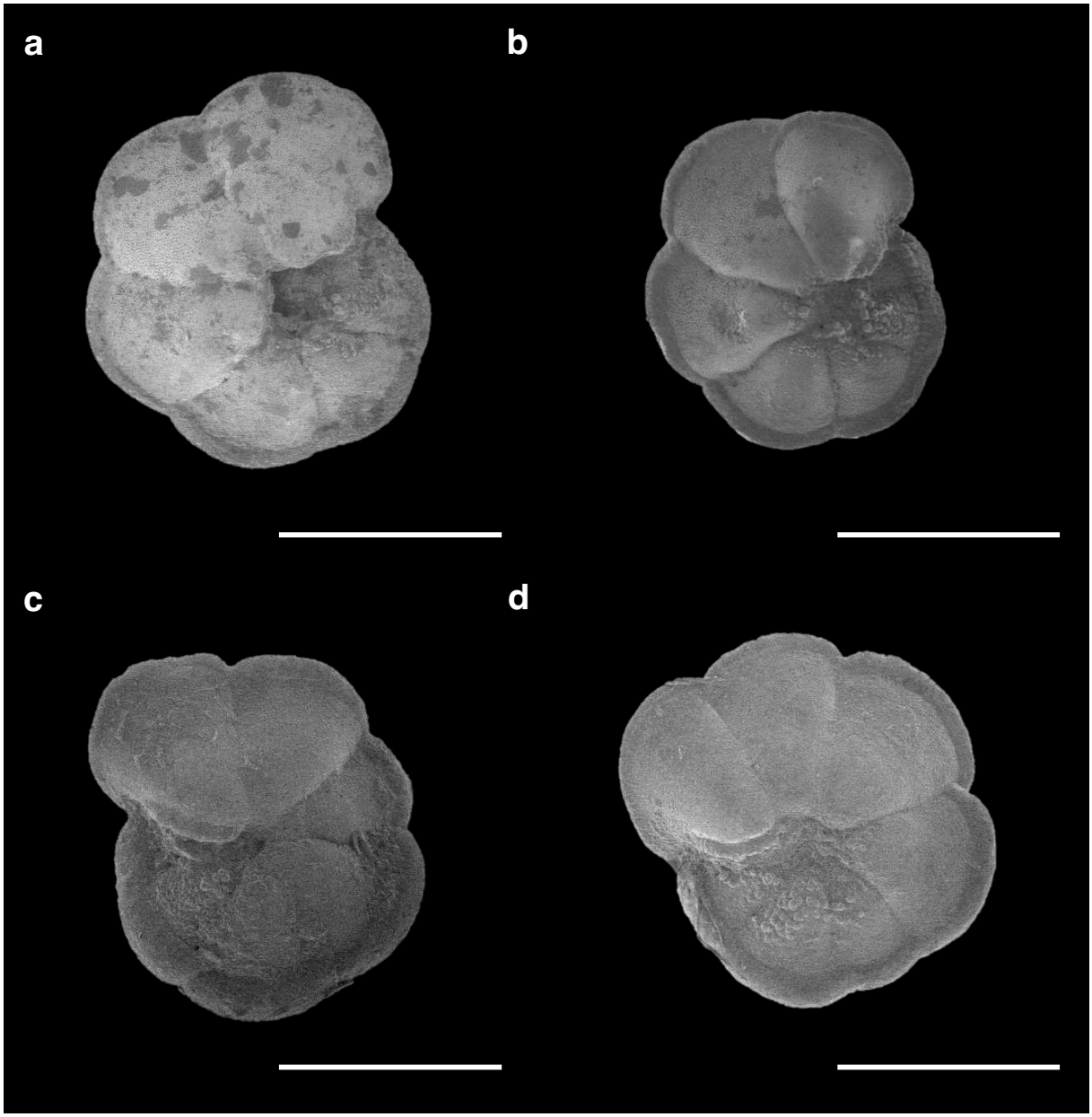

Figure A.1 Type specimens of Miocene *Menardella* species: **a-b)** hypotype specimens of *Menardella limbata* and **c-d)** holotype specimens of *Menardella multicamerata*. The scale bar is 500 µm.

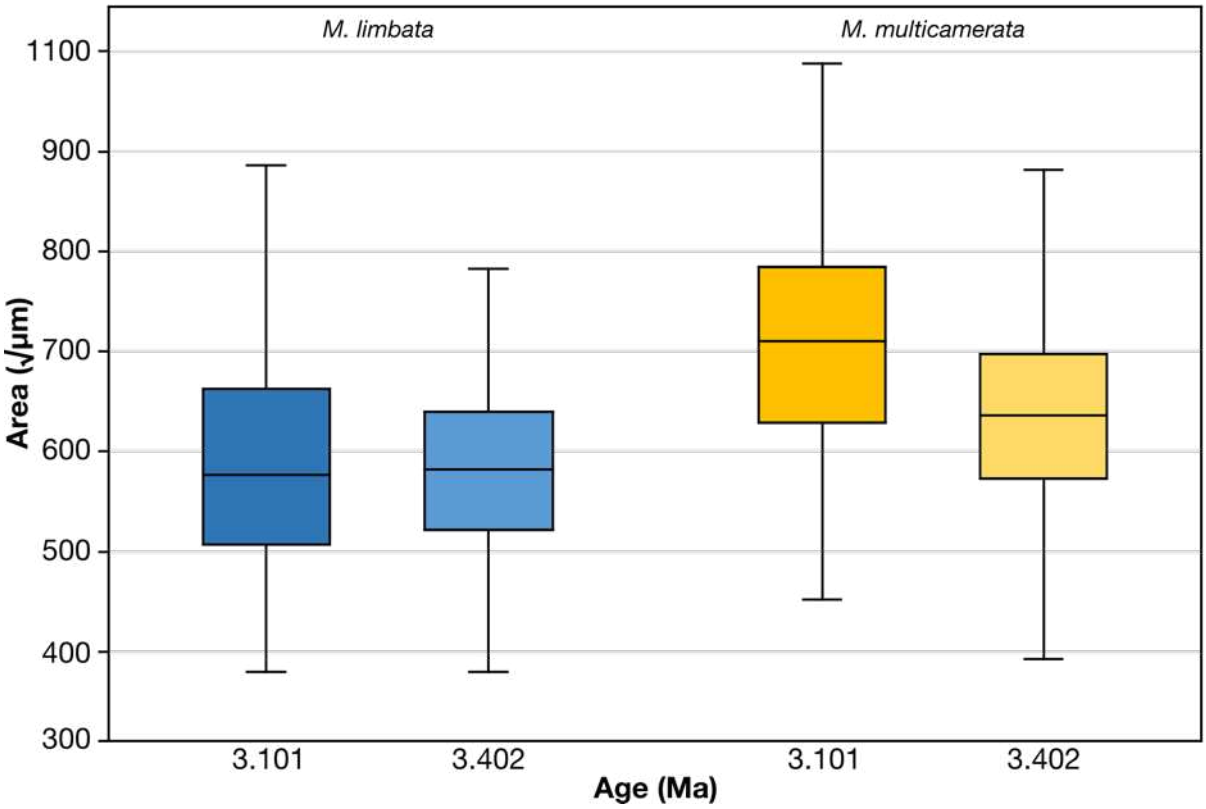

Figure A.2 Square root of the whole test area (√µm) of *Menardella limbata* (light to dark blue) and *Menardella multicamerata* (light to dark yellow) across 3.101 and 3.402 Ma.

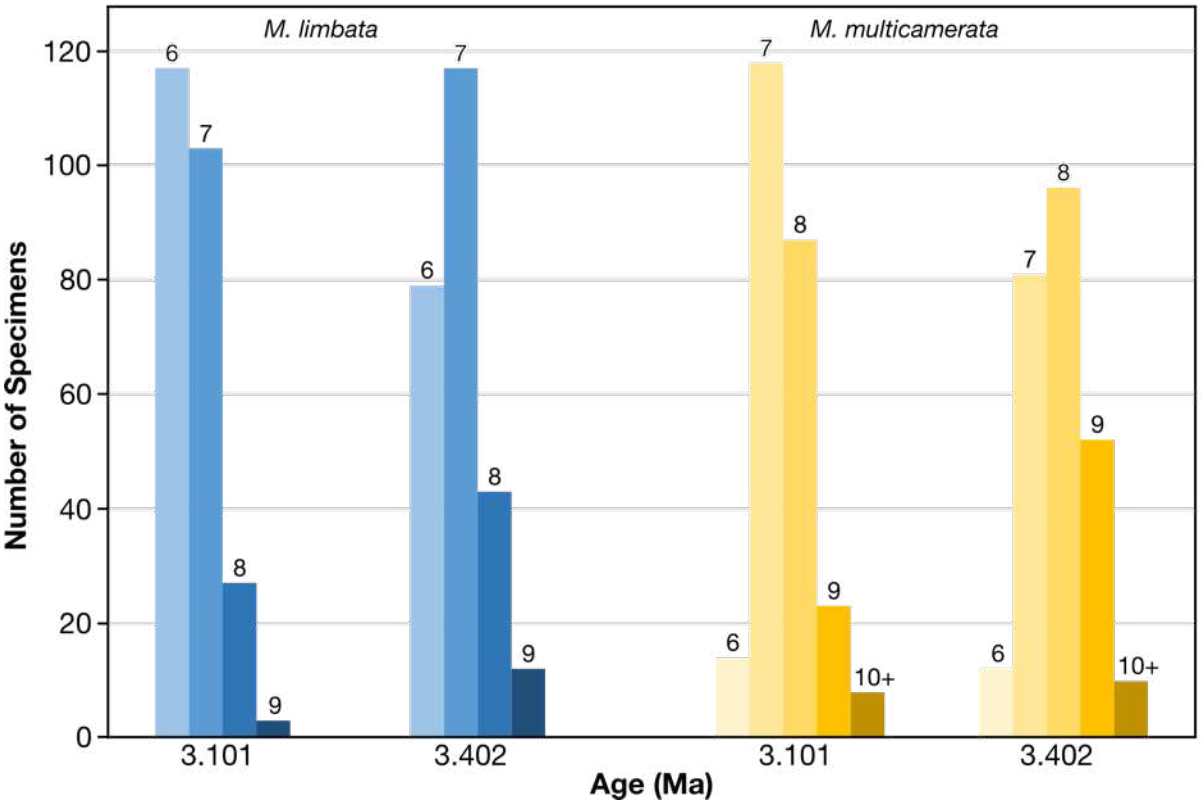

Figure A.3 Number of specimens of *Menardella limbata* (light to dark blue) and *Menardella multicamerata* (light to dark yellow) across 3.101 and 3.402 Ma for each group of final whorl chamber number.

Table A.1 The whole test area (√µm) range and mean of *Menardella limbata* and *Menardella multicamerata* for 3.101 and 3.402 Menardella and for 3.101 and 3.402 Ma combined (All), with standard deviation and 95 % confidence interval.

Species	***Menardella limbata***			***Menardella multicamerata***		
Age	**3.402**	**3.101**	**All**	**3.402**	**3.101**	**All**
Test area range (√µm)	363.01 – 767.34	380.97 – 949.45	363.01 – 949.45	389.27 – 879.95	449.91 – 988.09	389.27 – 988.09
Test area mean (√µm)	569.98	594.78	581.86	633.36	709.66	671.36
Standard deviation	77.65	105.52	93.35	91.55	100.20	103.19
Confidence interval (95%)	0.408	0.418	0.262	0.362	0.397	0.289

Appendix B Supplementary Material for Error! Reference source not found.

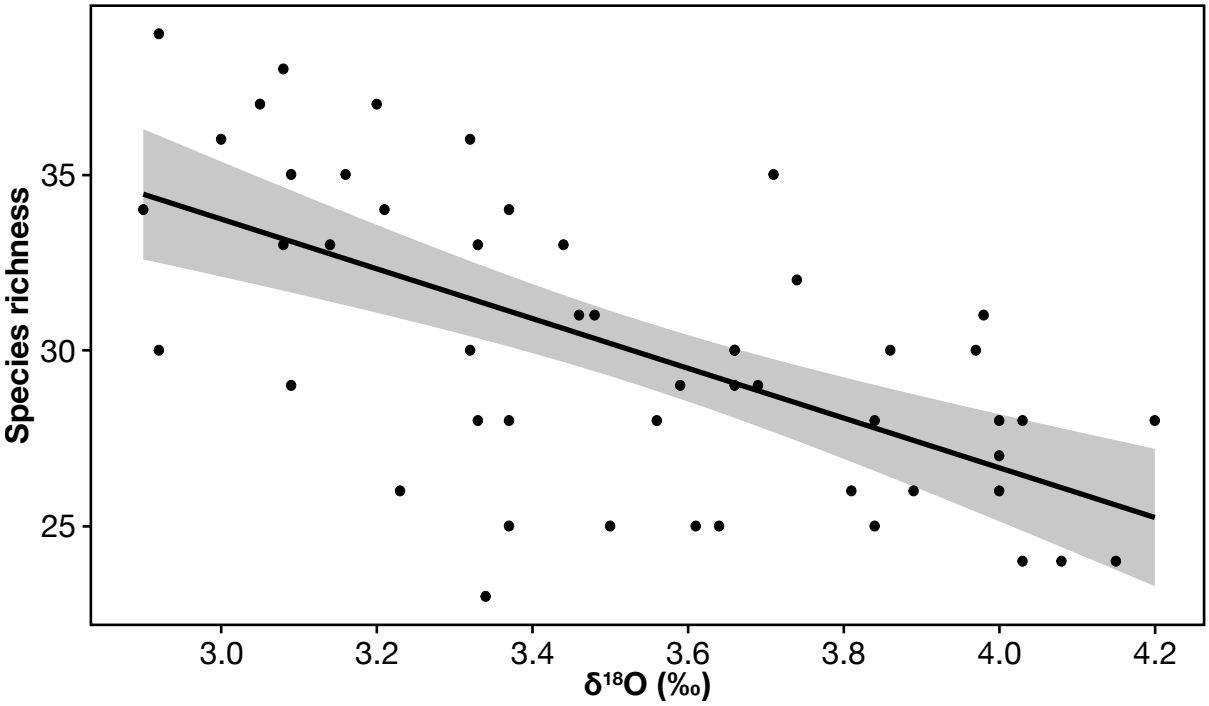

Figure B.1 Regression for observed diversity values (*q*0) and oxygen isotopes ($\delta^{18}O$ (‰) (Lisiecki and Raymo, 2005)) using a linear mixed model (t = -5.639), with a 95% confidence interval band.

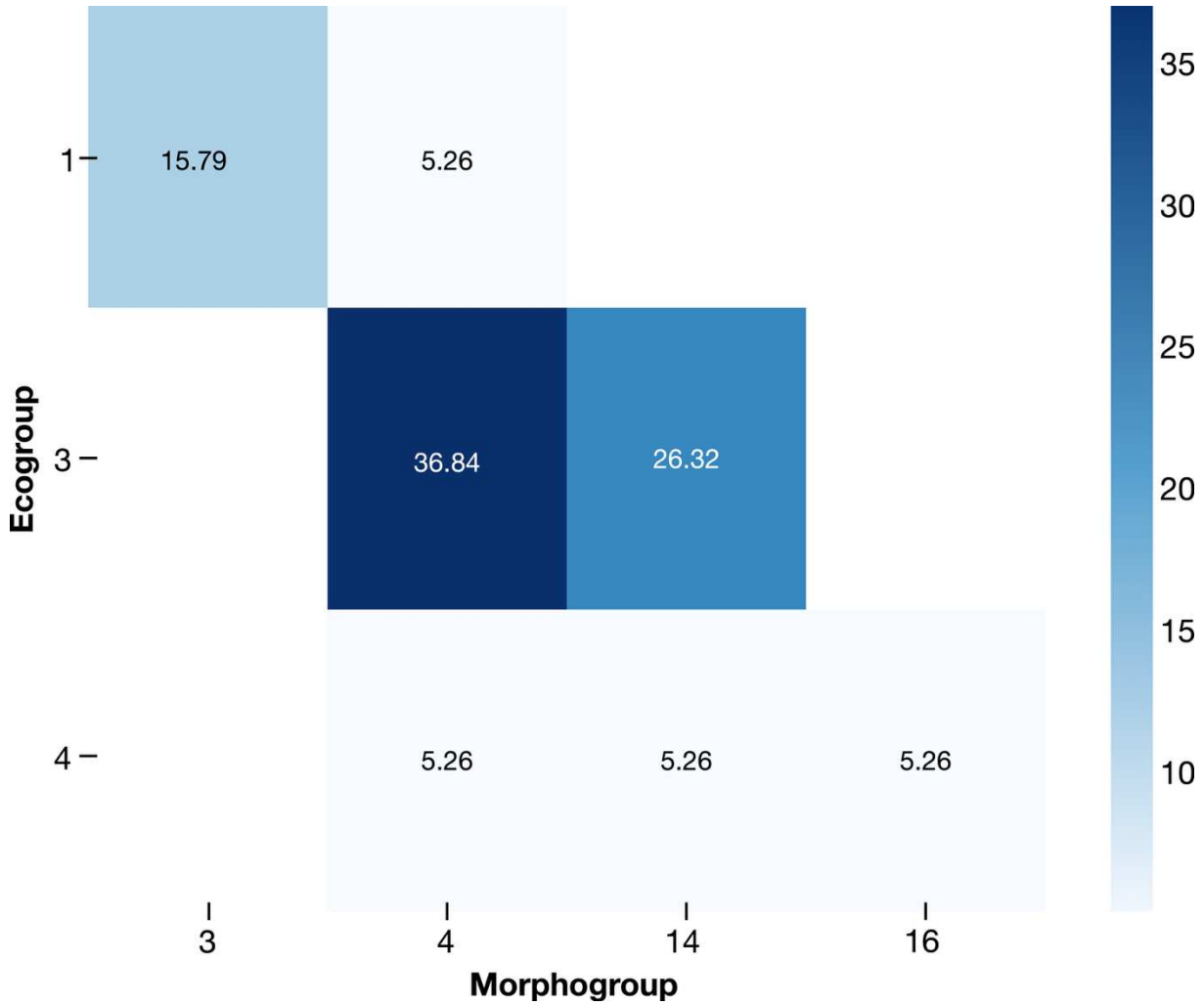

Figure B.2 Extinction percentage heatmap by combined ecogroup and morphogroup for the 19 species extinctions at ODP Site 925 in the Plio-Pleistocene. The darker shades represent higher extinction rates. **Ecogroup:** 1 = Open ocean mixed layer tropical/subtropical, with symbionts, 2 = Open ocean thermocline, 4 = Open ocean sub-thermocline. **Morphogroup:** 3 = Spinose, globular with supplementary apertures, 7 = Non-spinose, globular, 14 = Non-spinose, globorotaliform, keeled, 16 = Non-spinose, globorotaliform, non-keeled. Ecogroup and Morphogroup definitions are from Aze *et al.* (2011).

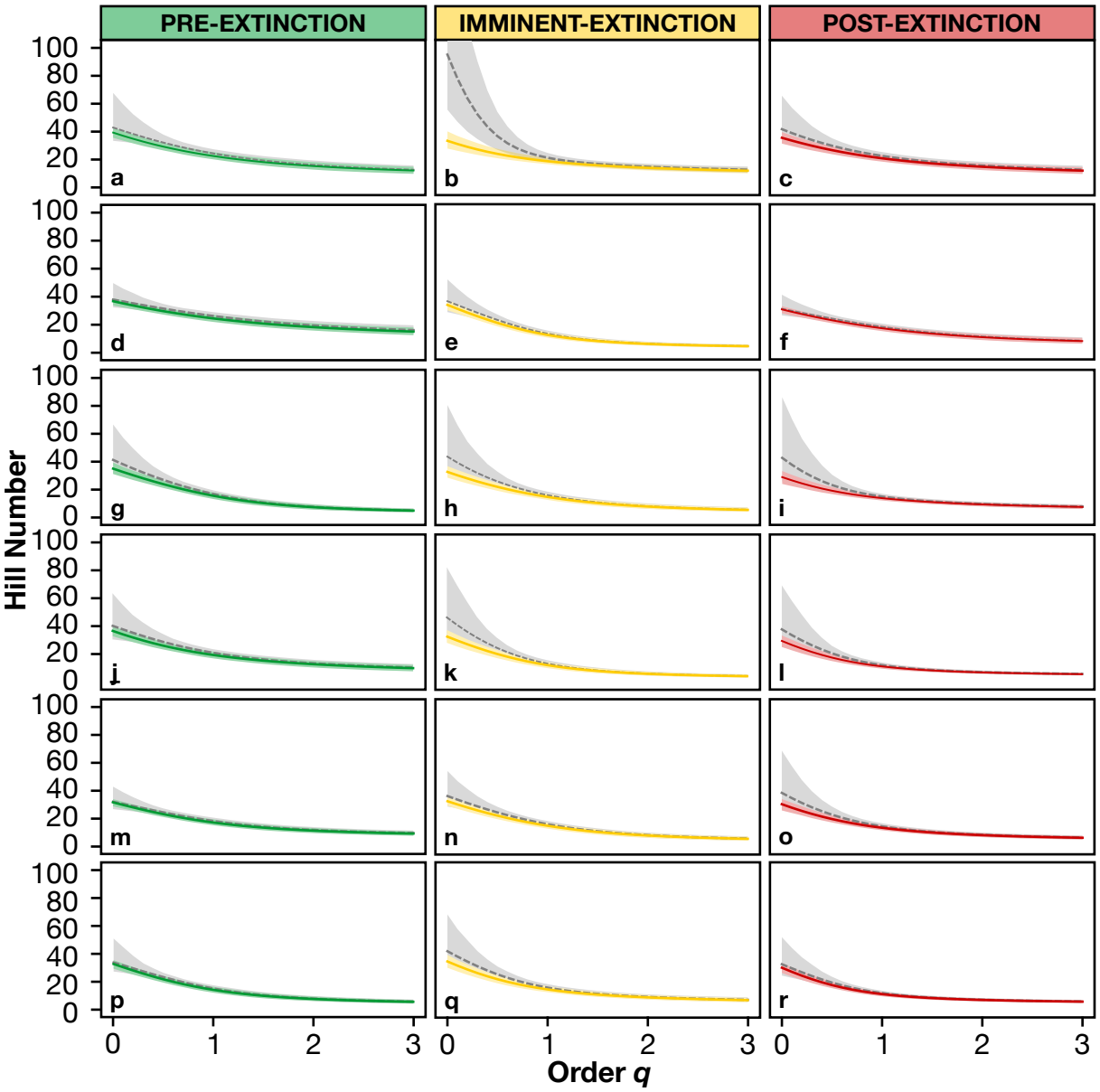

Figure B.3 Observed (solid line) and estimated (grey dashed line) diversity profiles for 1-5 of the individual species extinctions. q = 0 to 3, plotted with 95% confidence intervals (corresponding shading) across the three extinction intervals: pre-extinction (green), imminent-extinction (yellow), and post-extinction (red). **a-c)** *Hirsutella margaritae*, **d-f)** *Sphaeroidinella kochi*, **g-i)** *Dentoglobigerina baroemoenensis* and *Dentoglobigerina venezuelana*, **j-l)** *Dentoglobigerina altispira,* **m-o)** *Sphaeroidinellopsis seminulina*, and **p-r)** *Sphaeroidinellopsis paenedehiscens*.

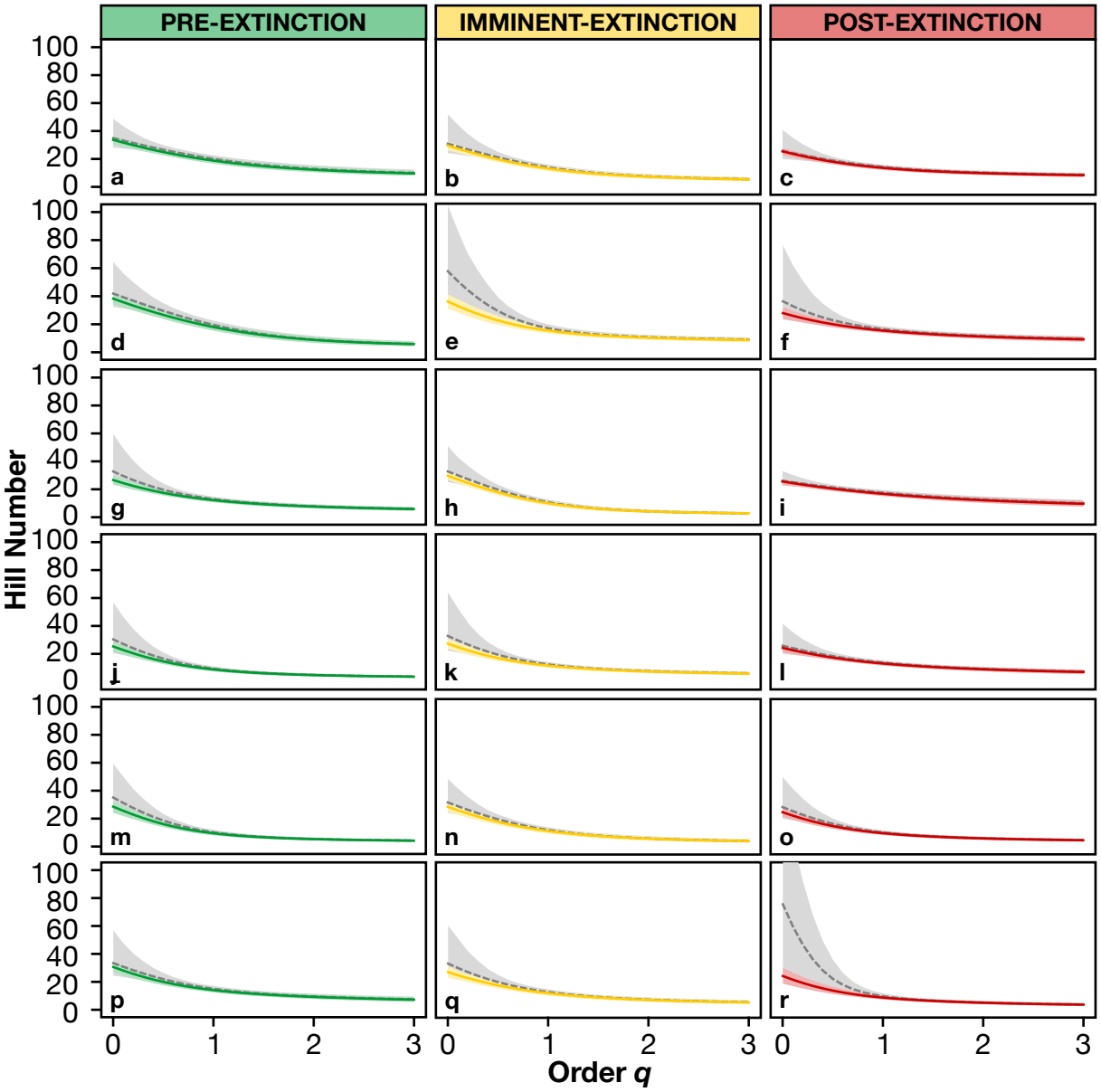

Figure B.4 Observed (solid line) and estimated (grey dashed line) diversity profiles for 6-10 of the individual species extinctions. q = 0 *to* 3, plotted with 95% confidence intervals (corresponding shading) across the three extinction intervals: pre-extinction (green), imminent-extinction (yellow), and post-extinction (red). **a-c)** *Hirsutella cibaoensis*, **d-f)** *Menardella limbata* and *Menardella multicamerata*, **g-i)** *Globoconella puncticulata*, **j-l)** *Menardella miocenica*, **m-o)** *Menardella pertenuis,* and **p-r)** *Menardella exilis*.

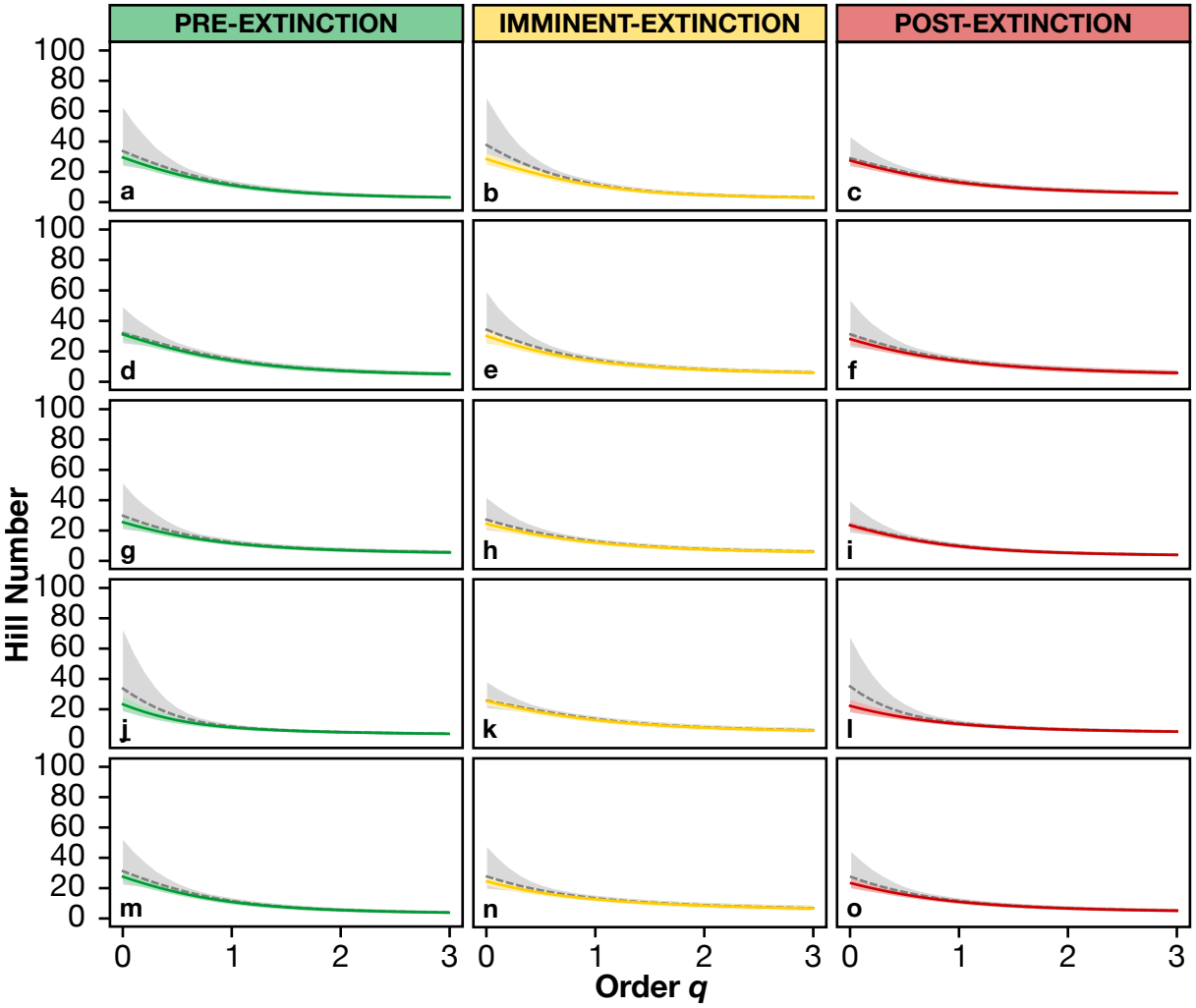

Figure B.5 Observed (solid line) and estimated (grey dashed line) diversity profiles for 11-15 of the individual species extinctions. q = 0 to 3, plotted with 95% confidence intervals (corresponding shading) across the three extinction intervals: pre-extinction (green), imminent-extinction (yellow), and post-extinction (red). **a-c)** *Globigerinoidesella fistulosa*, **d-f)** *Neogloboquadrina humerosa*, **g-i)** *Neogloboquadrina acostaensis*, **j-l)** *Globigerinoides extremus*, and **m-o)** *Globigerinoides obliquus*.

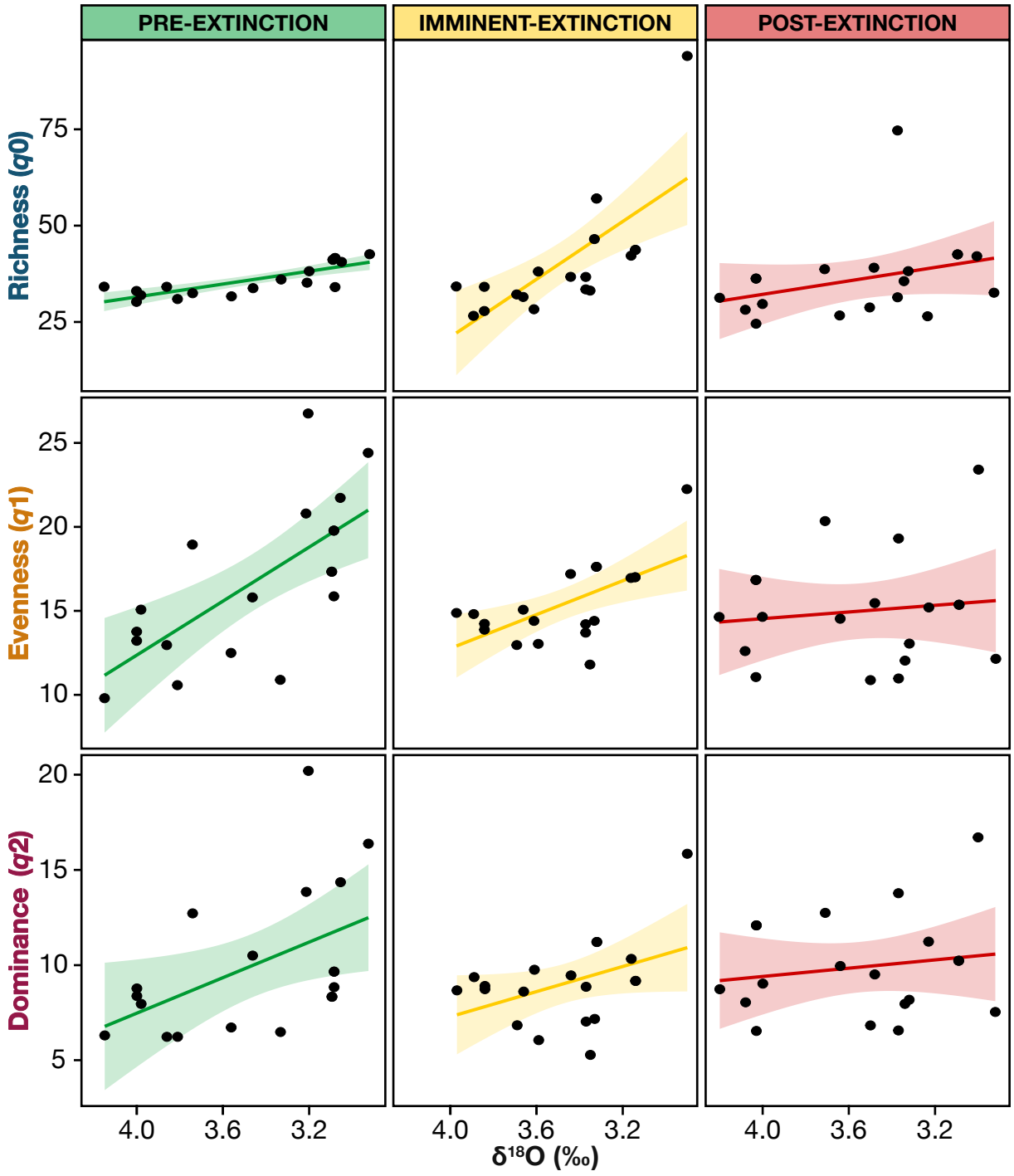

Figure B.6 Change in regression slopes and strengths for estimated values (*q*0, *q*1, and *q*2) and oxygen isotopes ($\delta^{18}O$ (‰) (Lisiecki and Raymo, 2005)) for pre- (green), imminent- (yellow), and post-extinction (red) intervals, with 95% confidence interval band from linear regressions

Table B.1 Last occurrence dates of individual species at Site 925, including ecogroups and morphogroups according to Aze *et al.* (2011). Global Age (Ma) is the last occurrence (LO) date from Aze *et al.* (2011) Shipboard Age (Ma) is the LO date from Chaisson & Pearson (1997), and LO (Ma) is the LO date from this study (see **3.2.2.1** for methodology). LO (Ma) age model is from Wilkens *et al.* (2017), and the oxygen isotope ($\delta^{18}O$ (‰)) is from Lisiecki and Raymo (2005).

	Species	Ecogroup*	Morpho group**	Global Age (Ma)	Shipboard Age (Ma)	LO (Ma)	$\delta^{18}O$ (‰)
1	*Hirsutella margaritae*	4	14	2.95	3.85	3.846	2.88
2	*Sphaeroidinellopsis kochi*	3	7	3.60	4.53	3.309	3.37
3	*Dentoglobigerina baroemoensis*	3	7	3.30	3.22	3.052	3.33
4	*Dentoglobigerina venezuelana*	4	7	3.30	3.11	3.052	3.33
5	*Dentoglobigerina altispira*	1	7	3.00	3.11	3.047	3.31
6	*Sphaeroidinellopsis seminulina*	3	7	2.30	3.11	2.990	3.18
7	*Sphaeroidinellopsis paenedehiscens*	3	7	2.30	3.11	2.959	3.08
8	*Hirsutella cibaoensis*	4	16	4.40	3.22	2.805	3.78
9	*Menardella limbata*	3	14	2.30	2.38	2.548	3.18
10	*Menardella multicamerata*	3	14	2.20	3.10	2.548	3.18
11	*Globoconella puncticulata*	3	7	2.30	1.61	2.421	3.35
12	*Menardella miocenica*	3	14	2.40	2.38	2.281	3.84
13	*Menardella pertenuis*	3	14	1.70	2.33	2.278	3.80
14	*Menardella exilis*	3	14	1.90	2.09	2.273	3.50
15	*Globigerinoidesella fistulosa*	1	3	2.00	1.88	1.335	4.19
16	*Neogloboquadrina humerosa*	3	7	1.60	1.58	1.122	4.47
17	*Neogloboquadrina acostaensis*	3	7	1.70	1.58	1.101	4.03
18	*Globigerinoides extremus*	1	3	1.60	1.98	1.086	3.89
19	*Globigerinoides obliquus*	1	3	1.30	1.30	1.075	3.48

***Ecogroup:** 1 = Open ocean mixed layer tropical/subtropical, with symbionts, 2 = Open ocean thermocline, 4 = Open ocean sub-thermocline. ****Morphogroup:** 3 = Spinose, globular with supplementary apertures, 7 = Non-spinose, globular, 14 = Non-spinose, globorotaliform, keeled, 16 = Non-spinose, globorotaliform, non-keeled.

Table B.2 Species count for assemblage counts conducted on sample 925D 8H2 140-142 cm, at 2.4285 Ma.

Sample Size	Species Count	Average	Standard Deviation	95% Confidence
10	8	6.3	1.059	0.657
10	6			
10	6			
10	5			
10	6			
10	6			
10	7			
10	8			
10	6			
10	5			
30	15	15.2	1.095	0.960
30	17			
30	15			
30	14			
30	15			
50	21	19.8	1.789	1.568
50	19			
50	21			
50	21			
50	17			
100	27	25.7	1.528	1.729
100	26			
100	24			
200	28	29.0	1.732	1.960
200	31			
200	28			
300	33	33.7	1.155	1.307
300	35			
300	33			
500	34	33.0	1.414	1.600
500	32			

Table B.3 The last occurrence samples and the pre- (PR), imminent- (IM) and post-extinction (PO) samples for all 19 species extinction events, with the number of species observed in a 300-specimen assemblage count from the sample (Count), with the oxygen isotope ($\delta^{18}O$ (‰)) for each sample as a representative of the environment. The age model is from Wilkens *et al.* (2017), and the $\delta^{18}O$ (‰) data is from Lisiecki and Raymo (2005)

Species Extinction		Last Occurrence Samples		Assemblage Samples			
		Age (Ma)	$\delta^{18}O$ (‰)	Interval	Age (Ma)	Count	$\delta^{18}O$ (‰)
1	*Hirsutella margaritae*	3.8458	2.88	PR	3.9010	39	2.92
				IM	3.8523	34	2.90
				PO	3.8009	36	3.00
2	*Sphaeroidinella kochi*	3.3050	3.42	PR	3.4237	37	3.20
				IM	3.3094	34	3.37
				PO	3.3007	31	3.71
3	*Dentoglobigerina baroemoenensis*	3.0523	3.33	PR	3.0724	35	3.09
				IM	3.0561	33	3.14
				PO	3.0350	29	3.09
4	*Dentoglobigerina venezuelana*	3.0523	3.33	PR	3.0724	35	3.09
				IM	3.0561	33	3.14
				PO	3.0350	29	3.09
5	*Dentoglobigerina altispira*	3.0467	3.31	PR	3.0659	37	3.05
				IM	3.0487	33	3.33
				PO	3.0259	30	3.32
6	*Sphaeroidinellopsis seminulina*	2.9903	3.18	PR	3.2960	32	3.74
				IM	3.0027	33	3.44
				PO	2.9756	31	3.48
7	*Sphaeroidinellopsis paenedehiscens*	2.9591	3.08	PR	3.0985	33	3.08
				IM	2.9648	35	3.16
				PO	2.9537	30	2.92
8	*Hirsutella cibaoensis*	2.8053	3.78	PR	2.9017	34	3.21
				IM	2.8124	30	3.66
				PO	2.7768	26	3.23
9	*Menardella limbata*	2.5480	3.18	PR	3.1015	38	3.08
				IM	2.5781	36	3.32
				PO	2.5265	28	4.03
10		2.5480	3.18	PR	3.1015	38	3.08

	Menardella multicamerata			IM	2.5781	36	3.32
				PO	2.5265	28	4.03
11	*Globoconella puncticulata*	2.4207	3.35	PR	2.4432	27	4.00
				IM	2.4285	30	3.66
				PO	2.4131	26	3.37
12	*Menardella miocenica*	2.3377	3.29	PR	2.6039	26	3.81
				IM	2.3465	28	3.37
				PO	2.3284	25	3.64
13	*Menardella pertenuis*	2.2779	3.80	PR	2.3852	29	3.33
				IM	2.2872	28	3.69
				PO	2.2733	25	3.50
14	*Menardella exilis*	2.2733	3.50	PR	2.2916	31	3.46
				IM	2.2813	28	3.84
				PO	2.2686	25	3.37
15	*Globigerinoidesella fistulosa*	1.3350	4.19	PR	1.9600	30	3.86
				IM	1.3500	29	3.59
				PO	1.3270	28	4.00
16	*Neogloboquadrina humerosa*	1.1321	4.05	PR	1.3650	31	3.98
				IM	1.1424	30	3.97
				PO	1.1166	28	4.20
17	*Neogloboquadrina acostaensis*	1.1063	4.03	PR	1.3260	26	4.00
				IM	1.1115	25	3.84
				PO	1.0960	24	4.03
18	*Globigerinoides extremus*	1.0805	3.89	PR	1.2970	24	4.15
				IM	1.0857	26	3.89
				PO	1.0702	23	3.34
19	*Globigerinoides obliquus*	1.0753	3.48	PR	1.4000	28	3.56
				IM	1.0805	25	3.61
				PO	1.0320	24	4.08

Table B.4 Observed and estimated *q* (0-2) values for pre- (PR), imminent- (IM) and post-extinction (PO) intervals for all 19 species extinction events, with the number of species observed in a 300-specimen assemblage count from the sample (Count). The age model is from Wilkens *et al.* (2017), and the oxygen isotope ($\delta^{18}O$ (‰)) is from Lisiecki and Raymo (2005).

Species Extinction		Sample				Observed			Estimated		
		Interval	Age (Ma)	Count	$\delta^{18}O$ (‰)	*q*0	*q*1	*q*2	*q*0	*q*1	*q*2
1	*Hirsutella margaritae*	PR	3.9010	39	2.92	39.000	20.282	13.330	46.537	22.081	13.905
		IM	3.8523	34	2.90	34.000	20.002	15.437	94.298	22.461	16.221
		PO	3.8009	36	3.00	36.000	21.429	15.401	41.980	23.070	16.183
2	*Sphaeroidinella kochi*	PR	3.4237	37	3.20	37.000	25.069	19.044	38.121	26.770	20.267
		IM	3.3094	34	3.37	33.000	13.626	7.278	34.780	14.485	7.434
		PO	3.3007	31	3.71	31.000	17.386	12.087	32.495	18.388	12.552
3	*Dentoglobigerina baroemoensis*	PR	3.0724	35	3.09	35.000	16.159	8.198	41.105	17.379	8.400
		IM	3.0561	33	3.14	33.000	15.588	8.906	43.631	16.818	9.147
		PO	3.0350	29	3.09	29.000	14.342	9.947	42.455	15.431	10.254
4	*Dentoglobigerina venezuelana*	PR	3.0724	35	3.09	35.000	16.159	8.198	41.105	17.379	8.400
		IM	3.0561	33	3.14	33.000	15.588	8.906	43.631	16.818	9.147
		PO	3.0350	29	3.09	29.000	14.342	9.947	42.455	15.431	10.254
5	*Dentoglobigerina altispira*	PR	3.0659	37	3.05	37.000	20.299	13.724	40.987	21.847	14.334
		IM	3.0487	33	3.33	33.000	13.096	7.010	46.455	14.192	7.154
		PO	3.0259	30	3.32	30.000	12.201	8.004	38.073	13.068	8.196
6	*Sphaeroidinellopsis seminulina*	PR	3.2960	32	3.74	36.000	19.351	12.225	42.105	20.848	12.702
		IM	3.0027	33	3.44	32.000	16.063	9.336	37.980	17.168	9.604
		PO	2.9756	31	3.48	31.000	14.431	9.323	37.379	15.432	9.589
7	*Sphaeroidinellopsis paenedehiscens*	PR	3.0985	33	3.08	33.000	14.792	8.545	34.780	15.725	8.767
		IM	2.9648	35	3.16	35.000	15.997	10.460	40.045	17.220	10.807
		PO	2.9537	30	2.92	30.000	11.455	7.361	32.442	12.143	7.521
8	*Hirsutella cibaoensis*	PR	2.9017	34	3.21	33.000	17.852	11.613	34.139	18.943	12.040
		IM	2.8124	30	3.66	30.000	14.078	8.381	31.329	14.867	8.594
		PO	2.7768	26	3.23	25.000	14.217	10.712	25.332	14.844	11.074
9	*Menardella limbata*	PR	3.1015	38	3.08	38.000	19.040	10.074	40.713	20.471	10.389
		IM	2.5781	36	3.32	36.000	15.819	10.833	57.054	17.460	11.202
		PO	2.5265	28	4.03	28.000	16.633	12.315	40.209	17.795	12.800
10	*Menardella multicamerata*	PR	3.1015	38	3.08	38.000	19.040	10.074	40.713	20.471	10.389
		IM	2.5781	36	3.32	36.000	15.819	10.833	57.054	17.460	11.202

		PO	2.5265	28	4.03	28.000	16.633	12.315	40.209	17.795	12.800
11	*Globoconella puncticulata*	PR	2.4432	27	4.00	27.000	12.935	8.129	30.115	13.639	8.327
		IM	2.4285	30	3.66	29.000	10.931	5.222	30.329	11.524	5.297
		PO	2.4131	26	3.37	26.000	10.108	6.310	28.492	10.632	6.424
12	*Menardella miocenica*	PR	2.6039	26	3.81	26.000	10.003	6.108	30.884	10.575	6.214
		IM	2.3465	28	3.37	28.000	12.547	8.456	33.316	13.328	8.673
		PO	2.3284	25	3.64	24.000	9.397	5.536	55.893	10.148	5.621
13	*Menardella pertenuis*	PR	2.3852	29	3.33	29.000	18.358	13.255	31.243	19.369	13.821
		IM	2.2872	28	3.69	30.000	12.038	6.652	32.243	12.749	6.780
		PO	2.2733	25	3.50	26.000	10.104	6.438	86.298	11.193	6.557
14	*Menardella exilis*	PR	2.2916	31	3.46	31.000	14.871	10.165	33.713	15.798	10.486
		IM	2.2813	28	3.84	28.000	13.108	8.449	32.485	13.888	8.666
		PO	2.2686	25	3.37	25.000	10.334	6.684	28.588	10.875	6.814
15	*Globigerinoidesella fistulosa*	PR	1.9600	30	3.86	31.000	12.428	6.127	34.488	13.220	6.234
		IM	1.3500	29	3.59	30.000	12.498	6.007	38.970	13.362	6.110
		PO	1.3270	28	4.00	27.000	12.856	8.182	31.153	13.577	8.383
16	*Neogloboquadrina humerosa*	PR	1.3650	31	3.98	31.000	14.258	7.765	31.886	15.070	7.945
		IM	1.1424	30	3.97	31.000	14.300	8.538	35.070	15.229	8.760
		PO	1.1166	28	4.20	24.000	12.820	8.622	25.495	13.394	8.848
17	*Neogloboquadrina acostaensis*	PR	1.3260	26	4.00	32.000	15.142	9.176	37.980	16.186	9.434
		IM	1.1115	25	3.84	31.000	14.524	8.686	35.884	15.488	8.916
		PO	1.0960	24	4.03	27.000	14.146	9.579	30.115	14.915	9.861
18	*Globigerinoides extremus*	PR	1.2970	24	4.15	24.000	9.208	6.023	31.973	9.750	6.126
		IM	1.0857	26	3.89	26.000	11.092	6.450	27.595	11.639	6.570
		PO	1.0702	23	3.34	24.000	11.351	7.631	30.229	11.958	7.804
19	*Globigerinoides obliquus*	PR	1.4000	28	3.56	28.000	12.069	6.599	30.492	12.734	6.725
		IM	1.0805	25	3.61	31.000	15.147	9.328	34.588	16.105	9.596
		PO	1.0320	24	4.08	27.000	12.146	7.700	30.115	12.808	7.877

Appendix C Supplementary material for Chapter 4

Table C.1 The mean diameter (µm) per species in the pre- (PR) and imminent- (IM) samples for all 19 species extinction events, with the oxygen isotope ($\delta^{18}O$ (‰)) for each sample as a representative of the environment. The age model is from Wilkens *et al.* (2017), and the $\delta^{18}O$ (‰) data is from Lisiecki and Raymo (2005)

Species Extinction		Assemblage Samples			
		Interval	Age (Ma)	Mean Diameter (µm)	$\delta^{18}O$ (‰)
1	*Hirsutella margaritae*	PR	3.9010	565.55	2.92
		IM	3.8523	486.33	2.90
2	*Sphaeroidinella kochi*	PR	3.4237	383.41	3.20
		IM	3.3094	506.64	3.37
3	*Dentoglobigerina baroemoenensis*	PR	3.0724	316.16	3.09
		IM	3.0561	325.31	3.14
4	*Dentoglobigerina venezuelana*	PR	3.0724	430.90	3.09
		IM	3.0561	361.69	3.14
5	*Dentoglobigerina altispira*	PR	3.0659	444.83	3.05
		IM	3.0487	488.08	3.33
6	*Sphaeroidinellopsis seminulina*	PR	3.2960	502.34	3.74
		IM	3.0027	476.63	3.44
7	*Sphaeroidinellopsis paenedehiscens*	PR	3.0985	478.05	3.08
		IM	2.9648	417.73	3.16
8	*Hirsutella cibaoensis*	PR	2.9017	272.02	3.21
		IM	2.8124	370.91	3.66
9	*Menardella limbata*	PR	3.1015	659.62	3.08
		IM	2.5781	563.01	3.32
10	*Menardella multicamerata*	PR	3.1015	692.72	3.08
		IM	2.5781	815.92	3.32
11	*Globoconella puncticulata*	PR	2.4432	435.20	4.00
		IM	2.4285	337.54	3.66
12	*Menardella miocenica*	PR	2.6039	460.55	3.81
		IM	2.3465	432.96	3.37
13	*Menardella pertenuis*	PR	2.3852	876.11	3.33
		IM	2.2872	661.23	3.69
14	*Menardella exilis*	PR	2.2916	837.87	3.46

		IM	2.2813	685.01	3.84
15	*Globigerinoidesella fistulosa*	PR	1.9600	857.07	3.86
		IM	1.3500	987.41	3.59
16	*Neogloboquadrina humerosa*	PR	1.3650	450.58	3.98
		IM	1.1424	413.97	3.97
17	*Neogloboquadrina acostaensis*	PR	1.3260	207.74	4.00
		IM	1.1115	332.92	3.84
18	*Globigerinoides extremus*	PR	1.2970	281.01	4.15
		IM	1.0857	324.23	3.89
19	*Globigerinoides obliquus*	PR	1.4000	365.67	3.56
		IM	1.0805	235.99	3.61

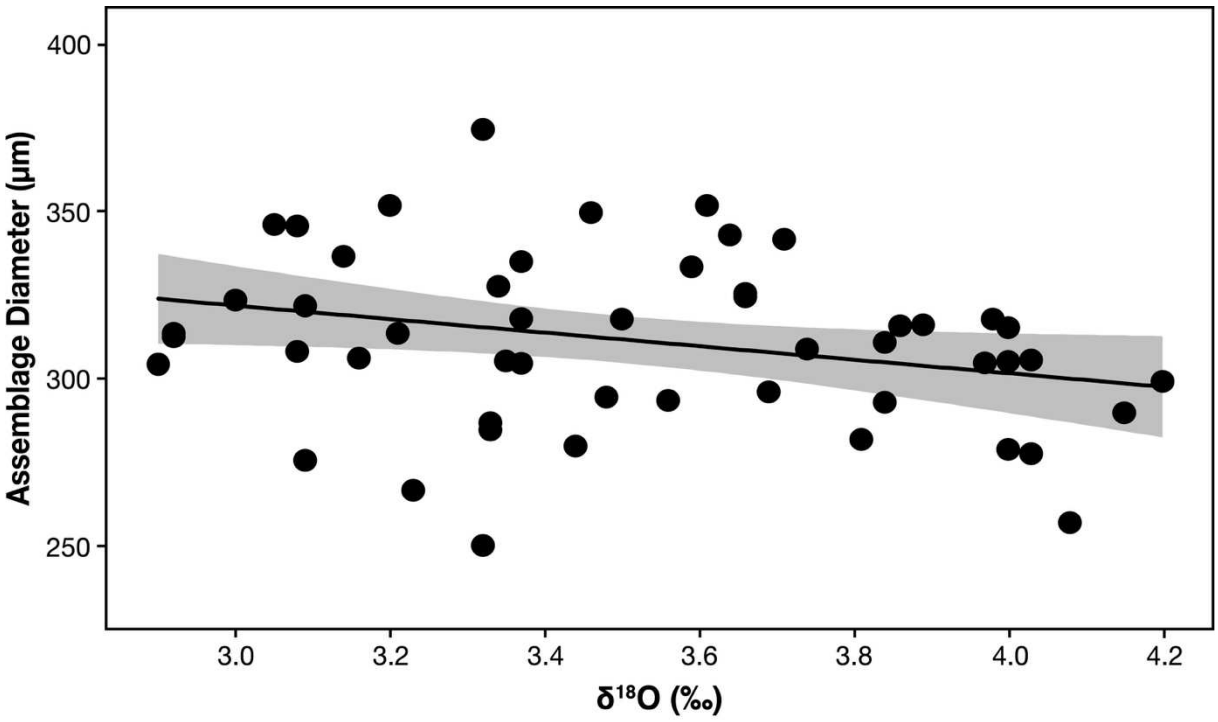

Figure C.1 Regression for the mean assemblage diameter (µm) and oxygen isotopes ($\delta^{18}O$ (‰) (Lisiecki and Raymo, 2005)) using a linear mixed model ($r = -0.279$, $p < 0.05$), with a 95% confidence interval band

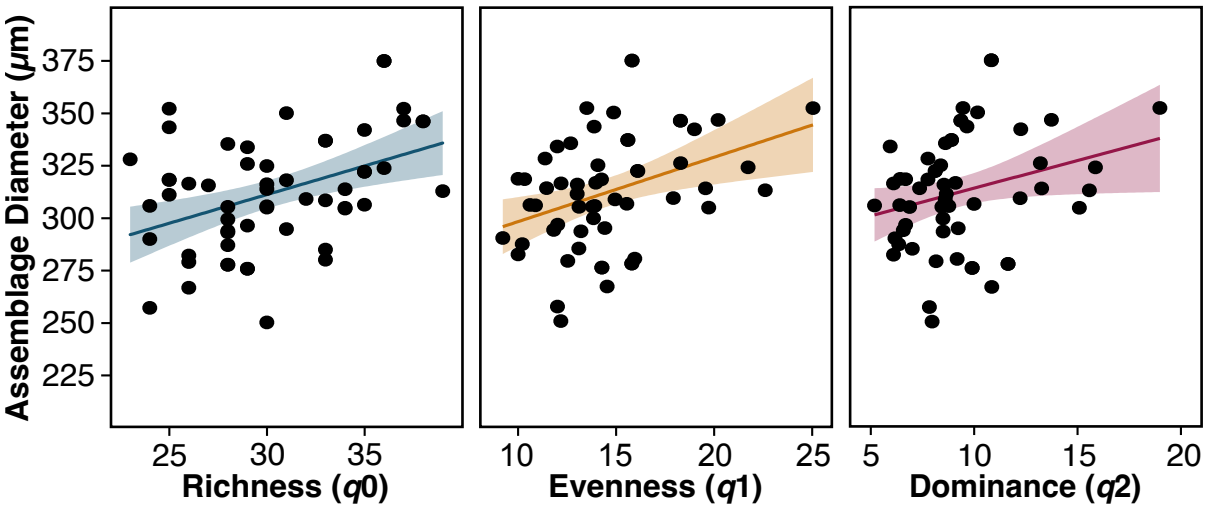

Figure C.2 Change in regression slopes and strengths for assemblage diameter and species richness (*q*0; dark blue), evenness (*q*1; orange), and dominance (*q*2; purple), with a 95% confidence interval band from linear regressions.

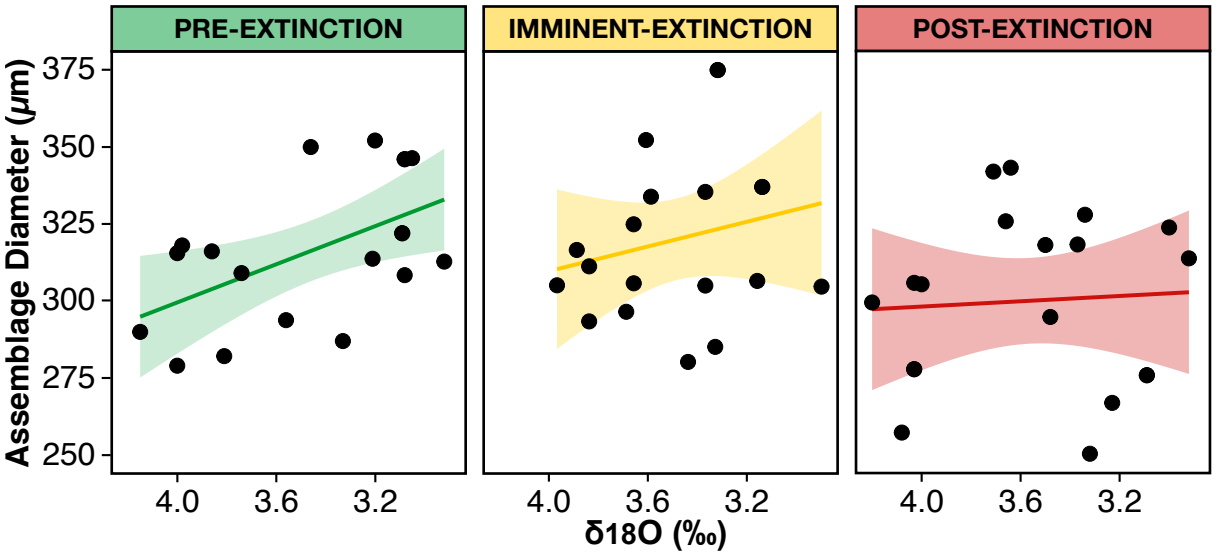

Figure C.3 Change in regression slopes and strengths for the assemblage size (μm) and oxygen isotopes ($\delta^{18}O$ (‰); Lisiecki and Raymo, 2005) for pre- (green), imminent- (yellow), and post-extinction (red) intervals, with 95% confidence interval bands from linear regressions.

Appendix D Neurodiversity: An Important Axis of Diversity in Ocean Sciences

Citation: Wilson, J.D., E. Sibert, M. Grigoratou, C.L.C. Jones, L. Rubin, and Z. Smilli. 2023. Neurodiversity: An important axis of diversity in ocean sciences. Oceanography 36(4):60-61, https://doi.org/10.5670/oceanog.2024.103

What is Neurodiversity?

Neurodiversity refers to variations in the human brain that affect information processing; it includes conditions, or "neurotypes," such as autism spectrum disorder (ASD), attention deficit hyperactivity disorder (ADHD), dyslexia, dyscalculia, and dyspraxia, among others. Neurodiversity can be conceptualized as significant differences in the ways that individuals process information; such differences may concern written or verbal language, sensory information, body language, or social interactions. These differences have been historically viewed within the medical model of disability, for example, as deficits in ability through a diagnosed condition, often associated with a goal of curing or managing the condition.

Neurodiversity as a term and concept is still very much evolving in its definition, use, and scope (Dwyer, 2022), but the concept of neurodiversity reflects a shift toward the social model of disability, which suggests that "disability" is defined by barriers inherent in society, such as implicit weighting of social interactions in an interview. In this article we refer to neurodiversity in the broad sense that a neurodivergent individual has a "spiky profile" of abilities (see **Figure 1**), where they may excel in some areas associated with information processing, such as processing time or working memory, but struggle significantly in others. This distinguishes them from neurotypical individuals who experience some variability, but to a lesser extent. Our aim here is to raise awareness about neurodiversity as it relates to efforts toward broader equality, diversity, and inclusion. The authors are neurodiverse ocean scientists who draw here on personal reflections and discussions to highlight key themes. Although discussions of neurodiversity often begin with a list of "average" strengths and weaknesses for specific neurotypes (e.g., Cope and Remington 2022), we felt this was not helpful here, as there can be diversity within neurotypes as well as comorbidity of neurotypes. Crucially, we suggest barriers to inclusion for neurodivergent individuals ultimately depend on the individual and not the relevant neurotype.

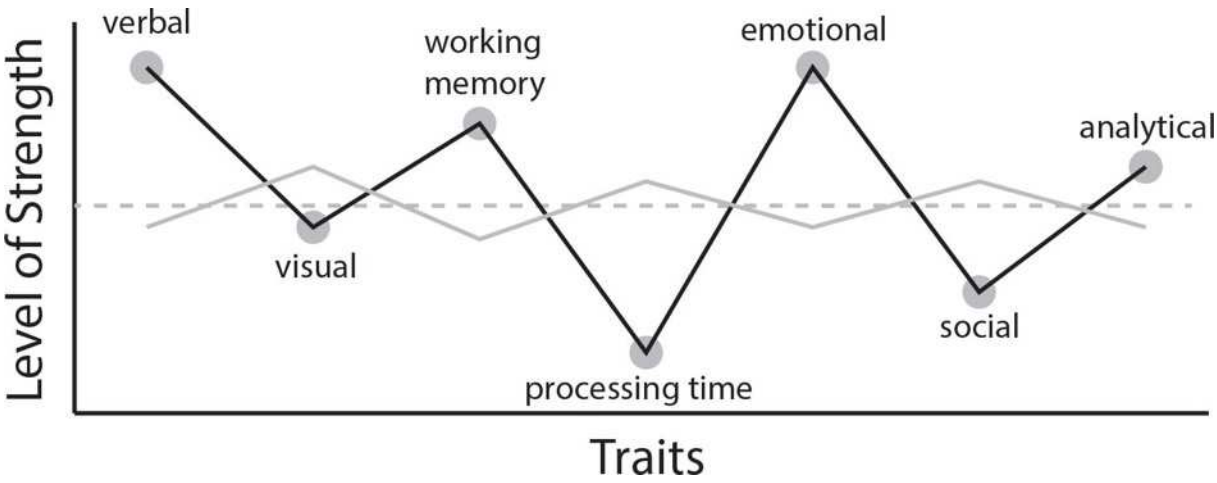

Figure 1 A common visual representation of neurodiversity (e.g., Doyle et al., 2020). This profile depicts relative areas of strengths and weaknesses in traits associated with information processing for an individual relative to an average level of ability (dashed line). A neurodiverse individual can be considered as having a "spiky profile," with significant variability in strengths and weaknesses across traits (black line). This is distinct from a neurotypical individual (gray line) who has less variability across traits. This representation promotes an inclusive view, indicating that neurodiverse individuals have particular strengths, bringing value to teams rather focusing on specific deficits.

Being Neurodiverse in Oceanography

Many of the challenges and solutions posed by neurodiversity in the ocean sciences will be common across the science, technology, engineering, and mathematics (STEM) disciplines (e.g., Joice and Tetlow, 2021; Sarju, 2021). The ocean sciences are inherently interdisciplinary and international, and thus benefit from research communities that offer highly diverse ways of approaching problems. As a group of neurodiverse authors, we found commonality in being drawn to the ocean sciences precisely because of their interdisciplinarity; however, the challenges we faced were based on our individual experiences and neurodivergence type(s). A unique aspect of oceanography within STEM is seagoing fieldwork, which can present specific challenges to neurodiverse individuals that include the sensory experience of being on a moving platform and include an intense social environment, changes in routine, and a need for rapid data collection and real-time documentation (e.g., Kingsbury et al., 2020). Even so, neurodivergent individuals can excel in these environments. For example, the constrained and demanding schedule aboard a research vessel proved to be a productive environment for one individual with ADHD, and an autistic person found the motion of the boat promoted focusing on the work at hand.

Other identities we hold as ocean scientists impact neurodiversity, including gender, race, nationality, socioeconomic background, and even career stage (Cosentino and Souviron-Priego, 2021). For example, multicultural teams in ocean sciences are common, which can pose intersectional challenges with social interaction and communication. The characteristics of

neurodiverse persons working within a multicultural team can sometimes be misinterpreted as language barriers or cultural issues related to communication. This misunderstanding can lead to a lack of recognition and accommodation for neurodiverse team members. Additionally, cultural differences in attitudes toward neurodiversity can further complicate matters. Some cultures may stigmatize neurodiverse conditions or have negative attitudes toward seeking help for these conditions, which can result in undiagnosed individuals not receiving the support they need to succeed (Botha and Gillespie-Lynch, 2022).

What is a well-supported environment for Neurodiverse individuals?

Ultimately, neurodiverse individuals are the experts in their lived experiences; they often have the best understanding of their own specific requirements, which need to be disclosed in order to overcome barriers. Neurodiversity declaration rates are the lowest in STEM disciplines generally, with just ~5% of STEM undergraduates revealing that they are neurodiverse, compared to 15% at a national level—among senior academics in the United Kingdom, the rate is just 0.9% (Joice and Tetlow, 2021; Sarju, 2021). One barrier to disclosure of a neurodiverse condition is the risk of exposure to stigma and negative stereotyping, which tends to link a diagnosis of a specific neurotype with the abilities (or lack of them) of an individual (LeFevre-Levy et al., 2023), for example, assumptions that the individual may not interact as expected at academic conferences or may not be able to produce papers at a desired level.

A well-supported environment for neurodiverse individuals provides space and flexibility across all aspects of research and education by allowing people to use their abilities in ways that work with, rather than against, their brains. Beyond disclosure, for example, this could involve offering a colleague flexibility in how and when to work and facilitating regular check ins to determine what is working and what is not. We six authors require six unique solutions or approaches to our neurodivergent-related needs, and we have found that such solutions can be achieved through open dialogue with colleagues.

Those whose brains process information differently are likely to approach a problem differently. Although it may initially be challenging to engage with someone who presents a new or radically different methodology or approach, applying that methodology or approach to the task at hand may enhance innovation, problem-solving, and creativity (Cope and Remington, 2022; LeFevre-Levy et al., 2023). It may be possible to engage specific skills—for example, the individual "spikes" in **Figure 1**—as well as novel approaches enabled by a combination of skills—the overall "spiky profile" in **Figure 1**. Neurodivergent individuals may also be more resilient and persistent in research, having navigated education systems in which they faced challenges related to their neurotypes. Addressing neurodiversity as an axis of diversity is an essential part

of equity, diversity, and inclusion efforts, and embracing and enabling neurodiverse individuals can enhance interdisciplinary and international research in ocean sciences.

Acknowledgments

JDW collaborated on the paper with ES, with input from all authors, who each contributed personal reflections on neurodiversity to form the basis for the article's content. The authors received no financial support for this article. We thank the editor and two reviewers for their constructive comments.

References

Botha, M., and K. Gillespie-Lynch. 2022. Come as you are: Examining autistic identity development and neurodiversity movement through an intersectional lens. *Human Development* 66(2):93–112, https://doi.org/10.1159/000524123.

Cope, R., and A. Remington. 2022. The strengths and abilities of autistic people in the workplace. *Autism in Adulthood* 4 (1):22–31, https://doi.org/10.1089/aut.2021.0037.

Cosentino, M., and L. Souviron-Priego. 2021. Think of the early career researchers! Saving the oceans through collaborations. *Frontiers in Marine Science* 8:574620, https://doi.org/10.3389/fmars.2021.574620.

Doyle, N. 2020. Neurodiversity at work: A biopsychosocial model and the impact on working adults. *British Medical Bulletin*135(1):108–125, https://doi.org/10.1093/bmb/ldaa021.

Dwyer, P. 2022. The neurodiversity approach(es): What are they and what do they mean for researchers? *Human Development* 66(2):73–92, https://doi.org/10.1159/000523723.

Joice, W., and A. Tetlow. 2021. Disability STEM data for students and academic staff in higher education 2007/08 to 2018/19. *Report by JISC for the Royal Society*, https://royalsociety.org/-/media/policy/topics/diversity-in-science/210118-disability-STEM-data-for-students-and-staff-in-higher-education.pdf.

Kingsbury, C.G., E.C. Sibert, Z. Killingback, and C.L. Atchison. 2020. "Nothing about us without us:" The perspectives of autistic geoscientists on inclusive instructional practices in geoscience education. *Journal of Geoscience Education* 68(4):302–310, https://doi.org/10.1080/10899995.2020.1768017.

LeFevre-Levy, R., A. Melson-Silimon, R. Harmata, A. Hulett, and N. Carter. 2023. Neurodiversity in the workplace: Considering neuroatypicality as a form of diversity. *Industrial and Organizational Psychology* 16(1):1–19, https://doi.org/10.1017/iop.2022.86.

Sarju, J.P. 2021. Nothing about us without us – Towards genuine inclusion of disabled scientists and science students post pandemic. *Chemistry: A European Journal* 27(41):10,489–10,494, https://doi.org/10.1002/chem.202100268.

References

Abramovich, S. *et al.* (2010) 'Global climate change and planktic foraminiferal response in the Maastrichtian: Maastrichtian climate and foraminifera', *Paleoceanography*, 25(2), p. PA2201. Available at: https://doi.org/10.1029/2009PA001843.

Adebayo, M.B. *et al.* (2023) 'Environmental controls of size distribution of Modern planktonic foraminifera in the tropical Indian Ocean', *Geochemistry, Geophysics, Geosystems*, 24(4), p. e2022GC010586. Available at: https://doi.org/10.1029/2022GC010586.

Agapow, P.-M. *et al.* (2004) 'The Impact of Species Concept on Biodiversity Studies', *The Quaterly Review of Biology*, 79(2), pp. 161–179. Available at: https://doi.org/10.1086/383542.

Akçakaya, H.R. *et al.* (2020) 'Assessing ecological function in the context of species recovery', *Conservation Biology*, 34(3), pp. 561–571. Available at: https://doi.org/10.1111/cobi.13425.

Aldridge, D., Beer, C.J. and Purdie, D.A. (2012) 'Calcification in the planktonic foraminifera *Globigerina bulloides* linked to phosphate concentrations in surface waters of the North Atlantic Ocean', *Biogeosciences*, 9(5), pp. 1725–1739. Available at: https://doi.org/10.5194/bg-9-1725-2012.

Alroy, J. (2008) 'Dynamics of origination and extinction in the marine fossil record', *Proceedings of the National Academy of Sciences*, 105(supplement_1), pp. 11536–11542. Available at: https://doi.org/10.1073/pnas.0802597105.

Al-Sabouni, N. *et al.* (2018) 'Reproducibility of species recognition in modern planktonic foraminifera and its implications for analyses of community structure', *Journal of Micropalaeontology*, 37(2), pp. 519–534. Available at: https://doi.org/10.5194/jm-37-519-2018.

Al-Sabouni, N., Kucera, M. and Schmidt, D.N. (2007) 'Vertical niche separation control of diversity and size disparity in planktonic foraminifera', *Marine Micropaleontology*, 63(1–2), pp. 75–90. Available at: https://doi.org/10.1016/j.marmicro.2006.11.002.

Alvarez, S.A. *et al.* (2019) 'Diversity decoupled from ecosystem function and resilience during mass extinction recovery', *Nature*, 574(7777), pp. 242–245. Available at: https://doi.org/10.1038/s41586-019-1590-8.

Anderson, O.R. *et al.* (1979) 'Trophic activity of planktonic foraminifera', *Journal of the Marine Biological Association of the United Kingdom*, 59(3), pp. 791–799. Available at: https://doi.org/10.1017/S002531540004577X.

André, A. *et al.* (2014) 'SSU rDNA Divergence in Planktonic Foraminifera: Molecular Taxonomy and Biogeographic Implications', *PLOS ONE*. Edited by V. Ketmaier, 9(8), p. e104641. Available at: https://doi.org/10.1371/journal.pone.0104641.

Antell, G.T. *et al.* (2020) 'Marine biodiversity and geographic dstributions are independent on large scales', *Current Biology*, 30(1), pp. 115-121.e5. Available at: https://doi.org/10.1016/j.cub.2019.10.065.

Antell, G.T. *et al.* (2021) 'Thermal niches of planktonic foraminifera are static throughout glacial–interglacial climate change', *Proceedings of the National Academy of Sciences*, 118(18), p. e2017105118. Available at: https://doi.org/10.1073/pnas.2017105118.

Armstrong, H.A. and Brasier, M.D. (2004) *Microfossils*. 1st edn. Wiley. Available at: https://doi.org/10.1002/9781118685440.

Arnold, A.J., Kelly, D.C. and Parker, W.C. (1995) 'Causality and Cope's Rule: Evidence from the Planktonic Foraminifera', *Journal of Paleontology*, 69(2), pp. 203–210.

Austen, G.E. *et al.* (2016) 'Species identification by experts and non-experts: comparing images from field guides', *Scientific Reports*, 6(1), p. 33634. Available at: https://doi.org/10.1038/srep33634.

Aze, T. *et al.* (2011) 'A phylogeny of Cenozoic macroperforate planktonic foraminifera from fossil data', *Biological Reviews*, 86(4), pp. 900–927. Available at: https://doi.org/10.1111/j.1469-185X.2011.00178.x.

Aze, T. (2022) 'Unraveling ecological signals from a global warming event of the past', *Proceedings of the National Academy of Sciences*, 119(13), p. e2201495119. Available at: https://doi.org/10.1073/pnas.2201495119.

Badger, M.P.S. *et al.* (2013) 'High-resolution alkenone palaeobarometry indicates relatively stable *p* CO_2 during the Pliocene (3.3–2.8 Ma)', *Philosophical Transactions of the Royal Society A: Mathematical, Physical and Engineering Sciences*, 371(2001), p. 20130094. Available at: https://doi.org/10.1098/rsta.2013.0094.

Bandy, O.L. (1972) 'Origin and Development of Globorotalia (Turborotalia) pachyderma (Ehrenberg)', *Micropaleontology*, 18(3), pp. 294–318. Available at: https://doi.org/10.2307/1485010.

Banerjee, A. and Boyajian, G.E. (1997) 'Selectivity of foraminiferal extinction in the late Eocene', *Paleobiology*, 23(3), pp. 347–357. Available at: https://doi.org/10.1017/S0094837300019722.

Banerji, R.K. (1981) '"Kummerforms" in planktonic foraminifera, its cause and distribution in Pacific waters', *Journal of the Paleontological Society of India*, 25, pp. 21–25.

Banner, F.T. and Blow, W.H. (1960) 'Some primary types of species belonging to the Superfamilt Globigerinaceae', *Contributions from the Cushman Foundation for Foraminiferal Research*, XI(204).

Barker, S. and Elderfield, H. (2002) 'Foraminiferal Calcification Response to Glacial-Interglacial Changes in Atmospheric CO_2', *Science*, 297(5582), pp. 833–836. Available at: https://doi.org/10.1126/science.1072815.

Barnosky, A.D. *et al.* (2011) 'Has the Earth's sixth mass extinction already arrived?', *Nature*, 471(7336), pp. 51–57. Available at: https://doi.org/10.1038/nature09678.

Bartoli, G., Hönisch, B. and Zeebe, R.E. (2011) 'Atmospheric CO_2 decline during the Pliocene intensification of Northern Hemisphere glaciations', *Paleoceanography*, 26(4), p. 2010PA002055. Available at: https://doi.org/10.1029/2010PA002055.

Bé, A.W.H. (1977) 'An ecological, zoogeographic and taxonomic review of recent planktonic foraminifera', in A.T.S. Ramsay (ed.) *Oceanic Micropaleontology*. Academic Press, p. 837. Available at: https://www.semanticscholar.org/paper/An-ecological%2C-zoogeographic-and-taxonomic-review-B%C3%A9/813bd31ef261d3cf88cc593262bf7673c7329c1d (Accessed: 11 January 2024).

Béjard, T.M. *et al.* (2022) 'Calcification response of planktic foraminifera to environmental change in the Western Mediterranean Sea during the industrial era'. Available at: https://doi.org/10.5194/egusphere-2022-711.

Berger, W.H. (1969) 'Planktonic Foraminifera: Basic Morphology and Ecologic Implications', *Journal of Paleontology*, 43(6), pp. 1369–1383.

Bernard-Verdier, B. *et al.* (2012) 'Community assembly along a soil depth gradient: contrasting patterns of plant trait convergence and divergence in a Mediterranean rangeland - Bernard-Verdier - 2012 - Journal of Ecology - Wiley Online Library', *Journal of Ecology*, 100(6), pp. 1422–1433. Available at: https://doi.org/10.1111/1365-2745.12003.

Biggs, C.R. *et al.* (2020) 'Does functional redundancy affect ecological stability and resilience? A review and meta-analysis', *Ecosphere*, 11(7), p. e03184. Available at: https://doi.org/10.1002/ecs2.3184.

Bijma, J., Faber, W.W. and Hemleben, C. (1990) 'Temperature and salinity limits for growth and survival of some planktonic foraminifers in laboratory cultures', *Journal of Foraminiferal Research*, 20(2), pp. 95–116. Available at: https://doi.org/10.2113/gsjfr.20.2.95.

Blow, W.H. (1969) *Late Middle Eocene to Recent Planktonic Foraminiferal Biostratigraphy*. E. J. Brill.

Bolli, H.M. and Bermudez, P.J. (1965) 'Zonation based on planktonic foraminifera of middle Miocene to Pliocene warm-water sediments', *Bol. Informativo, Asoc. Venez. Geol., Min. Petrol.*, 8(5), pp. 121–149.

Boscolo-Galazzo, F. *et al.* (2022) 'Late Neogene evolution of modern deep-dwelling plankton', *Biogeosciences*, 19(3), pp. 743–762. Available at: https://doi.org/10.5194/bg-19-743-2022.

Boscolo-Galazzo, F. *et al.* (2024) 'Mg/Ca and $\delta^{18}O$ in multiple species of planktonic foraminifera from 15 Ma to Recent', *EGUsphere*, [preprint]. Available at: https://doi.org/10.5194/egusphere-2024-1608.

BouDagher-Fadel, M.K. (2015) *Biostratigraphic and Geological Significance of Planktonic Foraminifera*. UCL Press. Available at: https://doi.org/10.14324/111.9781910634257.

Brombacher, A. *et al.* (2017) 'The Breakdown of Static and Evolutionary Allometries during Climatic Upheaval', *The American Naturalist*, 190(3), pp. 350–362. Available at: https://doi.org/10.1086/692570.

Brombacher, A. *et al.* (2018) 'Temperature is a poor proxy for synergistic climate forcing of plankton evolution', *Proceedings of the Royal Society B: Biological Sciences*, 285(1883), p. 20180665. Available at: https://doi.org/10.1098/rspb.2018.0665.

Brombacher, A. *et al.* (2022) 'Analysing planktonic foraminiferal growth in three dimensions with foram3D: an R package for automated trait measurements from CT scans', *Journal of Micropalaeontology*, 41(2), pp. 149–164. Available at: https://doi.org/10.5194/jm-41-149-2022.

Brombacher, A. *et al.* (2023) 'Morphological variation across space does not predict phenotypic change through time in two Neogene planktonic foraminifera species', *Frontiers in Ecology and Evolution*, 11. Available at: https://www.frontiersin.org/articles/10.3389/fevo.2023.1165174 (Accessed: 5 February 2024).

Brown, K.A. *et al.* (2023) 'Trait-based approaches as ecological time machines: Developing tools for reconstructing long-term variation in ecosystems', *Functional Ecology*, 37(10), pp. 2552–2569. Available at: https://doi.org/10.1111/1365-2435.14415.

Brummer, G.-J.A. and Kučera, M. (2022) 'Taxonomic review of living planktonic foraminifera', *Journal of Micropalaeontology*, 41(1), pp. 29–74. Available at: https://doi.org/10.5194/jm-41-29-2022.

Burnham, K.P. and Anderson, D.R. (eds) (2004) *Model Selection and Multimodel Inference*. New York, NY: Springer. Available at: https://doi.org/10.1007/b97636.

Canadell, J.G. and Jackson, R.B. (2021) 'Ecosystem Collapse and Climate Change: An Introduction', in J.G. Canadell and R.B. Jackson (eds) *Ecosystem Collapse and Climate Change*. Cham: Springer International Publishing, pp. 1–9. Available at: https://doi.org/10.1007/978-3-030-71330-0_1.

Cardinale, B.J. *et al.* (2012) 'Biodiversity loss and its impact on humanity', *Nature*, 486(7401), pp. 59–67. Available at: https://doi.org/10.1038/nature11148.

Caron, D.A., Faber, W.W. and Bé, A.W.H. (1987) 'Effects of temperature and salinity on the growth and survival of the planktonic foraminifer *Globigerinoides sacculifer*', *Journal of the Marine Biological Association of the United Kingdom*, 67(2), pp. 323–341. Available at: https://doi.org/10.1017/S0025315400026643.

Ceballos, G. *et al.* (2015) 'Accelerated modern human–induced species losses: Entering the sixth mass extinction', *Science Advances*, 1(5), p. e1400253. Available at: https://doi.org/10.1126/sciadv.1400253.

Chaisson, W.P. and Pearson, P.N. (1997) 'Planktonic foraminifer biostratigraphy at Site 925: Middle Miocene-Pleistocene', in N.J. Shackleton et al. (eds) *Proc. ODP, Sci. Results*. College Station, TX: Ocean Drilling Program, pp. 3–31. Available at: doi:10.2973/odp.proc.sr.154.104.1997.

Chao, A. *et al.* (2014) 'Rarefaction and extrapolation with Hill numbers: a framework for sampling and estimation in species diversity studies', *Ecological Monographs*, 84(1), pp. 45–67. Available at: https://doi.org/10.1890/13-0133.1.

Chao, A. and Jost, L. (2012) 'Coverage-based rarefaction and extrapolation: standardizing samples by completeness rather than size', *Ecology*, 93(12), pp. 2533–2547. Available at: https://doi.org/10.1890/11-1952.1.

Chao, A. and Jost, L. (2015) 'Estimating diversity and entropy profiles via discovery rates of new species', *Methods in Ecology and Evolution*, 6(8), pp. 873–882. Available at: https://doi.org/10.1111/2041-210X.12349.

Cifelli, R. (1969) ‘Radiation of Cenozoic Planktonic Foraminifera’, *Systematic Zoology*, 18(2), p. 154. Available at: https://doi.org/10.2307/2412601.

Colles, A., Liow, L.H. and Prinzing, A. (2009) ‘Are specialists at risk under environmental change? Neoecological, paleoecological and phylogenetic approaches’, *Ecology Letters*, 12(8), pp. 849–863. Available at: https://doi.org/10.1111/j.1461-0248.2009.01336.x.

Condamine, F.L., Rolland, J. and Morlon, H. (2013) ‘Macroevolutionary perspectives to environmental change’, *Ecology Letters*. Edited by H. Maherali, 16(s1), pp. 72–85. Available at: https://doi.org/10.1111/ele.12062.

Coxall, H.K. *et al.* (2007) ‘Iterative evolution of digitate planktonic foraminifera’, *Paleobiology*, 33(4), pp. 495–516. Available at: https://doi.org/10.1666/06034.1.

Cushman, J.A. and Jarvis, P.W. (1930) ‘Miocene Foraminifera from Buff Bay, Jamaica’, *Journal of Paleontology*, 4(4), pp. 353–368.

Cusson, M. *et al.* (2015) ‘Relationships between biodiversity and the stability of marine ecosystems: Comparisons at a European scale using meta-analysis’, *Journal of Sea Research*, 98, pp. 5–14. Available at: https://doi.org/10.1016/j.seares.2014.08.004.

Da, J. *et al.* (2019) ‘Low CO2 levels of the entire Pleistocene epoch’, *Nature Communications*, 10(1), p. 4342. Available at: https://doi.org/10.1038/s41467-019-12357-5.

Dal Corso, J. *et al.* (2022) ‘Environmental crises at the Permian–Triassic mass extinction’, *Nature Reviews Earth & Environment*, 3(3), pp. 197–214. Available at: https://doi.org/10.1038/s43017-021-00259-4.

Darling, K.F. *et al.* (1996) ‘Molecular phylogeny of the planktic foraminifera’, *The Journal of Foraminiferal Research*, 26(4), pp. 324–330. Available at: https://doi.org/10.2113/gsjfr.26.4.324.

Darling, K.F. and Wade, C.M. (2008) ‘The genetic diversity of planktic foraminifera and the global distribution of ribosomal RNA genotypes’, *Marine Micropaleontology*, 67(3–4), pp. 216–238. Available at: https://doi.org/10.1016/j.marmicro.2008.01.009.

Dayrat, B. (2005) ‘Towards integrative taxonomy’, *Biological Journal of the Linnean Society*, 85(3), pp. 407–417. Available at: https://doi.org/10.1111/j.1095-8312.2005.00503.x.

De Schepper, S. *et al.* (2013) ‘Northern Hemisphere Glaciation during the Globally Warm Early Late Pliocene’, *PLoS ONE*. Edited by V.C. Smith, 8(12), p. e81508. Available at: https://doi.org/10.1371/journal.pone.0081508.

De Vargas, C. *et al.* (1999) 'Molecular evidence of cryptic speciation in planktonic foraminifers and their relation to oceanic provinces', *Proceedings of the National Academy of Sciences*, 96(6), pp. 2864–2868. Available at: https://doi.org/10.1073/pnas.96.6.2864.

De Villiers, S. (2004) 'Optimum growth conditions as opposed to calcite saturation as a control on the calcification rate and shell-weight of marine foraminifera', *Marine Biology*, 144(1), pp. 45–49. Available at: https://doi.org/10.1007/s00227-003-1183-8.

Díaz, S. *et al.* (2006) 'Biodiversity loss threatens human well-being', *PLOS Biology*, 4(8), p. e277. Available at: https://doi.org/10.1371/journal.pbio.0040277.

Doncaster, C.P. *et al.* (2016) 'Early warning of critical transitions in biodiversity from compositional disorder', *Ecology*, 97(11), pp. 3079–3090. Available at: https://doi.org/10.1002/ecy.1558.

Dowsett, H., Robinson, M. and Foley, K. (2015) 'A global planktic foraminifer census data set for the Pliocene ocean', *Scientific Data*, 2(1), p. 150076. Available at: https://doi.org/10.1038/sdata.2015.76.

Dowsett, H.J. and Caballero Gill, R.P. (2010) 'Pliocene Climate', *Stratigraphy*, 7(2–3), pp. 105–110. Available at: https://doi.org/10.29041/strat.07.2.01.

Dutkiewicz, A. and Müller, R.D. (2022) 'The History of Cenozoic Carbonate Flux in the Atlantic Ocean Constrained by Multiple Regional Carbonate Compensation Depth Reconstructions', *Geochemistry, Geophysics, Geosystems*, 23(11), p. e2022GC010667. Available at: https://doi.org/10.1029/2022GC010667.

Elmqvist, T. *et al.* (2003) 'Response diversity, ecosystem change, and resilience', *Frontiers in Ecology and the Environment*, 1(9), pp. 488–494. Available at: https://doi.org/10.1890/1540-9295(2003)001[0488:RDECAR]2.0.CO;2.

Elphick, C.S. (2008) 'How you count counts: the importance of methods research in applied ecology', *Journal of Applied Ecology*, 45(5), pp. 1313–1320. Available at: https://doi.org/10.1111/j.1365-2664.2008.01545.x.

Ezard, T.H., Pearson, P.N. and Purvis, A. (2010) 'Algorithmic approaches to aid species' delimitation in multidimensional morphospace', *BMC Evolutionary Biology*, 10(1), p. 175. Available at: https://doi.org/10.1186/1471-2148-10-175.

Ezard, T.H.G. *et al.* (2011) 'Interplay between changing climate and species' ecology drives macroevolutionary dynamics', *Science*, 332(6027), pp. 349–351. Available at: https://doi.org/10.1126/science.1203060.

Ezard, Thomas H. G. *et al.* (2011) 'The meaning of birth and death (in macroevolutionary birth–death models)', *Biology Letters*, 8(1), pp. 139–142. Available at: https://doi.org/10.1098/rsbl.2011.0699.

Ezard, T.H.G. and Purvis, A. (2016) 'Environmental changes define ecological limits to species richness and reveal the mode of macroevolutionary competition', *Ecology Letters*. Edited by H. Morlon, 19(8), pp. 899–906. Available at: https://doi.org/10.1111/ele.12626.

Fabbrini, A. *et al.* (2021) 'Systematic taxonomy of middle Miocene Sphaeroidinellopsis (planktonic foraminifera)', *Journal of Systematic Palaeontology*, 19(13), pp. 953–968. Available at: https://doi.org/10.1080/14772019.2021.1991500.

Fabbrini, A. *et al.* (2023) 'Bridging the extant and fossil record of planktonic foraminifera: implications for the *Globigerina* lineage', *Palaeontology*, 66(6), p. e12676. Available at: https://doi.org/10.1111/pala.12676.

Fabbrini, A. *et al.* (2024) 'Rediscovering *Globigerina bollii* Cita and Premoli Silva 1960', *Journal of Micropalaeontology*, 43(1), pp. 121–138. Available at: https://doi.org/10.5194/jm-43-121-2024.

Fayolle, F. and Wade, B.S. (2021) 'The evolution of Eocene planktonic foraminifera Dentoglobigerina', *Journal of Systematic Palaeontology*, 19(5), pp. 333–376. Available at: https://doi.org/10.1080/14772019.2021.1904021.

Fenton, I.S. *et al.* (2016) 'Environmental predictors of diversity in Recent planktonic foraminifera as recorded in marine sediments', *PLOS ONE*. Edited by D.P. Gillikin, 11(11), p. e0165522. Available at: https://doi.org/10.1371/journal.pone.0165522.

Fenton, I.S. *et al.* (2021) 'Triton, a new species-level database of Cenozoic planktonic foraminiferal occurrences', *Scientific Data*, 8(1), p. 160. Available at: https://doi.org/10.1038/s41597-021-00942-7.

Fenton, I.S. *et al.* (2023) 'Origination of the modern-style diversity gradient 15 million years ago', *Nature*, 614(7949), pp. 708–712. Available at: https://doi.org/10.1038/s41586-023-05712-6.

Ferraro, S. *et al.* (2020) 'Morphometric response of late Aptian planktonic foraminiferal communities to environmental changes: A case study of *Paraticinella rohri* at Poggio le Guaine

(central Italy)', *Palaeogeography, Palaeoclimatology, Palaeoecology*, 538, p. 109384. Available at: https://doi.org/10.1016/j.palaeo.2019.109384.

Fetzer, I. *et al.* (2015) 'The extent of functional redundancy changes as species' roles shift in different environments', *Proceedings of the National Academy of Sciences*, 112(48), pp. 14888–14893. Available at: https://doi.org/10.1073/pnas.1505587112.

Finnegan, S. *et al.* (2015) 'Paleontological baselines for evaluating extinction risk in the modern oceans', *Science*, 348(6234), pp. 567–570. Available at: https://doi.org/10.1126/science.aaa6635.

Fornasini, C. (1902) 'Sinossi metodica dei foraminiferi sin qui rinvenuti nella sabbia del Lido di Rimini', *Academia de la scienze di Bologna* [Preprint].

Fox, L. *et al.* (2020) 'Quantifying the Effect of Anthropogenic Climate Change on Calcifying Plankton', *Scientific Reports*, 10(1), p. 1620. Available at: https://doi.org/10.1038/s41598-020-58501-w.

Fraass, A.J., Kelly, D.C. and Peters, S.E. (2015) 'Macroevolutionary history of the planktic foraminifera', *Annual Review of Earth and Planetary Sciences*, 43(1), pp. 139–166. Available at: https://doi.org/10.1146/annurev-earth-060614-105059.

Fraley, C. and Raftery, A.E. (2002) 'Model-Based Clustering, Discriminant Analysis, and Density Estimation', *Journal of the American Statistical Association*, 97(458), pp. 611–631. Available at: https://doi.org/10.1198/016214502760047131.

Gaston, K.J. (2008) 'Biodiversity and extinction: the importance of being common', *Progress in Physical Geography: Earth and Environment*, 32(1), pp. 73–79. Available at: https://doi.org/10.1177/0309133308089499.

Goswami, A. (2015) 'Phenome10K: a free online repository for 3-D scans of biological and palaeontological specimens'. Available at: www.phenome10k.org.

Goswami, M. *et al.* (2017) 'Functional Diversity: An Important Measure of Ecosystem Functioning', *Advances in Microbiology*, 7(1), pp. 82–93. Available at: https://doi.org/10.4236/aim.2017.71007.

Gray, W.R. and Evans, D. (2019) 'Nonthermal Influences on Mg/Ca in Planktonic Foraminifera: A Review of Culture Studies and Application to the Last Glacial Maximum', *Paleoceanography and Paleoclimatology*, 34(3), pp. 306–315. Available at: https://doi.org/10.1029/2018PA003517.

Grigoratou, M. *et al.* (2019) 'A trait-based modelling approach to planktonic foraminifera ecology', *Biogeosciences*, 16(7), pp. 1469–1492. Available at: https://doi.org/10.5194/bg-16-1469-2019.

Hackett, T.D. *et al.* (2024) 'Multi-habitat landscapes are more diverse and stable with improved function', *Nature*, 633(8028), pp. 114–119. Available at: https://doi.org/10.1038/s41586-024-07825-y.

Hallock, P., Premoli Silva, I. and Boersma, A. (1991) 'Similarities between planktonic and larger foraminiferal evolutionary trends through Paleogene paleoceanographic changes', *Palaeogeography, Palaeoclimatology, Palaeoecology*, 83(1–3), pp. 49–64. Available at: https://doi.org/10.1016/0031-0182(91)90075-3.

Hannisdal, B. *et al.* (2017) 'Common species link global ecosystems to climate change: dynamical evidence in the planktonic fossil record', *Proceedings of the Royal Society B: Biological Sciences*, 284(1858), p. 20170722. Available at: https://doi.org/10.1098/rspb.2017.0722.

Harnik, P.G. *et al.* (2012) 'Extinctions in ancient and modern seas', *Trends in Ecology and Evolution*, 27(11), pp. 608–617. Available at: https://doi.org/10.1016/j.tree.2012.07.010.

Haynes, J.R. (1981) *Foraminifera*. London: Palgrave Macmillan UK. Available at: https://doi.org/10.1007/978-1-349-05397-1.

Hemleben, C., Spindler, M. and Anderson, O.R. (1989) *Modern Planktonic Foraminifera*. New York Berlin Heidelberg London Paris Tokyo: Springer-Verlag.

Hill, M.O. (1973) 'Diversity and evenness: A unifying notation and its consequences', *Ecology*, 54(2), pp. 427–432. Available at: https://doi.org/10.2307/1934352.

Hinsbergen, D.J.J. van *et al.* (2015) 'A Paleolatitude Calculator for Paleoclimate Studies', *PLOS ONE*, 10(6), p. e0126946. Available at: https://doi.org/10.1371/journal.pone.0126946.

Hönisch, B. *et al.* (2012) 'The Geological Record of Ocean Acidification', *Science*, 335(6072), pp. 1058–1063. Available at: https://doi.org/10.1126/science.1208277.

Honjo, S. and Berggren, W.A. (1967) 'Scanning Electron Microscope Studies of Planktonic Foraminifera', *Micropaleontology*, 13(4), pp. 393–406. Available at: https://doi.org/10.2307/1484717.

Hooper, D.U. *et al.* (2005) 'Effects of Biodiversity on Ecosystem Functioning: A Consensus of Current Knowledge', *Ecological Monographs*, 75(1), pp. 3–35. Available at: https://doi.org/10.1890/04-0922.

Hopkins, G.W. and Freckleton, R.P. (2002) 'Declines in the numbers of amateur and professional taxonomists: implications for conservation', *Animal Conservation*, 5(3), pp. 245–249. Available at: https://doi.org/10.1017/S1367943002002299.

Huber, B.T., Bijma, J. and Darling, K. (1997) 'Cryptic speciation in the living planktonic foraminifer *Globigerinella siphonifera* (d'Orbigny)', *Paleobiology*, 23(1), pp. 33–62. Available at: https://doi.org/10.1017/S0094837300016638.

Huber, R. *et al.* (1999) 'Data Report: Counting experiments on different size fractions: Examples from Site 984', in M.E. Raymo et al. (eds) *Proc. ODP Sci. Results*. College Station, TX: Ocean Drilling Program. Available at: doi: 10.2973/odp.proc.sr.162.034.1999 (Accessed: 12 January 2024).

Hull, P.M. and Norris, R.D. (2011) 'Diverse patterns of ocean export productivity change across the Cretaceous-Paleogene boundary: New insights from biogenic barium', *Paleoceanography*, 26(3). Available at: https://doi.org/10.1029/2010PA002082.

IPCC (2021) 'Climate Change 2021 – The Physical Science Basis: Working Group I Contribution to the Sixth Assessment Report of the Intergovernmental Panel on Climate Change', in V. Masson-Delmotte et al. (eds). Cambridge, United Kingdom and New York, NY, USA: Cambridge University Press, p. 2391. Available at: doi: 10.1017/9781009157896 (Accessed: 11 January 2024).

IPCC (2023) 'IPCC, 2023: Summary for Policymakers', in *Climate Change 2023: Synthesis Report. Contribution of Working Groups I, II and III to the Sixth Assessment Report of the Intergovernmental Panel on Climate Change [Core Writing Team, H. Lee and J. Romero (eds)]*. First. Geneva, Switzerland: Intergovernmental Panel on Climate Change (IPCC). Available at: https://doi.org/10.59327/IPCC/AR6-9789291691647.

Isbell, F. *et al.* (2015) 'Biodiversity increases the resistance of ecosystem productivity to climate extremes', *Nature*, 526(7574), pp. 574–577. Available at: https://doi.org/10.1038/nature15374.

Ives, A.R., Cardinale, B.J. and Snyder, W.E. (2005) 'A synthesis of subdisciplines: predator–prey interactions, and biodiversity and ecosystem functioning', *Ecology Letters*, 8(1), pp. 102–116. Available at: https://doi.org/10.1111/j.1461-0248.2004.00698.x.

Ives, A.R. and Carpenter, S.R. (2007) 'Stability and Diversity of Ecosystems', *Science*, 317(5834), pp. 58–62. Available at: https://doi.org/10.1126/science.1133258.

Ives, A.R., Klug, J.L. and Gross, K. (2000) 'Stability and species richness in complex communities', *Ecology Letters*, 3(5), pp. 399–411. Available at: https://doi.org/10.1046/j.1461-0248.2000.00144.x.

Jablonski, D. (2005) 'Mass extinctions and macroevolution', *Paleobiology*, 31(sp5), pp. 192–210. Available at: https://doi.org/10.1666/0094-8373(2005)031[0192:MEAM]2.0.CO;2.

Kearns, L.E. *et al.* (2021) 'Searching for function: Reconstructing adaptive niche changes using geochemical and morphological data in planktonic foraminifera', *Frontiers in Ecology and Evolution*, 9, p. 679722. Available at: https://doi.org/10.3389/fevo.2021.679722.

Kearns, L.E. *et al.* (2023) 'The Influence of Geochemical Variation Among *Globigerinoides ruber* Individuals on Paleoceanographic Reconstructions', *Paleoceanography and Paleoclimatology*, 38(4), p. e2022PA004549. Available at: https://doi.org/10.1029/2022PA004549.

Keller, G. (1988) 'Extinction, Survivorship and Evolution of Planktic Foraminifera across the Cretaceous/Tertiary Boundary at E1 Kef, Tunisia', *Marine Micropaleontology*, 13, pp. 239–263.

Keller, G. and Abramovich, S. (2009) 'Lilliput effect in late Maastrichtian planktic foraminifera: Response to environmental stress', *Palaeogeography, Palaeoclimatology, Palaeoecology*, 284(1), pp. 47–62. Available at: https://doi.org/10.1016/j.palaeo.2009.08.029.

Kennett, J.P. and Srinivasan, M.S. (1983) *Neogene Planktonic Foraminifera: A Phylogenetic Atlas*. Stroudsberg, Pennsylvania: Hutchinson Ross Publishing Company.

Kinoshita, S. *et al.* (2022) 'Response of Planktic Foraminiferal Shells to Ocean Acidification and Global Warming Assessed Using Micro-X-Ray Computed Tomography', *Paleontological Research*, 26(4). Available at: https://doi.org/10.2517/PR200043.

Kirchner, J.W. and Weil, A. (2000) 'Delayed biological recovery from extinctions throughout the fossil record', *Nature*, 404(6774), pp. 177–180. Available at: https://doi.org/10.1038/35004564.

Knappertsbusch, M. (2007) 'Morphological variability of Globorotalia menardii (planktonic foraminifera) in two DSDP cores from the Caribbean Sea and the Eastern Equatorial Pacific', *Carnets de géologie (Notebooks on geology)* [Preprint], (Articles). Available at: https://doi.org/10.4267/2042/8455.

Knappertsbusch, M. (2016) ‘Evolutionary prospection in the Neogene planktic foraminifer Globorotalia menardii and related forms from ODP Hole 925B (Ceara Rise, western tropical Atlantic): evidence for gradual evolution superimposed by long distance dispersal?’, *Swiss Journal of Palaeontology*, 135(2), pp. 205–248. Available at: https://doi.org/10.1007/s13358-016-0113-6.

Koch, P.L. and Barnosky, A.D. (2006) ‘Late Quaternary Extinctions: State of the Debate’, *Annual Review of Ecology, Evolution, and Systematics*, 37(1), pp. 215–250. Available at: https://doi.org/10.1146/annurev.ecolsys.34.011802.132415.

Kolbe, S.E., Lockwood, R. and Hunt, G. (2011) ‘Does morphological variation buffer against extinction? A test using veneroid bivalves from the Plio-Pleistocene of Florida’, *Paleobiology*, 37(3), pp. 355–368. Available at: https://doi.org/10.1666/09073.1.

Kucera, M. (2007) ‘Chapter Six Planktonic Foraminifera as Tracers of Past Oceanic Environments’, in *Developments in Marine Geology*. Elsevier, pp. 213–262. Available at: https://doi.org/10.1016/S1572-5480(07)01011-1.

Kürzel, K. *et al.* (2022) ‘Correct Species Identification and Its Implications for Conservation Using Haploniscidae (Crustacea, Isopoda) in Icelandic Waters as a Proxy’, *Frontiers in Marine Science*, 8. Available at: https://doi.org/10.3389/fmars.2021.795196.

Laliberté, E. *et al.* (2010) ‘Land-use intensification reduces functional redundancy and response diversity in plant communities’, *Ecology Letters*, 13(1), pp. 76–86. Available at: https://doi.org/10.1111/j.1461-0248.2009.01403.x.

Laureto, L.M.O., Cianciaruso, M.V. and Samia, D.S.M. (2015) ‘Functional diversity: an overview of its history and applicability’, *Natureza & Conservação*, 13(2), pp. 112–116. Available at: https://doi.org/10.1016/j.ncon.2015.11.001.

Lea, D.W. (2014) ‘Elemental and Isotopic Proxies of Past Ocean Temperatures’, in *Treatise on Geochemistry*. Elsevier, pp. 373–397. Available at: https://doi.org/10.1016/B978-0-08-095975-7.00614-8.

Lennon, J.J. *et al.* (2004) ‘Contribution of rarity and commonness to patterns of species richness’, *Ecology Letters*, 7(2), pp. 81–87. Available at: https://doi.org/10.1046/j.1461-0248.2004.00548.x.

Lipps, J.H. (1970) ‘Plankton evolution’, *Evolution*, 24(1), pp. 1–22. Available at: https://doi.org/10.1111/j.1558-5646.1970.tb01737.x.

Lisiecki, L.E. and Raymo, M.E. (2005) 'A Pliocene-Pleistocene stack of 57 globally distributed benthic $\delta^{18}O$ records', *Paleoceanography*, 20(1), p. 2004PA001071. Available at: https://doi.org/10.1029/2004PA001071.

Lisiecki, L.E. and Raymo, M.E. (2007) 'Plio–Pleistocene climate evolution: trends and transitions in glacial cycle dynamics', *Quaternary Science Reviews*, 26(1–2), pp. 56–69. Available at: https://doi.org/10.1016/j.quascirev.2006.09.005.

Lloyd, G.T. *et al.* (2012) 'Sampling bias and the fossil record of planktonic foraminifera on land and in the deep sea', *Paleobiology*, 38(4), pp. 569–584. Available at: https://doi.org/10.1666/11041.1.

Lombard, F. *et al.* (2009) 'Modelling the temperature dependent growth rates of planktic foraminifera', *Marine Micropaleontology*, 70(1–2), pp. 1–7. Available at: https://doi.org/10.1016/j.marmicro.2008.09.004.

Lombard, F. *et al.* (2010) 'Effect of carbonate ion concentration and irradiance on calcification in planktonic foraminifera', *Biogeosciences*, 7(1), pp. 247–255. Available at: https://doi.org/10.5194/bg-7-247-2010.

Lombard, F. *et al.* (2011) 'Modelling planktic foraminifer growth and distribution using an ecophysiological multi-species approach', *Biogeosciences*, 8(4), pp. 853–873. Available at: https://doi.org/10.5194/bg-8-853-2011.

Lombard1, F. *et al.* (2009) 'Temperature effect on respiration and photosynthesis of the symbiont-bearing planktonic foraminifera Globigerinoides ruber, Orbulina universa, and Globigerinella siphonifera', *Limnology and Oceanography*, 54(1), pp. 210–218. Available at: https://doi.org/10.4319/lo.2009.54.1.0210.

Loreau, M. *et al.* (2001) 'Biodiversity and ecosystem functioning: Current knowledge and future challenges', *Science*, 294(5543), pp. 804–808. Available at: https://doi.org/10.1126/science.1064088.

Loreau, M. (2004) 'Does Functional Redundancy Exist?', *Oikos*, 104(3), pp. 606–611. Available at: https://doi.org/10.1111/j.0030-1299.2004.12685.x.

Louca, S. and Pennell, M.W. (2020) 'Extant timetrees are consistent with a myriad of diversification histories', *Nature*, 580(7804), pp. 502–505. Available at: https://doi.org/10.1038/s41586-020-2176-1.

Lowery, C.M. *et al.* (2020) 'Ecological Response of Plankton to Environmental Change: Thresholds for Extinction'.

Lucini, F.A. *et al.* (2020) 'Diversity increases the stability of ecosystems', *PLOS ONE*. Edited by J. Hewitt, 15(4), p. e0228692. Available at: https://doi.org/10.1371/journal.pone.0228692.

Lyons, K.G. *et al.* (2005) 'Rare species and ecosystem functioning', *Conservation Biology*, 19(4), pp. 1019–1024. Available at: https://doi.org/10.1111/j.1523-1739.2005.00106.x.

MacDougall, A.S. *et al.* (2013) 'Diversity loss with persistent human disturbance increases vulnerability to ecosystem collapse', *Nature*, 494(7435), pp. 86–89. Available at: https://doi.org/10.1038/nature11869.

Malmgren, B. and Kennett, J.P. (1976) 'Biometric analysis of phenotypic variation in Recent*Globigerina bulloides* d'Orbigny in the southern Indian Ocean', *Marine Micropaleontology*, 1, pp. 3–25. Available at: https://doi.org/10.1016/0377-8398(76)90003-7.

Malmgren, B.A., Berggren, W.A. and Lohmann, G.P. (1983) 'Evidence for punctuated gradualism in the Late Neogene *Globorotalia tumida* lineage of planktonic foraminifera', *Paleobiology*, 9(4), pp. 377–389. Available at: https://doi.org/10.1017/S0094837300007843.

Marshall, C.R. (2017) 'Five palaeobiological laws needed to understand the evolution of the living biota', *Nature Ecology & Evolution*, 1(6), p. 0165. Available at: https://doi.org/10.1038/s41559-017-0165.

Martínez-Botí, M.A. *et al.* (2015) 'Plio-Pleistocene climate sensitivity evaluated using high-resolution CO2 records', *Nature*, 518(7537), pp. 49–54. Available at: https://doi.org/10.1038/nature14145.

Mary, Y. (2013) *Morphologic, biogeographic and ontogenetic investigation of Mid-Pliocene menardellids (planktonic foraminifera)*. University of Basel. Available at: 10.5451/unibas-006194467.

Mary, Y. and Knappertsbusch, M.W. (2013) 'Morphological variability of menardiform globorotalids in the Atlantic Ocean during Mid-Pliocene', *Marine Micropaleontology*, 101, pp. 180–193. Available at: https://doi.org/10.1016/j.marmicro.2012.12.001.

Mayr, E. (1968) 'The Role of Systematics in Biology', *Science*, 159. Available at: https://doi.org/10.1126/science.159.3815.595.

McCann, K.S. (2000) ‘The diversity–stability debate’, *Nature*, 405(6783), pp. 228–233. Available at: https://doi.org/10.1038/35012234.

Media Cybernetics (2017) ‘Image-Pro Premier: 2D image analysis software’. Available at: https://my.mediacy.com/support/updates/image-pro-premier-9-2-9-3-415.

Meilland, J. *et al.* (2021) ‘Population dynamics and reproduction strategies of planktonic foraminifera in the open ocean’, *Biogeosciences*, 18(20), pp. 5789–5809. Available at: https://doi.org/10.5194/bg-18-5789-2021.

Moller, T., Schulz, H. and Kucera, M. (2013) ‘The effect of sea surface properties on shell morphology and size of the planktonic foraminifer Neogloboquadrina pachyderma in the North Atlantic’, *Palaeogeography, Palaeoclimatology, Palaeoecology*, 391, pp. 34–48. Available at: https://doi.org/10.1016/j.palaeo.2011.08.014.

Morard, R. *et al.* (2024) ‘The global genetic diversity of planktonic foraminifera reveals the structure of cryptic speciation in plankton’, *Biological Reviews*, 99(4), pp. 1218–1241. Available at: https://doi.org/10.1111/brv.13065.

Mouillot, D. *et al.* (2013) ‘A functional approach reveals community responses to disturbances’, *Trends in Ecology & Evolution*, 28(3), pp. 167–177. Available at: https://doi.org/10.1016/j.tree.2012.10.004.

Mouillot, D. *et al.* (2014) ‘Functional over-redundancy and high functional vulnerability in global fish faunas on tropical reefs’, *Proceedings of the National Academy of Sciences*, 111(38), pp. 13757–13762. Available at: https://doi.org/10.1073/pnas.1317625111.

Mulqueeney, J.M. *et al.* (2024) ‘How many specimens make a sufficient training set for automated three-dimensional feature extraction?’, *Royal Society Open Science*, 11(6), p. rsos.240113. Available at: https://doi.org/10.1098/rsos.240113.

Norris, R.D. (1991) ‘Biased extinction and evolutionary trends’, *Paleobiology*, 17(4), pp. 388–399. Available at: https://doi.org/10.1017/S0094837300010721.

Norris, R.DeWitt. and Corfield, R.M. (1998) *Isotope paleobiology and paleoecology*. Fayetteville, AR: Paleontological Society (The Paleontological Society papers, v. 4).

Olsson, R.K. (1973) ‘What Is a Kummerform Planktonic Foraminifer?’, *Journal of Paleontology*, 47(2), pp. 327–329.

Ottens, J.J. and Nederbragt, A.J. (1992) 'Planktic foraminiferal diversity as indicator of ocean environments', *Marine Micropaleontology*, 19(1–2), pp. 13–28. Available at: https://doi.org/10.1016/0377-8398(92)90019-G.

Parker, F.L. (1973) 'Late Cenozoic biostratigraphy (Planktonic Foraminifera) of tropical Atlantic deep-sea sections', *Revista española de micropaleontología*, 5(2), pp. 253–289.

Pärtel, M., Szava-Kovats, R. and Zobel, M. (2011) 'Dark diversity: shedding light on absent species', *Trends in Ecology & Evolution*, 26(3), pp. 124–128. Available at: https://doi.org/10.1016/j.tree.2010.12.004.

Payne, J.L. *et al.* (2016) 'Ecological selectivity of the emerging mass extinction in the oceans', *Science*, 353(6305), pp. 1284–1286. Available at: https://doi.org/10.1126/science.aaf2416.

Payne, J.L. and Finnegan, S. (2007) 'The effect of geographic range on extinction risk during background and mass extinction', *Proceedings of the National Academy of Sciences*, 104(25), pp. 10506–10511. Available at: https://doi.org/10.1073/pnas.0701257104.

Pearson, P.N. (1998) 'Speciation and Extinction Asymmetries in Paleontological Phylogenies: Evidence for Evolutionary Progress', *Paleobiology*, 24(3), pp. 305–335. Available at: https://doi.org/10.1666/0094-8373(1998)024[0305:SAEAIP]2.3.CO;2.

Pearson, P.N. *et al.* (2001) 'Warm tropical sea surface temperatures in the Late Cretaceous and Eocene epochs', *Nature*, 413(6855), pp. 481–487. Available at: https://doi.org/10.1038/35097000.

Pearson, P.N. and Ezard, T.H.G. (2014) 'Evolution and speciation in the Eocene planktonic foraminifer Turborotalia', *Paleobiology*, 40(1), pp. 130–143. Available at: https://doi.org/10.1666/13004.

Peres-Neto, P.R., Jackson, D.A. and Somers, K.M. (2005) 'How many principal components? stopping rules for determining the number of non-trivial axes revisited', *Computational Statistics & Data Analysis*, 49(4), pp. 974–997. Available at: https://doi.org/10.1016/j.csda.2004.06.015.

Petchey, O.L. and Gaston, K.J. (2006) 'Functional diversity: back to basics and looking forward', *Ecology Letters*, 9(6), pp. 741–758. Available at: https://doi.org/10.1111/j.1461-0248.2006.00924.x.

Peters, S.E., Kelly, D.C. and Fraass, A.J. (2013) 'Oceanographic controls on the diversity and extinction of planktonic foraminifera', *Nature*, 493(7432), pp. 398–401. Available at: https://doi.org/10.1038/nature11815.

Pfuhl, H.A. and Shackleton, N.J. (2004) 'Changes in coiling direction, habitat depth and abundance in two menardellid species', *Marine Micropaleontology*, 50(1–2), pp. 3–20. Available at: https://doi.org/10.1016/S0377-8398(03)00063-X.

Pinheiro, J. *et al.* (2024) 'Linear and nonlinear mixed effects models'. Available at: https://svn.r-project.org/R-packages/trunk/nlme/.

Pires, A.P.F., Srivastava, D.S. and Farjalla, V.F. (2018) 'Is biodiversity able to buffer ecosystems from climate change? What we know and what we don't', *BioScience*, 68(4), pp. 273–280. Available at: https://doi.org/10.1093/biosci/biy013.

Poole, C.R. and Wade, B.S. (2019) 'Systematic taxonomy of the *Trilobatus sacculifer* plexus and descendant *Globigerinoidesella fistulosa* (planktonic foraminifera)', *Journal of Systematic Palaeontology*, 17(23), pp. 1989–2030. Available at: https://doi.org/10.1080/14772019.2019.1578831.

Quental, T.B. and Marshall, C.R. (2010) 'Diversity dynamics: Molecular phylogenies need the fossil record', *Trends in Ecology and Evolution*, 25(8), pp. 434–441. Available at: https://doi.org/10.1016/j.tree.2010.05.002.

R Core Team (2023) 'R: A Language and Environment for Statistical Computing'. Vienna, Austria: R Foundation for Statistical Computing. Available at: https://www.r-project.org/.

Reich, P.B. *et al.* (2012) 'Impacts of Biodiversity Loss Escalate Through Time as Redundancy Fades', *Science*, 336(6081), pp. 589–592. Available at: https://doi.org/10.1126/science.1217909.

Rillo, M.C. *et al.* (2019) 'On the mismatch in the strength of competition among fossil and modern species of planktonic Foraminifera', *Global Ecology and Biogeography*. Edited by D. Tittensor, 28(12), pp. 1866–1878. Available at: https://doi.org/10.1111/geb.13000.

Rillo, M.C. (2019) *Unravelling macroecological patterns in extant planktonic Foraminifera*. Doctor of Philosophy. University of Southampton.

Rillo, M.C. *et al.* (2020) 'Intraspecific size variation in planktonic foraminifera cannot be consistently predicted by the environment', *Ecology and Evolution*, 10(20), pp. 11579–11590. Available at: https://doi.org/10.1002/ece3.6792.

Roberts, D.L., Elphick, C.S. and Reed, J.M. (2010) 'Identifying Anomalous Reports of Putatively Extinct Species and Why It Matters', *Conservation Biology*, 24(1), pp. 189–196. Available at: https://doi.org/10.1111/j.1523-1739.2009.01292.x.

Rohling, E.J. *et al.* (2004) 'Reconstructing past planktic foraminiferal habitats using stable isotope data: a case history for Mediterranean sapropel S5', *Marine Micropaleontology*, 50(1–2), pp. 89–123. Available at: https://doi.org/10.1016/S0377-8398(03)00068-9.

Rutherford, S., D'Hondt, S. and Prell, W. (1999) 'Environmental controls on the geographic distribution of zooplankton diversity', *Nature*, 400(6746), pp. 749–753. Available at: https://doi.org/10.1038/23449.

Schiebel, R. and Hemleben, C. (2005) 'Modern planktic foraminifera', *Paläontologische Zeitschrift*, 79(1), pp. 135–148. Available at: https://doi.org/10.1007/BF03021758.

Schiebel, R. and Hemleben, C. (2017) *Planktic Foraminifers in the Modern Ocean*. Berlin, Heidelberg: Springer Berlin Heidelberg. Available at: https://doi.org/10.1007/978-3-662-50297-6.

Schmidt, D.N., Thierstein, H.R., *et al.* (2004) 'Abiotic Forcing of Plankton Evolution in the Cenozoic', *Science*, 303(5655), pp. 207–210. Available at: https://doi.org/10.1126/science.1090592.

Schmidt, D.N., Renaud, S., *et al.* (2004) 'Size distribution of Holocene planktic foraminifer assemblages: biogeography, ecology and adaptation', *Marine Micropaleontology*, 50(3–4), pp. 319–338. Available at: https://doi.org/10.1016/S0377-8398(03)00098-7.

Schmidt, D.N. *et al.* (2006) 'Biogeography and evolution of body size in marine plankton', *Earth-Science Reviews*, 78(3–4), pp. 239–266. Available at: https://doi.org/10.1016/j.earscirev.2006.05.004.

Schmidt, D.N. *et al.* (2016) 'Morphological response of planktic foraminifers to habitat modifications associated with the emergence of the Isthmus of Panama', *Marine Micropaleontology*, 128, pp. 28–38. Available at: https://doi.org/10.1016/j.marmicro.2016.08.003.

Schmidt, D.N., Renaud, S. and Bollmann, J. (2003) 'Response of planktic foraminiferal size to late Quaternary climate change', *Paleoceanography*, 18(2), p. 2002PA000831. Available at: https://doi.org/10.1029/2002PA000831.

Schmidt, D.N., Thierstein, H. and Bollmann, J. (2004) 'The evolutionary history of size variation of planktic foraminiferal assemblages in the Cenozoic', *Palaeogeography, Palaeoclimatology, Palaeoecology*, 212(1–2), pp. 159–180. Available at: https://doi.org/10.1016/S0031-0182(04)00312-8.

Schmidt, M.W., Vautravers, M.J. and Spero, H.J. (2006) 'Western Caribbean sea surface temperatures during the late Quaternary', *Geochemistry, Geophysics, Geosystems*, 7(2), p. 2005GC000957. Available at: https://doi.org/10.1029/2005GC000957.

Schulte, P. *et al.* (2010) 'The Chicxulub Asteroid Impact and Mass Extinction at the Cretaceous-Paleogene Boundary', *Science*, 327(5970), pp. 1214–1218. Available at: https://doi.org/10.1126/science.1177265.

Scott, G.H. (2011) 'Holotypes in the taxonomy of planktonic foraminiferal morphospecies', *Marine Micropaleontology*, 78(3), pp. 96–100. Available at: https://doi.org/10.1016/j.marmicro.2010.11.001.

Scrucca, L. *et al.* (2016) 'mclust 5: Clustering, Classification and Density Estimation Using Gaussian Finite Mixture Models', *The R Journal*, 8(1), p. 289. Available at: https://doi.org/10.32614/RJ-2016-021.

Sexton, P.F., Wilson, P.A. and Pearson, P.N. (2006) 'Microstructural and geochemical perspectives on planktic foraminiferal preservation: "Glassy" versus "Frosty"', *Geochemistry Geophysics Geosystems*, 7(12), p. Q12P19.

Shackleton, N.J. (1977) 'Oxygen isotopes, ice volume and sea level', *Quaternary Science Reviews*, 6(3–4), pp. 193–190. Available at: https://doi.org/10.1016/0277-3791(87)90003-5.

Shackleton, N.J. and Vincent, E. (1978) 'Oxygen and carbon isotope studies in recent foraminifera from the southwest Indian ocean', *Marine Micropaleontology*, 3(1), pp. 1–13. Available at: https://doi.org/10.1016/0377-8398(78)90008-7.

She, Y. *et al.* (2023) 'Relationship between Species Diversity and Community Stability in Degraded Alpine Meadows during Bare Patch Succession', *Plants*, 12(20), p. 3582. Available at: https://doi.org/10.3390/plants12203582.

Shipboard Scientific Party (1995) 'Site 925', in W.B. Curry, N.J. Shackleton, and C. Richter (eds) *Proc. ODP. Init. Repts.* College Station, TX: Ocean Drilling Program, pp. 55–152. Available at: doi:10.2973/odp.proc.ir.154.104.1995.

Simmons, B.I. *et al.* (2020) 'Estimating the risk of species interaction loss in mutualistic communities', *PLOS Biology*, 18(8), p. e3000843. Available at: https://doi.org/10.1371/journal.pbio.3000843.

Stachowicz, J.J., Bruno, J.F. and Duffy, J.E. (2007) 'Understanding the Effects of Marine Biodiversity on Communities and Ecosystems', *Annual Review of Ecology, Evolution, and Systematics*, 38(1), pp. 739–766. Available at: https://doi.org/10.1146/annurev.ecolsys.38.091206.095659.

Stewart, D.R.M. (2003) *Evolution of Neogene globorotaliid foraminifera and Miocene climate change*. Doctor of Philosophy. University of Bristol.

Swain, A. *et al.* (2024) 'Biogeographic response of marine plankton to Cenozoic environmental changes', *Nature*, pp. 1–8. Available at: https://doi.org/10.1038/s41586-024-07337-9.

Tabachnick, R.E. and Bookstein, F.L. (1990) 'The Structure of Individual Variation in Miocene globorotalia', *Evolution*, 44(2), pp. 416–434. Available at: https://doi.org/10.2307/2409418.

The NOW Community (2024) 'New and Old Wrolds Database of Fossil Mammals (NOW)'. Available at: https://doi.org/10.5281/zenodo.4268068.

Thomson, S.A. *et al.* (2018) 'Taxonomy based on science is necessary for global conservation', *PLOS Biology*, 16(3), p. e2005075. Available at: https://doi.org/10.1371/journal.pbio.2005075.

Thunell, R.C. (1981) 'Cenozoic palaeotemperature changes and planktonic foraminiferal speciation', *Nature*, 289(5799), pp. 670–672. Available at: https://doi.org/10.1038/289670a0.

Tilman, D., Isbell, F. and Cowles, J.M. (2014) 'Biodiversity and Ecosystem Functioning', *Annual Review of Ecology, Evolution, and Systematics*, 45(Volume 45, 2014), pp. 471–493. Available at: https://doi.org/10.1146/annurev-ecolsys-120213-091917.

Todd, C.L. *et al.* (2020) 'Planktic Foraminiferal Test Size and Weight Response to the Late Pliocene Environment', *Paleoceanography and Paleoclimatology*, 35(1), p. e2019PA003738. Available at: https://doi.org/10.1029/2019PA003738.

Torres-Silva, A.I. and Hohenegger, J. (2024) 'Objective identification of Lepidocyclina (Foraminifera) species from the Eocene of Cuba based on growth-invariant morphometric characters', *Journal of Systematic Palaeontology*, 22(1), p. 2287728. Available at: https://doi.org/10.1080/14772019.2023.2287728.

Tyszka, J. *et al.* (2017) 'Energy flow in Foraminifera: from empirical to theoretical models', in. *Foraminifera and Nannofossil Meeting 2017*. Available at: https://pure.royalholloway.ac.uk/en/publications/energy-flow-in-foraminifera-from-empirical-to-theoretical-models (Accessed: 5 March 2025).

Uhen, M.D. *et al.* (2023) 'Paleobiology Database User Guide Version 1.0', *PaleoBios*, 40(11). Available at: https://doi.org/10.5070/P9401160531.

Urban, M.C. (2015) 'Accelerating extinction risk from climate change', *Science*, 348.6234, pp. 571–573.

Urbanek, A. (1993) 'Biotic crises in the history of Upper Silurian graptoloids: A Palaeobiological model', *Historical Biology*, 7(1), pp. 29–50. Available at: https://doi.org/10.1080/10292389309380442.

Vaes, B. *et al.* (2023) 'A global apparent polar wander path for the last 320 Ma calculated from site-level paleomagnetic data', *Earth-Science Reviews*, 245, p. 104547. Available at: https://doi.org/10.1016/j.earscirev.2023.104547.

Wade, B.S. *et al.* (2011) 'Review and revision of Cenozoic tropical planktonic foraminiferal biostratigraphy and calibration to the geomagnetic polarity and astronomical time scale', *Earth-Science Reviews*, 104(1–3), pp. 111–142. Available at: https://doi.org/10.1016/j.earscirev.2010.09.003.

Wade, B.S. and Olsson, R.K. (2009) 'Investigation of pre-extinction dwarfing in Cenozoic planktonic foraminifera', *Palaeogeography, Palaeoclimatology, Palaeoecology*, 284(1–2), pp. 39–46. Available at: https://doi.org/10.1016/j.palaeo.2009.08.026.

Waterson, A.M. *et al.* (2017) 'Quantifying the stability of planktic foraminiferal physical niches between the Holocene and Last Glacial Maximum', *Paleoceanography*, 32(1), pp. 74–89. Available at: https://doi.org/10.1002/2016PA002964.

Wei, K.-Y. and Kennett, J.P. (1986) 'Taxonomic evolution of Neogene planktonic foraminifera and paleoceanographic relations', *Paleoceanography*, 1(1), pp. 67–84. Available at: https://doi.org/10.1029/PA001i001p00067.

Weinkauf, M.F. *et al.* (2014) 'Disruptive selection and bet-hedging in planktonic Foraminifera: shell morphology as predictor of extinctions', *Frontiers in Ecology and Evolution*, 2. Available at: https://doi.org/10.3389/fevo.2014.00064.

Weinkauf, M.F.G. *et al.* (2013) 'Calcification intensity in planktonic Foraminifera reflects ambient conditions irrespective of environmental stress', *Biogeosciences*, 10(10), pp. 6639–6655. Available at: https://doi.org/10.5194/bg-10-6639-2013.

Weinkauf, M.F.G. *et al.* (2019) 'An extinction event in planktonic Foraminifera preceded by stabilizing selection', *PLOS ONE*. Edited by R. Rosa, 14(10), p. e0223490. Available at: https://doi.org/10.1371/journal.pone.0223490.

Weinkauf, M.F.G., Siccha, M. and Weiner, A.K.M. (2022) 'Reproduction dynamics of planktonic microbial eukaryotes in the open ocean', *Journal of The Royal Society Interface*, 19(187), p. 20210860. Available at: https://doi.org/10.1098/rsif.2021.0860.

Westerhold, T. *et al.* (2020) 'An astronomically dated record of Earth's climate and its predictability over the last 66 million years', *Science*, 369(6509), pp. 1383–1387. Available at: https://doi.org/10.1126/science.aba6853.

Wiens, J.J. (2004) 'The Role of Morphological Data in Phylogeny Reconstruction', *Systematic Biology*, 53(4), pp. 653–661. Available at: https://doi.org/10.1080/10635150490472959.

Wilkens, R.H. *et al.* (2017) 'Revisiting the Ceara Rise, equatorial Atlantic Ocean: isotope stratigraphy of ODP Leg 154 from 0 to 5 Ma', *Climate of the Past*, 13(7), pp. 779–793. Available at: https://doi.org/10.5194/cp-13-779-2017.

Woodhouse, A. *et al.* (2021) 'Adaptive ecological niche migration does not negate extinction susceptibility', *Scientific Reports*, 11(1), p. 15411. Available at: https://doi.org/10.1038/s41598-021-94140-5.

Woodhouse, A. *et al.* (2023) 'Paleoecology and evolutionary response of planktonic foraminifera to the mid-Pliocene Warm Period and Plio-Pleistocene bipolar ice sheet expansion', *Biogeosciences*, 20(1), pp. 121–139. Available at: https://doi.org/10.5194/bg-20-121-2023.

Woodruff, D.S. (2001) 'Populations, species and conservation genetics', *Encyclopedia of Bidiversity*, 4, pp. 811–829.

Worm, B. *et al.* (2006) 'Impacts of biodiversity loss on ocean ecosystem services', *Science*, 314(5800), pp. 787–790. Available at: https://doi.org/10.1126/science.1132294.

Yasuhara, M. *et al.* (2009) 'Temporal latitudinal-gradient dynamics and tropical instability of deep-sea species diversity', *Proceedings of the National Academy of Sciences*, 106(51), pp. 21717–21720. Available at: https://doi.org/10.1073/pnas.0910935106.

Yasuhara, M. *et al.* (2017) 'Combining marine macroecology and palaeoecology in understanding biodiversity: microfossils as a model: Marine macroecology-palaeoecology integration', *Biological Reviews*, 92(1), pp. 199–215. Available at: https://doi.org/10.1111/brv.12223.

Yasuhara, M. *et al.* (2020) 'Past and future decline of tropical pelagic biodiversity', *Proceedings of the National Academy of Sciences*, 117(23), pp. 12891–12896. Available at: https://doi.org/10.1073/pnas.1916923117.

Zeebe, R.E. and Wolf-Gladrow, D.A. (2009) 'Carbon Dioxide, Dissolved (Ocean)', in *Encylopedia of Paleoclimatology and Ancient Environments*. Dordrecht: Springer Netherlands, pp. 123–127.